

Utah State University

DigitalCommons@USU

---

All Graduate Theses and Dissertations

Graduate Studies

---

5-2002

## Geometry and Physical Properties of the Chelungpu Fault, Taiwan, and Their Effect on Fault Rupture

Richard V. Heermance  
*Utah State University*

Follow this and additional works at: <https://digitalcommons.usu.edu/etd>

 Part of the [Geology Commons](#)

---

### Recommended Citation

Heermance, Richard V., "Geometry and Physical Properties of the Chelungpu Fault, Taiwan, and Their Effect on Fault Rupture" (2002). *All Graduate Theses and Dissertations*. 6720.

<https://digitalcommons.usu.edu/etd/6720>

This Thesis is brought to you for free and open access by the Graduate Studies at DigitalCommons@USU. It has been accepted for inclusion in All Graduate Theses and Dissertations by an authorized administrator of DigitalCommons@USU. For more information, please contact [digitalcommons@usu.edu](mailto:digitalcommons@usu.edu).



GEOMETRY AND PHYSICAL PROPERTIES OF THE CHELUNGPU FAULT, TAIWAN,  
AND THEIR EFFECT ON FAULT RUPTURE

by

Richard V. Heermance

A thesis submitted in partial fulfillment  
of the requirements for the degree

of

MASTER OF SCIENCE

in

Geology

Approved

UTAH STATE UNIVERSITY  
Logan, Utah

2002

## ABSTRACT

Geometry and Physical Properties of the Chelungpu Fault,  
Taiwan, and Their Effect on Fault Rupture

by

Richard V. Heermance, Master of Science

Utah State University, 2002

Major Professor: Dr. James P. Evans  
Department: Geology

Rupture of the Chelungpu fault during the September 21, 1999, 7.6  $M_w$  earthquake in Taiwan caused a 90-km-long surface rupture with variable displacement along strike. Analysis of core from two holes drilled through the fault zone, combined with geologic mapping and detailed investigation from three outcrops, define the fault geometry and physical properties of the Chelungpu fault in its northern and southern regions. In the northern region, the fault dips 45-60° east parallel to bedding and consists of a narrow (1-20 cm) core of dark-gray, sheared clay gouge at the base of a 30-50 m zone of increased fracture density that is confined asymmetrically to the hanging wall. Microstructural analysis of the fault gouge indicates the presence of extremely narrow clay zones (50-300  $\mu\text{m}$  thick) that are interpreted as the fault rupture surfaces. Few shear indicators are observed outside of the fault gouge, which implies that slip was localized in the gouge in the northern region. Slip localization along a bed-parallel surface resulted in less high-frequency ground motion and larger displacements during the earthquake than in the southern region. Observations from the southern region indicate that the fault dips 20-30° at the surface and consists of a wide (20-70 m-thick) zone of sheared, foliated shale with numerous gouge zones. A footwall-ramp geometry juxtaposes 2000-3000 m of flat-lying Quaternary Toukoshan Formation in the footwall with Pliocene and Miocene, east-dipping siltstone and mudstone in the hanging wall. The wide, diffuse fault zone contributed to the lower displacement and higher frequency ground motion in the southern region during the 1999 earthquake. The structure in the northern region is the result of the fault being a very young (<50 ka) fault segment in the hanging wall of an older segment of the Chelungpu fault, buried in the Taichung basin. The fault in the southern region is located on an older (~1 Ma) fault

trace. The contrasting fault properties in the different regions are responsible for the variability in strong-motion and displacement observed during the 1999 earthquake.

(126 pages)

## ACKNOWLEDGMENTS

This work was funded by a National Science Foundation Grant #EAR00-98108 to J. P. Evans at Utah State University. Funding for the drilling was provided primarily by the Japanese Marine, Science and Technology Center (J.M.S.T.E.C.). Dr. Hidemi Tanaka (Ehime University, Japan) and Dr. Jih-Hao Hung (National Central University (NCU), Taiwan) were the principal investigators on the drill site. Japanese collaborators on the Chelungpu Fault Drilling Project included Dr. Masataka Ando, Dr. Arito Sakaguchi, Dr. Kotaro Ujiie, and Dr. Kazuko Saruwatari. Field work on the drill site in Taiwan was assisted by Zoe Shipton and Matt Pachell from Utah State University, and for their help I am indebted. Discussion with Dr. Jih-Hao Hung (NCU), Dr. Jien-Chen Lee (Academica Sinica, Taiwan), Dr. Yuen-Hsi Lee (National Taiwan University, Taiwan), Dr. Siang-Rong Song (NCU), Dr. Cyi-Tyi Lee (NCU), and Dr. Chien-Ying Wang (NCU) in Taiwan greatly assisted with my understanding of local and regional geology in Taiwan. John Demera, James, Amigo Wang, and the entire Filipino crew from Groundmat Construction, LTD. controlled the operations on the drill site, and for their help I am appreciative. Matt Mosdell, Angela Carter, and Natalie Jorgensen traveled to Taiwan with J. P. Evans and me in February, 2002, and their help was invaluable for understanding the fault structure. Dr. Pete Kolesar guided me through the x-ray diffraction analyses of the samples.

I would like to thank my advisor, Dr. James P. Evans, who gave me the opportunity to come to Utah and work with him on the structural geology of the Chelungpu fault. His work ethic and enthusiasm have truly been an inspiration, and are one of the main reasons I want to continue my study of geology. I also thank my other committee members, Zoe Shipton and Susanne Janecke, for their discussion and review of these papers. They put up with my last minute, sometimes frantic work.

Finally, there are my friends at Utah State University. Steve Klassen and Amelia Henry, for being such understanding and fun roommates during my often chaotic schedule. Dr. Brad Ritts for

his discussion, skiing, and biking assistance; Lori Hirschi for her never-ending patience with my demands; and Cam Snow, Matt Anders, and Adrian Berry for their comradeship in the geology department. I want to thank the rest of the grad students in the Geology Department, as well as all my friends I've made here at Utah State. Finally, to Liz Langenberg, who had to put up with me as an office-mate and roommate, but mostly a great friend. Without any of you, this thesis would have been much more difficult. Thanks!

Dick Heermance

## CONTENTS

|   | Page |
|---|------|
| ABSTRACT .....  | ii   |
| ACKNOWLEDGMENTS .....   | iv   |
| CONTENTS.....   | vi   |
| LIST OF FIGURES .....   | viii |
| CHAPTER   |      |
| 1. INTRODUCTION.....  | 1    |
| Introduction .....  | 1    |
| Regional Setting.....   | 4    |
| Objectives .....  | 9    |
| Methods .....   | 12   |
| References.....   | 13   |
| 2. CONTROLS ON FAULT SLIP AND GROUND MOTION DURING THE<br>1999 RUPTURE OF THE CHELUNGPU FAULT, TAIWAN ..... | 25   |
| Abstract.....   | 25   |
| Introduction .....  | 26   |
| Geologic Setting .....  | 29   |
| Study Locations .....   | 31   |
| Northern Region: Fengyuan Drill Site.....   | 31   |
| Northern Region: Takeng Site.....   | 35   |
| Northern Region: Tachia River Site.....   | 38   |
| Southern Region: Nantou Drill Site.....   | 39   |
| Southern Region: Tongtong Bridge Site.....  | 40   |
| Southern Region: Peikou Stream.....   | 41   |
| Discussion .....  | 41   |
| Brecciated Zone formation .....   | 43   |
| Rupture Properties.....   | 44   |
| Conclusions .....   | 46   |
| References.....   | 46   |
| 3. GEOMETRIC EVOLUTION OF THE SANYI/CHELUNGPU FAULT AND<br>THE EFFECTS OF RAMPS ON FAULT STRUCTURE .....    | 67   |
| Abstract.....   | 67   |
| Introduction .....  | 68   |

|  |     |
|--|-----|
|  | vii |
| Regional Geology .....                       | 69  |
| Sanyi Region .....                           | 70  |
| Northern Region of the Chelungpu Fault ..... | 71  |
| Southern Region of the Chelungpu Fault ..... | 72  |
| Geomorphology .....                          | 73  |
| Timing of faulting .....                     | 77  |
| Fault Structure .....                        | 77  |
| Discussion .....                             | 78  |
| Conclusions .....                            | 80  |
| References .....                             | 81  |
| 4. CONCLUSIONS .....                         | 94  |
| References .....                             | 98  |
| APPENDIX .....                               | 99  |



## LIST OF FIGURES

| Figure  | Page |
|---|------|
| 1-1 Location map of the Chelungpu fault rupture and generalized geologic map of the region.....   | 19   |
| 1-2 Chelungpu fault scarp through the Tachia River and this dam near the northern end of the rupture. Vertical displacement here was 9.8 m (Central Geological Survey, 1999)..... | 20   |
| 1-3 Accelerogram data from strong motion stations along the Chelungpu fault trace, showing vertical, E-W, and N-S movement. ....  | 21   |
| 1-4 Tectonic setting of Taiwan. ....  | 22   |
| 1-5 Schematic cross section across Taiwan.....  | 23   |
| 1-6 Stratigraphic column of the Western Foothills fold-and-thrust belt.....   | 24   |
| 2-1 Location map of the Chelungpu fault rupture and generalized geologic map of the Chelungpu/Sanyi fault region. ....  | 53   |
| 2-2 Cross-section A-A' and B-B' through the northern and southern regions of the Chelungpu fault. ....  | 54   |
| 2-3 Geologic map of the northern drill site showing local stratigraphy.....   | 55   |
| 2-4 Determination of bedding dips within the core. ....   | 56   |
| 2-5 Cross-section C-C' through Fengyuan drill site.....   | 57   |
| 2-6 Typical core lithology and structures. ....   | 58   |
| 2-7 Thin section photomicrographs of core samples.....  | 59   |
| 2-8 Histograms showing the fracture density in the core and their relation to the largest fractures. ....   | 60   |
| 2-9 Photo of the core box from 325-329 m. ....  | 61   |
| 2-10 Oblique photo of the Chlungpu fault in the Tali River near Takeng City.....  | 62   |
| 2-11 Cross-polarized photomicrographs from the 1999 rupture surface of the Chelungpu fault and hanging wall rocks.....  | 63   |
| 2-12 Scanning electron microscope image of the Chelungpu fault slip-surface from sample CDR-8.....  | 64   |
| 2-13 X-ray diffraction analysis from the Takeng fault outcrop. ....   | 65   |

|      |  |    |
|------|--|----|
| 2-14 | Chelungpu fault outcrop exposure in the Chingshui River at the Tungtou Bridge.....                   | 66 |
| 3-1  | Digital elevation model of the Chelungpu fault region.....   | 85 |
| 3-2  | Geologic map of the Chelungpu/Sanyi fault region.....  | 86 |
| 3-3  | Cross-section A-A' through the northern region of the Chelungpu fault.....                           | 87 |
| 3-4  | Cross-section B-B' through the Sanyi region.....   | 88 |
| 3-5  | Cross-section C-C' of the southern Chelungpu region.....   | 89 |
| 3-6  | Geologic map of northern region of Chelungpu fault showing lateritic terrace relationships.....      | 90 |
| 3-7  | Uplifted lateritic terrace in hanging wall of the Chelungpu fault northern region.....               | 91 |
| 3-8  | Fault zone outcrop from the Tongtou Bridge site at the southern terminus of the Chelungpu fault..... | 92 |
| 3-9  | Schematic cross sections through time of the Chelungpu fault in the northern region.....             | 93 |

## CHAPTER 1

### INTRODUCTION

#### Introduction

The Chelungpu fault of central Taiwan ruptured in a  $M_w$  7.6 earthquake at 1:47 AM local time on September 21, 1999. The earthquake is referred to as the Chi-Chi earthquake, or simply the 9/21/99 earthquake. The earthquake lasted 45 seconds, caused 2470 deaths, destroyed over 100,000 structures, and produced a 90-km-long rupture trace (Shin and Teng, 2001). Strong motion data and surface displacement from the earthquake was extremely well documented due a dense network of strong-motion recorders, GPS monuments, and an easily accessible surface rupture (Shin and Teng, 2001; Yu et al., 2001). The locations of high-frequency ground acceleration and rupture magnitude varied considerably along strike, and we compare these characteristics with the Chelungpu fault structure and surface lithology in order to understand the controls on fault rupture during the earthquake. The 9/21/99 earthquake thus provides one of the best data sets on the seismic slip and co-seismic deformation ever recorded.

The surface rupture from the 9/21/99 earthquake produced some of the largest displacements ever documented during a single earthquake (Wells and Coppersmith, 1994). The largest displacements were restricted to the northern end of the rupture approximately 40-50 km north of the epicenter. For this reason, I divided the fault into the northern and southern regions based on surface displacement and ground motion characteristics (Fig. 1-1). Typical vertical displacements of 5-7 m (4 m average) in the northern region reached a maximum of 12-15 m at the Shihkang Dam on the Tachia River (Fig. 1-2) (Y. H. Lee et al., 2001; Y. G. Chen et al., 2001; W.S. Chen et al., 2001a). Horizontal displacements in the northern region averaged 7 to 9 m and reached a maximum of 11.1 m (Lin et al., 2001; W. S. Chen et al., 2001a). Slip vectors here were  $320-330^\circ$  based on surface rupture piercing points and GPS data, indicating oblique thrust motion (Fig. 1-1)

(Chen et al., 2001a; Yu et al., 2001). In contrast, the southern region had vertical and horizontal displacements of approximately 2 m. Slip vectors were  $270\text{-}290^\circ$  along a  $20\text{-}30^\circ$  dipping fault plane (Lin et al., 2001; W. S. Chen et al., 2001a), indicating almost pure thrust movement in the southern region.

Ground shaking and surface displacements from the earthquake also varied considerably between the northern and southern regions. These were well documented due to the recently completed Taiwan Strong-Motion Instrumentation Program, which contains over 600 digital ground-motion instruments (Shin and Teng, 2001). The data from the earthquake was quickly made available to the public for analysis (Ma et al., 1999). Subsurface slip along the fault was inverted from the strong motion data, and showed that slip in the northern region averaged 8 m, while slip was only 1-3 m in the southern region near the epicenter (Ma et al., 2001). These slip values are consistent with empirical relationships for fault ruptures, which indicate that average subsurface slip is less than the average surface displacement during an earthquake (Wells and Coppersmith, 1994). Low frequency ( $<1$  Hz), long wavelength ground accelerations were dominant in the northern region, where surface displacement reached a maximum (Fig. 1-3) (Huang et al., 2001; Ouchi et al., 2001; Chi et al., 2001; Ma et al., 2001). High frequency (2-3 Hz) ground accelerations were the dominant strong-motion observed in the southern region during the earthquake. Rupture propagation velocity in the north was modeled at 1.2 km/sec, whereas the rupture propagated at 3.0 km/sec near the epicenter (Dalguer et al., 2001). The higher frequency accelerations and faster rupture propagation in the south produced much building damage, whereas in the north, where displacement was greatest, damage to buildings and loss of life was less.

Coseismic displacements (ground movement at surface) during the earthquake were monitored on a dense global positioning system (GPS) network in Taiwan. The GPS data agreed with the subsurface slip inverted from strong motion data and direct measurements of surface displacement along the fault rupture, in that displacement increased along the fault from the south to the north (Yu et al., 2001). GPS measurements showed that total displacement across the fault

ranged from 2.4 to 10.1 m (Yu et al., 2001). Horizontal displacement ranged from 1.1 to 9.1 m in the hanging wall, while vertical displacements ranged from 2.2 to 4.5 m (Yu et al., 2001; Ma et al., 2001; Lin et al., 2001). Additionally, the GPS data indicated that approximately 90% of the movement during the earthquake occurred in the hanging wall. These observations are in agreement with a model of the Chelungpu fault that predicts more motion in the hanging wall than in the footwall of thrust faults (Oglesby and Day, 2001; Oglesby et al., 2000). Deformation (uplift) occurred on the ground surface within 10 km of the hanging wall in the southern region, whereas deformation occurred 30 km into the hanging wall in the northern region, consistent with much larger displacements in the northern region (Yu et al., 2001).

Observations made along the Chelungpu fault as a result of the 9/21/99 earthquake provide an outstanding data set with which to study the fault. The established seismic monitoring network in Taiwan provides the unique opportunity for direct comparison of fault structure with surface displacement and ground-shaking during an earthquake. The purpose of this comparison is to understand how slip is distributed along the fault from the hypocenter to the surface. The observed surface ruptures in earthquakes are often larger than those modeled from strong motion data (Brune and Anooshepoor, 1998) indicating that direct observations of fault zones in the upper several km of the earth are important in constraining the processes of rupture propagation to the surface. The shallow dip of the Chelungpu fault makes subsurface portions more accessible through drilling and shallow seismic reflection methods. This study reports the results from two boreholes across the fault zone at localities in the northern and the southern region, as well as results from 3 surface outcrops. These results determined in this investigation are compared with data from other boreholes, and with previous investigations of the 9/21/99 earthquake, to try and understand how fault properties affect fault rupture on the Chelungpu fault. Insight gained from this comparison will be invaluable for understanding earthquake processes.

## Regional Setting

Taiwan is located on the tectonically active plate boundary of the Eurasian continental plate and the Philippine oceanic plate (Fig. 1-4). The northwestern corner of the Philippine plate is converging obliquely in a northwesterly direction at the rate of approximately 7 cm per year (Seno et al., 1993) relative to the Eurasian plate. This convergence has resulted in the northward subduction of the Philippine plate into the Ryukyu Trench northeast of Taiwan, and eastward subduction of the South China Sea below the Philippine Sea Plate to the south of Taiwan above the Manila trench (Fig. 1-4). Taiwan island has developed as the accretionary wedge over the southern subduction zone. Stratigraphic evidence indicates that the Philippine sea plate collided with the Eurasian margin approximately at 4 Ma (Chi et al., 1981), although zircon fission track dates across northern Taiwan show that accretion and mountain-building began as early as 5-6 Ma (Hsieh, 1990). Regardless of the exact timing, plate collision began near the early Pliocene in the northern part of the island, and the collision is propagating southward as the Philippine Sea Plate collides obliquely with the Eurasian continental plate (Suppe, 1987). On the northern half of the island, the Central Mountains have reached a steady state topographically, balanced between tectonic growth and erosion. To the south, however, where plate collision has begun more recently, the mountains are growing more rapidly and have not reached a topographical steady state (Suppe, 1987). Therefore, the Central Mountains decrease in height towards the south on the island. Development of the accretionary prism has only just begun south of Taiwan, where mountain building has initiated below sea level (Suppe, 1987).

Four major geologic provinces have developed from the plate collision and subsequent accretion of the Eurasian margin sediments along the Philippine/Eurasian plate boundary (Fig. 1-4). These include 1) the Eastern Coastal Range, 2) the Central Mountains, 3) the Western Foothills and 4) the Western Coastal Plain. The stratigraphy in these provinces records the timing of development of the island.

The Eastern Coastal Range consists of allochthonous volcanic and sedimentary rocks that have been accreted along the eastern edge of Taiwan. These rocks include ophiolites and volcanoclastic sedimentary rocks from the Philippine sea plate. These rocks lie unconformably underneath Plio-Pleistocene sedimentary formations derived from uplift of the Taiwan Central Mountains (Chi et al., 1981). The longitudinal valley on the eastern side of Taiwan represents the faulted boundary between the Eastern Coastal Range and Central Mountains, and is considered the suture zone between the Philippine and Eurasian plates.

The Central Mountains consist of metamorphic rocks that are the oldest rocks exposed in Taiwan. These Mesozoic and early Cenozoic meta-sedimentary rocks were derived from the Eurasian passive margin (Ho, 1976, 1986). They have been thrust up from at-least greenschist-facies depths since the initiation of the mountain-building during the Pliocene (Liou and Ernst, 1984) (Fig. 1-5). These structurally complex rocks contain thrusts and folds that generally trend parallel to the active plate boundary.

The Western Foothills are the active part of the accretionary prism, and form the advancing front of the accretionary wedge. They consist of a series of westward-verging, eastward-dipping thrust faults that sole into one or two basal decollement surfaces (Fig. 1-5) (Suppe, 1980a, 1980b; Kao and Chen, 2000). Shortening of between 140 and 200 km has occurred in the Western Foothills fold and thrust belt since the Pliocene (Suppe, 1980a). Global Positioning System (GPS) data indicates that between 20 and 45 mm/year of shortening are accommodated within the Western Foothills and 7-10 mm/yr. on average was accommodated on the Chelungpu fault from 1992-1999 (Yu et al., 2001). Decollement surfaces in Taiwan are generally weak, shale-rich horizons with high pore fluid pressure, and the basal detachment is a lower Miocene unit near the Oligo-Miocene boundary (Hung and Suppe, 2000; Suppe, 1987). Generally, the thrust-faults in the Western Foothills strike N-NE, are sub-parallel, and become younger towards the west (Davis et al., 1983). The geometry and kinematics of these folds have been modeled, but there is not detailed field mapping on the 100-1000 m scale of these structures. The youngest fault is the Changhua fault, a

blind thrust fault that produced a hanging wall anticline in the Pleistocene sedimentary units in the Western Coastal Plain (Fig. 1-5). The Chelungpu fault is immediately eastward of the frontal Changhua thrust in the fold-and-thrust belt.

The stratigraphy of the Western Foothills of Taiwan has been extensively studied due to hydrocarbon potential and complex structural evolution in the region (Deffontaines et al., 1997; Hung and Wiltschko, 1993; Hung and Yang, 1991; Kuan, 1972; Kuan and Wu, 1986; Namson, 1981; Suppe, 1980b). The formations in the Western Foothills consist of Pliocene and Miocene, shallow-marine facies rocks (Fig. 1-6) (W. S. Chen et al., 2001b). The dominant rocks in the region of the Chelungpu fault are of the Pliocene Cholan and Chinsui Formations. These are moderately-poorly consolidated, shallow marine, tidal and sub-tidal, siltstone and shale (Covey, 1984). The thrust faults in this province cause fault-bend folding in the hanging wall of the faults, and often are imbricate with multiple thrusts to the surface (Suppe and Medwedeff, 1990; Suppe, 1987).

The Western Coastal Plain consists of foreland deposits of the accretionary wedge, and is being impinged upon by the fold-and-thrust belt to the east. The basin consists of primarily Pleistocene and Pliocene, shallow-marine and fluvial sedimentary rocks derived from the Central mountains and Western Foothills of Taiwan (Covey, 1984; W. S. Chen et al., 2001b). Present erosion rates are 5-6 km/Ma (Li, 1976), and deposition rates in the foreland basin have been 1900 m/Ma since the initiation of faulting in the Western Foothills at approximately 1.25 Ma (W. S. Chen et al., 2001b).

The 1999 rupture along the Chelungpu fault was an out-of sequence event in the Western Foothills fold-and-thrust belt based on its geographic location behind the frontal Changhua thrust (Morley, 1988; Wang et al., 2000; Kao and Chen, 2000). The foremost thrust fault in the belt, the Changhua thrust, cuts through Plio-Pleistocene basin deposits to the west of the Chelungpu fault (Chang, 1971). The Chelungpu fault actually defines the boundary between the foothills and the "piggy-back" Taichung basin, currently being uplifted behind the foremost Changhua fault. Recent investigation has indicated that the Chelungpu fault may be migrating eastward from its original trace



and that fault propagation is controlled at the northern end by a south plunging Pliocene syncline (Y. G. Chen et al., 2001; Lee et al., 2002). The Chelungpu fault had been mapped prior to the 1999 rupture, but had been considered to pose a low seismic risk due to low seismicity in the area (Wang et al., 2000).

Geologic and seismic data, moment tensor solutions, and inversion of strong-motion data indicate the Chelungpu fault dips 20-35° east at 5-10 km depth, and strikes generally due north (Suppe 1980a; Hung and Suppe, 2000; Wang et al., 2000; Ma et al., 2001; W. S. Chen et al., 2001a; Y. G. Chen et al., 2001; Kao and Chen, 2000; J. C. Lee et al., 2001). Aftershocks from the 1999 earthquake indicated two zones of seismicity, the primary east-dipping zone at approximately 8 km depth, and a second east-dipping zone at approximately 25 kilometers depth (Fig. 1-5). This pattern may indicate that the Chelungpu fault moved within the hanging wall of a deeper decollement sheet (Fig. 1-5) (Kao and Chen, 2000).

The Chelungpu fault has been divided into two regions for this study, though other workers have subdivided the fault into four (Lin et al., 2001; Ouchi, et al., 2001; W. S. Chen et al., 2001b) or five (Y. H. Lee, personal communication, 2002) segments based on rupture properties. The subdivisions in this investigation are based on displacement style, magnitude, and slip direction, which all generally change just north of Wufeng city (Fig. 1-1). Previously defined fault segments are A) the E-W striking segment at the northern rupture terminus in the Tachia and Taan River valleys (large, south to north thrust displacement dominated by fault-related folding), B) the N-S striking segment from Fengyuan south to Wufeng (large, southeast to northwest displacement), C) the N-S striking segment from Wufeng south to Nantou (small, east to west displacement), and D) the southernmost segment south of Nantou (small, northeast to southwest displacement) (Lin et al., 2001; Ouchi et al., 2001). W. S. Chen et al. (2001a) assign the names Cholan, Shihkang, Tsaotun and Chushan to these 4 segments respectively. Y. H. Lee (personal communication, 2002) includes a fifth segment at the southern terminus where displacement was dominantly strike slip. The southern region for our investigation combines the southern segments C and D (and the southern terminus),

based on similar fault structure, displacement, and seismic characteristics from the 9/21/99 earthquake (Fig. 1-1). The northern region includes segments A and B. The specifics of the rupture in segment A have been discussed thoroughly in recent literature (J. C. Lee et al., 2001; Lin et al., 2001; Lee et al., 2002), and the unique characteristics of this termination are not the subject of this investigation. The northern and southern regions are defined in this investigation by their distinctly different rupture (magnitude, dip) and seismic characteristics (strong-motion), and changes in slip vector were not considered.

In the northern region, the hanging wall of the fault near the rupture trace consists of the Miocene Kuechulin Formation, the early Pliocene Chinsui Shale, and late Pliocene Cholan Formation. The footwall consists of the Miocene Kuechulin Formation or early Pliocene Chinsui Shale, in most places covered with only a thin veneer (<100 m) of Quaternary alluvial deposits (Y. H. Lee, personal communication, 2001). This suggests that the fault plane be confined within siltstone along a bed-parallel, footwall-flat geometry within at least the near surface (<300 m). The fault has been interpreted as a bedding-slip fault within late Pliocene and early Miocene Formations, based on seismic profiles and industry borehole data across the fault (Suppe, 1980a; W. S. Chen, 2001a; Wang et al., 2000). Surface outcrops define a steeply dipping (45-60°) fault, parallel to bedding, that ruptured with oblique left lateral thrust motion. Lin et al. (2001) observed similar surface outcrops dipping 50-85° east. Bedding becomes gentler (20-40°) eastward away from the fault trace towards the axis of the Toukashan syncline (Lo et al., 1999) (Fig. 1-1). The fault may therefore ramp to the surface along bedding in the west limb of the syncline.

In contrast to the northern region, the fault in the southern region dips 12-35° in the near surface (Lee et al, 2001) and is interpreted as a footwall ramp between Quaternary alluvium in the footwall and Pliocene shale in the hanging wall (Wang et al., 2000). The alluvium in the footwall is estimated to be approximately 2000-3000 m thick in this region (Chang, 1971). This suggests that the

fault juxtaposes two different lithologies for a significant portion of its rupture length (5-10%), and the rupture does not follow pre-existing bedding planes, at least in the near surface (< 2 km).

### Objectives

We investigated the structural properties of the Chelungpu fault in order to address questions regarding how structure affects coseismic slip within faults, and how energy and slip radiate to the ground surface. Why does the fault structure change along strike, and what are the implications of this change in structure? Why is the largest offset at the northern end of the rupture and not near the epicenter? What are the causes of the spatial variation in slip and surface displacement along strike, and how does the geology within the upper few hundred meters of the surface affect fault rupture? Oglesby and Day (2001) have determined that fault geometry plays a primary role in controlling the magnitude and strong motion during an earthquake rupture. Additionally, Ma et al. (2001) determined that variation in the geometry of the Chelungpu fault caused the different slip magnitude and ground motion observed along the fault strike during the 9/21/99 earthquake. Lee et al. (2002) showed how the location of the rupture was controlled by regional structure in the northern region. Therefore, it is important to document the structure of the fault to determine the relationship between fault thickness and geometry with rupture magnitude and ground shaking.

Drilling into recently ruptured faults can reveal significant data about the composition and structure of active faults (Ohtani et al., 2000). The width of the fault zone is of primary interest because width is used when modeling fluid pressures during earthquake rupture (Ma et al., submitted), and fault width also provides insight into how slip is distributed (localized or diffuse) in the fault zone. Ma et al. (submitted) interpret the lack of high-frequency motion in the north to result from a narrow (cm-scale) "smooth" slip surface parallel to bedding. Modeling of general fault rupture dynamics by Kanamori and Heaton (2000) describe how a narrow fault zone that, with elevated pore-pressures, would have reduced friction during earthquake rupture. Similarly, Brodsky

and Kanamori (2001) discuss how as displacement and velocity during fault rupture increases, and if the fault zone material behaves as a viscous fluid, then fluid pressure in the fault zone rises. This would create a lubricated fault surface that would decrease high-frequency radiation in a fault zone. Therefore, determining the width and composition of fault zones are important to understanding the rupture process. Documentation and characterization of the slip surface will either support these fault models, or discount their applicability to the Chelungpu fault zone.

It is important to document the fault properties soon after an earthquake rupture. As time passes after an earthquake, the fault zone is exposed to fluid flow and weathering processes that can obscure or eliminate any earthquake-induced breaks in the core. The fault scarp immediately begins to denude, especially in tropical climates such as Taiwan, after an earthquake. A denuded scarp can make finding surface outcrops difficult or impossible a short time after the earthquake. For the same reasons, it is important to log the core on site, during drilling. Otherwise, the core may sit around and dry out while waiting to be taken to the lab. Drying may cause new fractures to form from the clay shrinking as it dehydrates, making the original fractures difficult to distinguish. Also, structural features such as striations within weak clay zones may be destroyed as the core is transported from the drill site. Therefore, in order to obtain a sample of the fault zone as it was during rupture, the drilling was completed within 16 months of the earthquake and the core was logged on-site during drilling.

Several models exist for how energy is dissipated near the earth's surface. One such model indicates that the upper few kilometers of the earth's surface acts as a weak layer, where fault propagation changes from depth (Wald and Heaton, 1994; Brune and Anooshehpour, 1998). Another model implies that the heterogeneous nature of overlying, unconsolidated sediments causes complexities in the surface expression of the fault rupture (Bray et al., 1994). But few observational data have been collected to determine which model may best explain energy and slip distributions in the near surface. Therefore, by understanding how fault width relates to slip distribution in the near surface, we can use these data to compare with properties from older, exhumed faults, in an effort to

understand their past-seismicity. Additionally, by understanding the local structure associated with faulting and fault zone geometry, we may attempt to predict the controlling factors for fault rupture.

It is clear that the Chelungpu fault properties, such as width, fracture density, and geometry within the upper 1 km of the surface played a role in fault rupture properties. Field data indicates that the Chelungpu fault in the near surface changes geometry from depth. It is important to understand this geometric variability along the fault, and the understanding of how these properties affect fault rupture. Seismologists need these fundamental data on faults, such as thickness of slip zone, smoothness of fault surface, and compositional variability of a fault zone in order to accurately model seismic slip. Additionally, any relationship that can be documented between surface rupture, ground motion, and fault geometry may be used in future earthquake hazard analysis, and to help prevent loss of life and property in future events. This thesis therefore describes the near-surface characteristics of the Chelungpu fault in order to provide some of these required data and better understand the rupture processes from the 9/21/99 earthquake.

The second chapter of this Masters thesis describes the structural properties observed for the Chelungpu fault. The structure at different locations along strike is compared to rupture and ground-shaking observations produced during the 9/21/99 earthquake. A correlation between structure and earthquake rupture characteristics is hypothesized.

Chapter 3 discusses the rupture history of the Chelungpu fault over the last 1 Ma. This history provides reasons for the different fault structure along strike of the Chelungpu fault, and provides insight into how thrust faults evolve on a temporal scale.

Finally, Chapter 4 summarizes the findings of this thesis. Chapter 4 concludes that the structure of the fault changes along strike from north to south, this structural change affected the rupture during the 9/21/99 earthquake, and the different structure is the result different evolution at different regions along strike.

## Methods

Fieldwork in Taiwan was performed to support the Chelungpu Fault Drilling project. The project involved drilling 2 holes through the fault within the upper 250 meters of the ground surface. A 50° angled hole was drilled in the northern region near the city of Fengyuan (Fig. 1-1) where it intersected the fault at approximately 327 meters (drillers depth). The other hole, drilled vertically (90°), was drilled in the southern region near Nantou City up-dip of the epicenter, where it intersected the fault at approximately 180 m vertical depth. Participants in the project included the faculty from National Central University (NCU) in Taiwan, Ehime and Nagoya Universities in Japan, and Utah State University. The drilling investigations were funded primarily by the Japanese Marine Science and Technology Center (JAMSTEC) with additional funding provided by NCU in Taiwan and the National Science Foundation (NSF) Grant # EAR00-98108 to J. P. Evans at Utah State University in the United States. The project oversight group consisted of Professors C.Y. Wang and J. H. Hung of NCU; Professor H. Tanaka of Ehime University in Japan; and Prof. M. Ando of Nagoya University in Japan. Prof. H. Tanaka acted as the on-site supervisor during the drilling. We logged structural and lithologic characteristics of the core immediately after it was drilled. Z. K. Shipton, M. Pachell, and I were on site for the daily drilling from 70 m to 350 m, for a total of 21 days of drilling at the northern site. The northern core from 350-450 m was logged in the lab after the completion of drilling. The southern core was logged after the completion of drilling in the lab at NCU. Drill logs from the Fengyuan site are shown in the Appendix.

Geologic mapping and drill core analysis were used to constrain the fault geometry and architecture in the northern region of the Chelungpu fault. Detailed geologic mapping was completed within 1 km around the drill site. Additionally, detailed outcrop mapping was completed at the rupture 6 km south of the drill site in the Tali River near Takeng City. Samples were collected, and the structural analysis of the outcrop was compared to the structural feature observed in the borehole at Fengyuan. Both compared favorably, indicating that fault width observed at the surface

extended to at least 250 m depth along the fault. The fault was also described at the fault scarp through the Tachia River, 5 km north of the Fengyuan drill site, where the bed-parallel structure and relatively little deformation in the fault zone was recorded. A detailed structural transect was also completed at the Putzu River, 8 km south of the Fengyuan drill site, where intensely folded and faulted Chinsui Shale is juxtaposed on Quaternary gravel. This site is the subject of research by Matt Mosdell and Angela Carter (2 undergraduate field assistants in Taiwan), and the details of their work will be reported later. Structural data from the southern region were collected from the borehole in Nantou city, as well as from a surface exposure of the fault at the southern terminus of the fault trace near the Tungtuo Bridge along the Chingshui River (Fig. 1-1). The structural data collected from the study sites were used to evaluate the relationship of the fault structure between the northern and southern regions of the fault, and relate these structures to the rupture characteristics observed during the earthquake.

#### References

- Bray, J. D., R. B. Seed, L. S., Cluff, and H. B. Seed (1994). Earthquake fault rupture propagation through soil, *J. Geotech. Eng.* **120**, 543-561.
- Brodsky, E. E., and H. Kanamori (2001). Elastohydrodynamic lubrication of faults, *J. Geophys. Res.* **106**, 16357-16374.
- Brune, J. N., and A. Anooshehpour (1998). A physical model of the effect of a shallow weak layer on strong ground motion for strike-slip ruptures, *Bull. Seismol. Soc. Am.* **88**, 1070-1078.
- Chang, S. S. L. (1971). Subsurface geologic study of the Taichung basin, *Petrol. Geol. Taiwan* **8**, 21-45.
- Chen, C. H., H. C. Ho, K. S. Shea, W. Lo, W. H. Lin, H. C. Chang, C. S. Huang, C. S. Huang, C. W. Lin, G. H. Chen, C. N. Yang, and Y. H. Lee (2000). Geologic map of Taiwan, Central Geol. Surv., Ministry of Economic Affairs, R.O.C., scale 1:500,000.
- Chen, W. S., B. S. Huang, Y. G. Chen, Y. H. Lee, C. N. Yang, C. H. Lo, H. C. Chang, Q. C. Sung, N. W. Huang, C. C. Lin, S. H. Sung, and K. J. Lee (2001a). 1999 Chi-Chi earthquake: a case study

- on the role of thrust-ramp structures for generating earthquakes, *Bull. Seismol. Soc. Am.* **91**, 986-994.
- Chen, W. S., K. D. Ridgeway, C. S. Horng, Y. G. Chen, K. S. Shea, and M. G. Yeh (2001b). Stratigraphic architecture, magnetotratigraphy, and incised-valley systems of the Pliocene-Pleistocene collisional margin foreland basin of Taiwan, *Geol. Soc. Amer. Bull.* **113**, 1249-1271.
- Chen, Y. G., W. S. Chen, J. C. Lee, Y. H. Lee, C. T. Lee, H. C. Chang, and C. H. Lo (2001). Surface rupture of 1999 Chi-Chi earthquake yields insights on active tectonics of central Taiwan, *Bull. Seismol. Soc. Am.* **91**, 977-985.
- Chen, Y. G., W. S. Chen, Y. Wang, P. W. Lo, T. K. Liu, and J. C. Lee (2002). Geomorphic evidence for prior earthquakes: lessons from the 1999 Chichi earthquake in central Taiwan, *Geology* **30**, 171-174.
- Chi, W. C., D. Dreger, and A. Kaverina (2001). Finite-source modeling of the 1999 Taiwan (Chi-Chi) earthquake derived from a dense strong-motion network, *Bull. Seismol. Soc. Am.* **91**, 1144-1157.
- Chi, W.R., J. Namson, and J. Suppe (1981). Stratigraphic record of plate interactions in the Coastal Range of eastern Taiwan, *Geol. Soc. China Mem.* **4**, 155-194.
- Covey, M. (1984). Lithofacies analysis and basin reconstruction, Plio-Pleistocene Western Taiwan foredeep, *Petrol. Geol. Taiwan*, **20**, 53-83.
- Dalguer, L. A., J. D. Irikura, J. D. Riera, and H. C. Chiu (2001). The importance of the dynamic source effects on strong ground motion during the 1999 Chi-Chi, Taiwan, earthquake: brief interpretation of the damage distribution on buildings, *Bull. Seismol. Soc. Am.* **91**, 1112-1127.
- Davis, D., J. Suppe, and F. A. Dahlen (1983). Mechanics of fold-and-thrust belts and accretionary wedges, *J. Geophys. Res.* **88**, 1153-1172.
- Deffontaines, B., O. Lacombe, J. Angelier, H. T. Chu, F. Mouthereau, C. T. Lee, J. Deramond, J. F. Lee, and P. M Liew (1997). Quaternary transfer faulting in the Taiwan Foothills: Evidence for a multisource approach, *Tectonophysics* **274**, 61-82.



- Ho, C.S. (1975). An introduction to the geology of Taiwan-explanatory text of the geologic map of Taiwan, Central Geol. Surv., Ministry of Economic Affairs, R.O.C., 153 p.
- Ho, C. S. (1986). A synthesis of the geologic evolution of Taiwan, *Tectonophysics* **125**, 1-16.
- Hsieh, M. L., Y. H. Lee, T. S. Shih, S. T. Lu, and W. Y. Wu (2001). Could we have pre-located the northeastern portion of the 1999 Chi-Chi earthquake rupture using geological and geomorphic data? *Terr., Atm. and Oceanic Sci.* **12**, 461-484.
- Hsieh, S. L. (1990). Fission-track dating of zircons from several east-west sections of Taiwan Island, MS thesis (in chinese), National Taiwan University, 134 p., as cited in Chen et al., 2001.
- Huang, W. G., J. H. Wang, B. S. Huang, K. C. Chen, T. M. Chang, R. D. Hwang, H. C. Chiu, and C. C. P. Tsai (2001). Estimates of source parameters for the 1999 Chi-Chi, Taiwan, earthquake based on Brune's source model, *Bull. Seismol. Soc. Am.* **91**, 1190-1198.
- Hung, J. H., and C. N. Yang (1991). Mesoscale deformation mechanisms in the Chuhuangkeng anticline, Miaoli, Taiwan, *Proceed. Geol. Soc. China* **34**, 17-42.
- Hung, J. H., and J. Suppe (2000). Subsurface geometry of the Chelungpu fault and surface deformation style, *Int. Workshop Annual Commem. Chi-Chi Earthquake* **1**, 133-144.
- Hung, J.H., and D.V. Wiltschko (1993). Structure and kinematics of arcuate thrust faults in the Miaoli-Cholan area of Western Taiwan, *Petrol. Geol. Taiwan*, **28**, 59-96.
- Kanamori, H., and T. H. Heaton (2000). Microscopic and macroscopic physics of earthquakes, *Am. Geoph. Un. Mono.* **120**, 147-161.
- Kao, H. and W. P. Chen (2000). The Chi-Chi earthquake sequence: active, out-of-sequence thrust faulting in Taiwan, *Science* **288**, 2346-2349.
- Kuan, M.Y. (1972). The evolution of the structures in the oil and gas fields in the Miaoli area, Taiwan, *Petrol. Geol. Taiwan* **10**, 123-139.
- Kuan, M. Y. and S. Wu (1986). Hydrocarbon potential in Western Taiwan, *Petrol. Geol. Taiwan* **22**, 201-226.

- Lee, J. C., Y. G. Chen, K. Sieh, K. Mueller, W. S. Chen, H. T. Chu, Y. C. Chan, C. Rubin, and R. Yates (2001). A vertical exposure of the 1999 surface rupture of the Chelungpu fault at Wufeng, western Taiwan: structural and paleoseismic implications for an active thrust fault, *Bull. Seismol. Soc. Am.* **91**, 914-929.
- Lee, J. C., H. T. Chu, J. Angelier, Y. C. Chan, J. C. Hu, C. Y. Lu, and R. J. Rau (2002). Geometry and structure of northern surface ruptures of the 1999 Mw=7.6 Chi-Chi, Taiwan earthquake: influence from inherited fold belt structures, *J. Struct. Geol.* **24**, 173-192.
- Lee, Y. H., W. Y. Wu, T. S. Shih, S. T. Lu, and M. L. Shieh (2001). Deformation characteristics of surface ruptures of the Chi-Chi earthquake, east of the Pifeng bridge. Central Geologic Survey, Ministry of Economic Affairs, *Special Issue* **12**, 1-40.
- Li, Y. H. (1976). Denudation of Taiwan island since the Pliocene epoch, *Geology* **4**, 105-107.
- Lin, A., T. Ouchi, A. Chen, and T. Maruyama (2001). Co-seismic displacements, folding and shortening structures along the Chelungpu surface rupture zone occurred during the 1999 Chi-Chi (Taiwan) earthquake, *Tectonophysics* **330**, 225-244.
- Liou, J. G., and W. G. Ernst (1984). Summary of Phanerozoic metamorphism in Taiwan, *Geol. Soc. China Mem.* **6**, 133-152.
- Lo, W., L. C. Wu, and H. W. Chen (1999). The geological map and explanatory text of Kuohsing, Taiwan, Central Geol. Surv., Ministry of Economic Affairs, R.O.C., scale 1:50,000.
- Ma, K. F., E. E. Brodsky, J. Mori, Ji, Chen, T. R. A. Song, and H. Kanamori (submitted, 2002). Evidence for fault lubrication during the 1999 Chi-Chi, Taiwan, earthquake (Mw7.6).
- Ma, K. F., J. Mori, S. J. Lee, and S. B. Yu (2001). Spatial and temporal distribution of slip for the 1999 Chi-Chi, Taiwan, earthquake, *Bull. Seism. Soc. Amer.* **91**, 1069-1087.
- Ma, K. F., C. T. Lee, and Y. B. Tsai (1999). The Chi-Chi Taiwan earthquake: Large surface displacements on an inland thrust fault, *EOS Trans. Amer. Geophys. Un.* **80**, 605-611.
- Morley, C. K. (1988). Out of sequence thrusts, *Tectonics* **7**, 539-561.

- Namson, J. (1981). Structure of the Western Foothills belt, Miaoli-Hsinchu area, Taiwan: (I) Southern part, *Petrol. Geol. Taiwan* **18**, 31-51.
- Oglesby, D. D., R. J. Archuleta, and S. B. Nielsen (2000). The three-dimensional dynamics of dipping faults, *Bull. Seismol. Soc. Am.* **90**, 616-628.
- Oglesby, D. D., and S. M. Day (2001). The effect of fault geometry on the 1999 Chi-Chi (Taiwan) earthquake, *Geophys. Res. Lett.* **28**, 1831-1834.
- Ohtani, T., K. Fujimoto, H. Ito, H. Tanaka, N. Tomida, and T. Higuchi (2000). Fault rocks and paleo- to-recent fluid characteristics from the borehole survey of the Nojima fault ruptured in the 1995 Kobe earthquake, Japan, *J. Geophys. Res.* **105**, 16,161-16,172.
- Ouchi, T., A. Lin, A. Chen, and T. Maruyama (2001). The 1999 Chi-Chi (Taiwan) earthquake: earthquake fault and strong ground motions, *Bull. Seismol. Soc. Am.* **91**, 966-976.
- Seno, T., S. Stein, and A. Gripp (1993). A model for the motion of the Philippine sea plate consistent with NUVEL-1 and geological data, *J. Geophys. Res.* **98**, 17941-17948.
- Shin, T. C., and T. L. Teng (2001). An overview of the 1999 Chi-Chi, Taiwan, earthquake, *Bull. Seismol. Soc. Am.* **91**, 895-914.
- Suppe, J. (1980a). A retrodeformable cross section of northern Taiwan, *Proc. Geol. Soc. China* **23**, 46-55.
- Suppe, J. (1980b). Imbricated structure of Western Foothills belt, southcentral Taiwan, *Petrol. Geol. Taiwan* **17**, 1-16.
- Suppe, J. (1987). The active Taiwan mountain belt, in *Anatomy of Mountain Chains*, J. P. Schaer and J. Rogers (Editors), Princeton University Press, 277-293.
- Suppe, J., and A. Medwedeff (1990). Geometry and kinematics of fault-propagation folding, *Eclogae Geol. Helv.* **83**, 409-454.
- Wald, D. J., and T. H. Heaton (1994). Spatial and temporal distribution of slip for the 1992 Landers, California, earthquake, *Bull. Seism. Soc. Am.* **84**, 668-691.

- Wang, C. Y., C. H. Chang, and H. Y. Yen (2000). An interpretation of the 1999 Chi-Chi earthquake in Taiwan based on the thin-skinned thrust model. *Terr., Atm. and Oceanic Sci.* **11**, 609-630.
- Wells, D. L., and K. J. Coppersmith (1994). New empirical relationships among magnitude, rupture length, rupture width, rupture area, and surface displacement, *Bull. Seism. Soc. Amer.* **84**, 974-1002.
- Yu, S. B., L. C. Kuo, Y. J. Hsu, H. H. Su, C. C. Lui, C. S. Hou, J. F. Lee, T. C. Lai, C. C. Liu, C. L. Liu, T. F. Tseng, C. S. Tsai, and T. C. Shin (2001). Preseismic deformation and coseismic displacements associated with the 1999 Chi-Chi, Taiwan, earthquake, *Bull. Seism. Soc. Amer.* **91**, 995-1912.

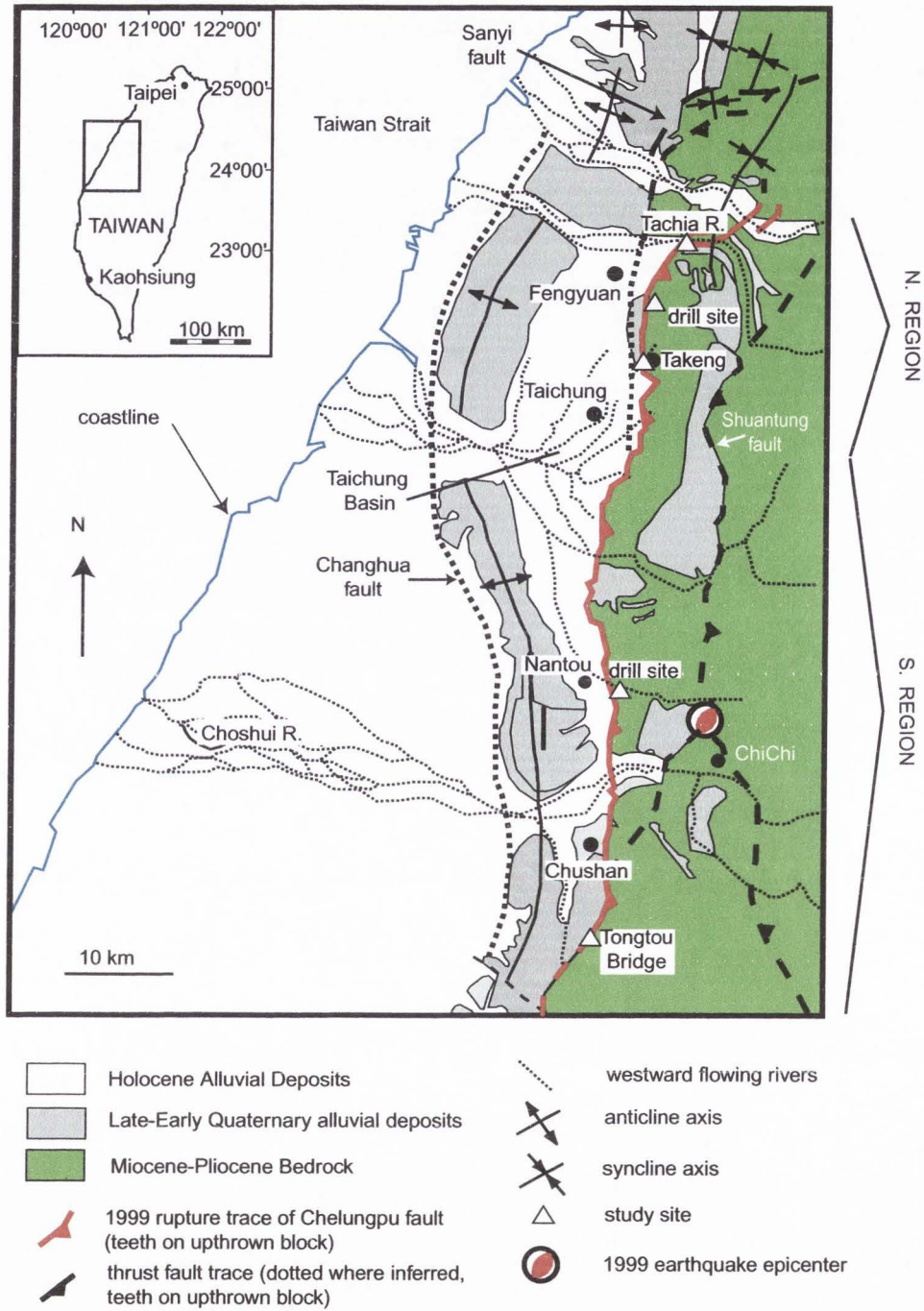


Figure 1-1. Location map of the Chelungpu fault rupture and generalized geologic map of the region. Mapping based from C. H. Chen et al. (2000), Hsieh et al. (2001), and Y. G. Chen et al. (2002). Epicenter position from Shin and Teng(2001). All faults are west vergent thrust faults.



Figure 1-2. Chelungpu fault scarp through the Tachia River and this dam near the northern end of the rupture. Vertical displacement here was 9.8 m, as shown by the difference in elevation of the top of the dam. Photo taken towards east.

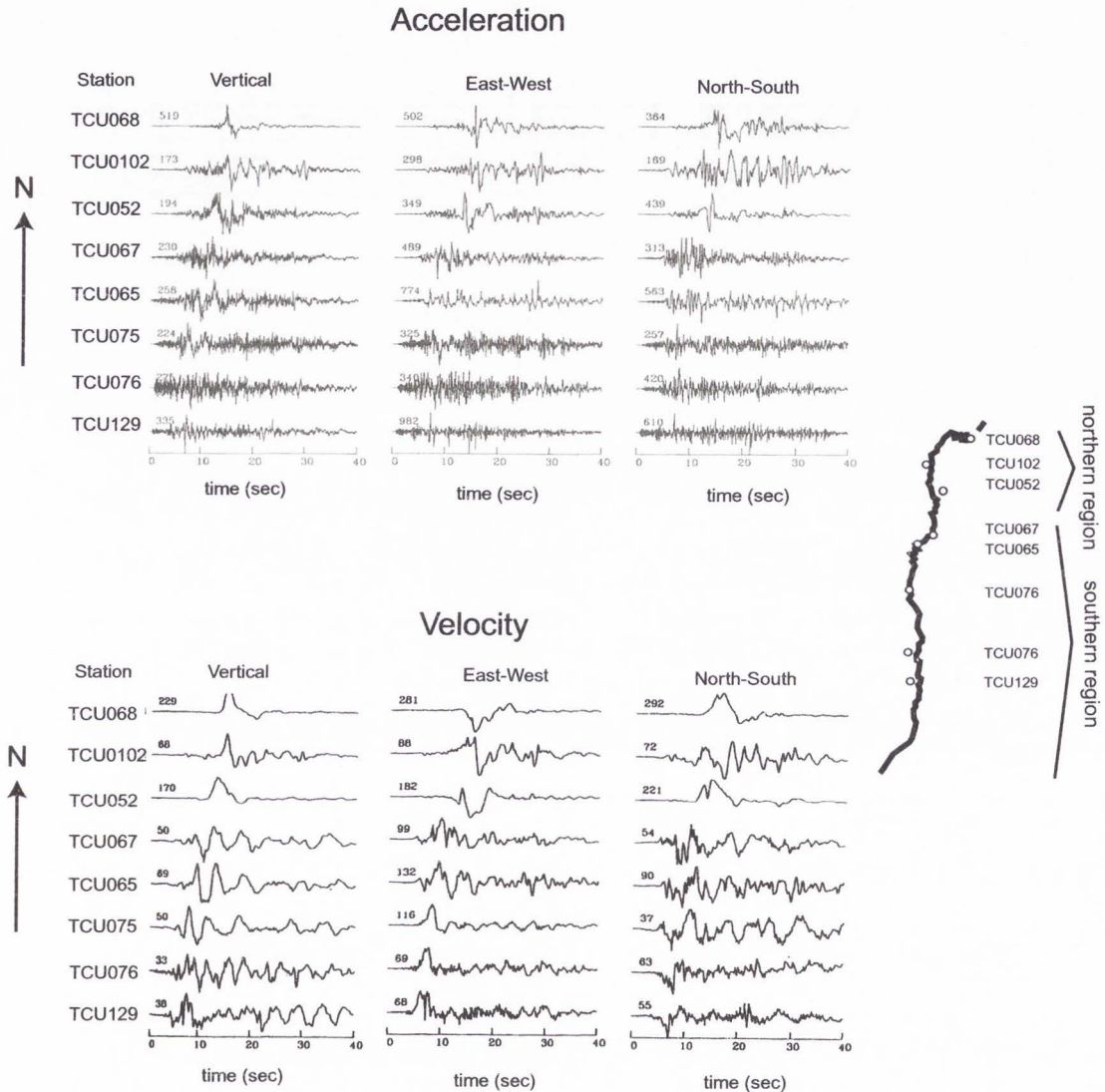


Figure 1-3. Accelerogram data from strong motion stations along the Chelungpu fault trace, showing vertical, E-W and N-S movement. Accelerations are shown in the upper graph, normalized to the peak value ( $\text{cm}/\text{sec}^2$ ) enumerated above each trace. Ground velocity data ( $\text{cm}/\text{sec}$ ) is integrated once from the accelerations. Peak velocities are enumerated above each trace. Station locations are shown on the fault sketch on the right. Figure modified from Huang et al. (2001). Ma et al. (2001) discuss in detail the differences between the ground-motion in the northern region (specifically TCU068 and TCU 052) and southern region. Slip occurred during a very short time ( $\sim 6$  sec) in the northern region, whereas in the southern region slip occurred for  $\sim 12$  sec. Shaking in the northern sites was dominated by "smooth," low-frequency ground movement and a fast slip velocity ( $2.3$  m/sec), while shaking in the southern sites had much-higher frequency ground motion and a slower slip velocity ( $0.5$  m/sec).

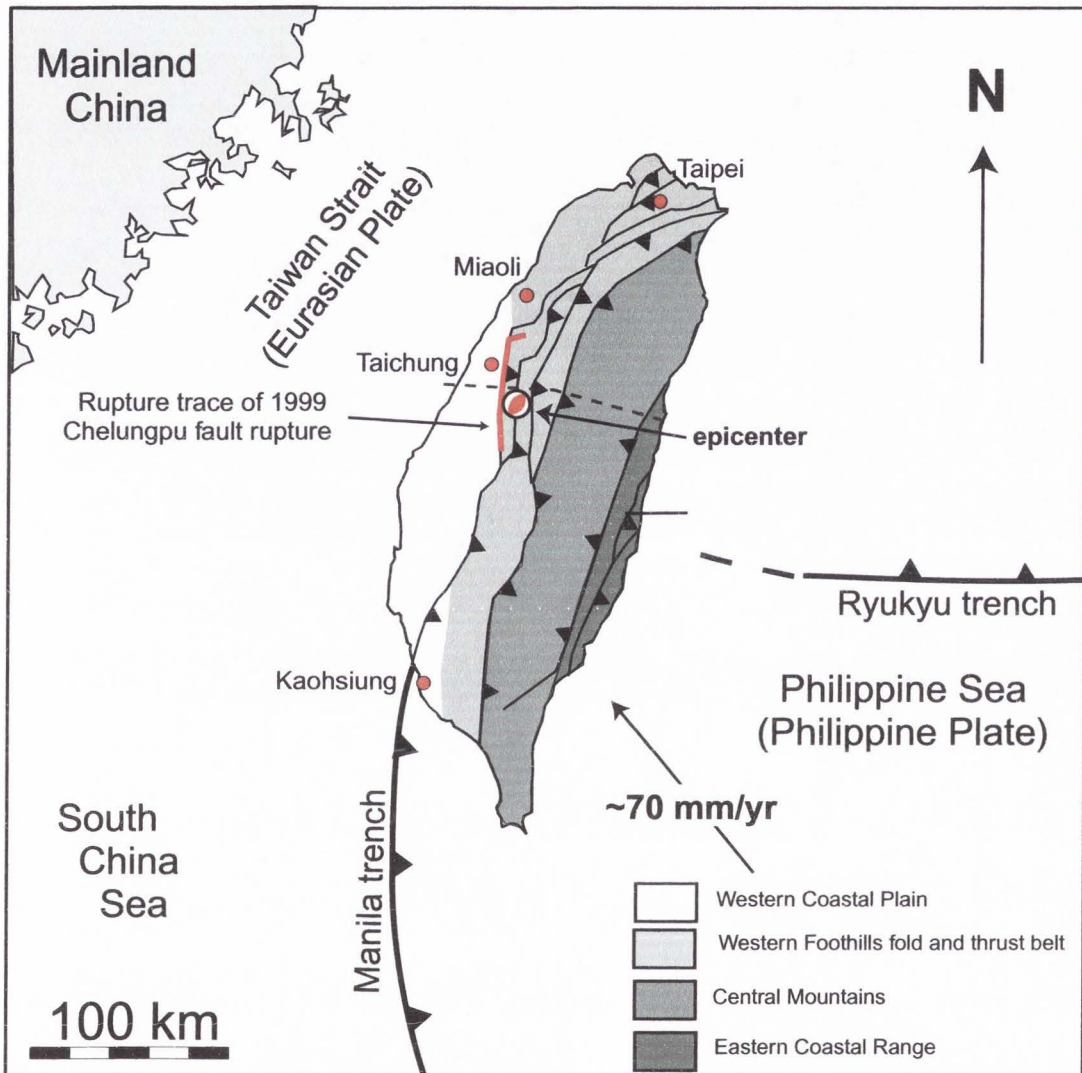


Figure 1-4. Tectonic setting of Taiwan. Heavy black lines in the oceans indicate plate boundaries with teeth on the overriding plate. Black lines on the island of Taiwan indicate faults with teeth on the upthrown side. Bold red line on Taiwan defines the 1999 trace of the Chelungpu fault. The focal mechanism shows the epicenter of the earthquake (Shin and Teng, 2001). Red dots indicate major cities in Taiwan. Figure 1-5 cross section location is indicated by the dashed line across Taiwan. The relative motion of Philippine Sea plate with Eurasia by Seno et al. (1993).



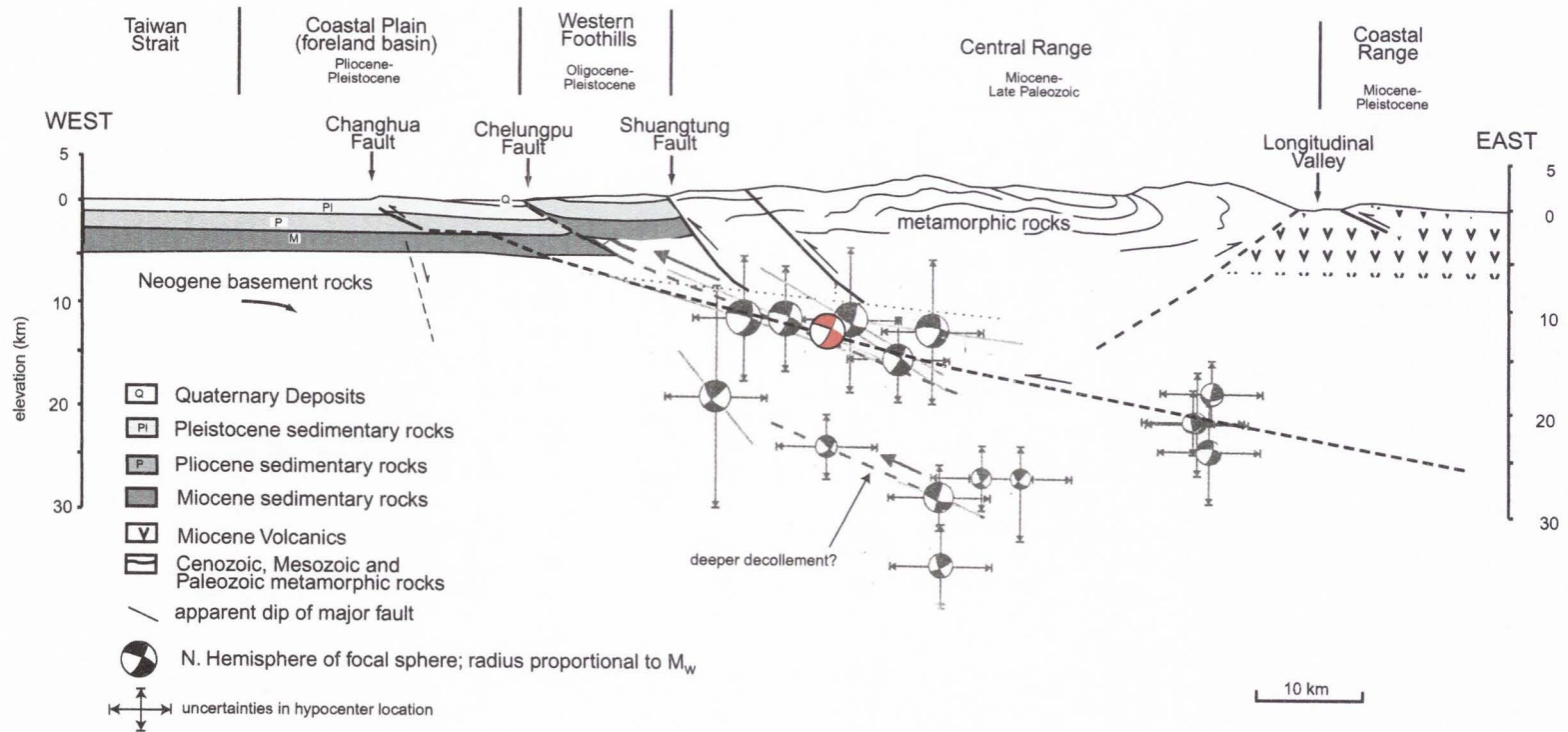


Figure 1-5. Schematic cross section across Taiwan (location shown on Fig. 1-4) showing the geologic provinces of Taiwan and the location of the Chelungpu fault in the fold and thrust belt. Section modified from W. S. Chen et al. (2001a). Major stratigraphic boundaries are also shown. Approximate location of main shock is shown in red. Selected aftershocks from the 9/21/99 earthquake are plotted in their spatial location (Kao and Chen, 2000).

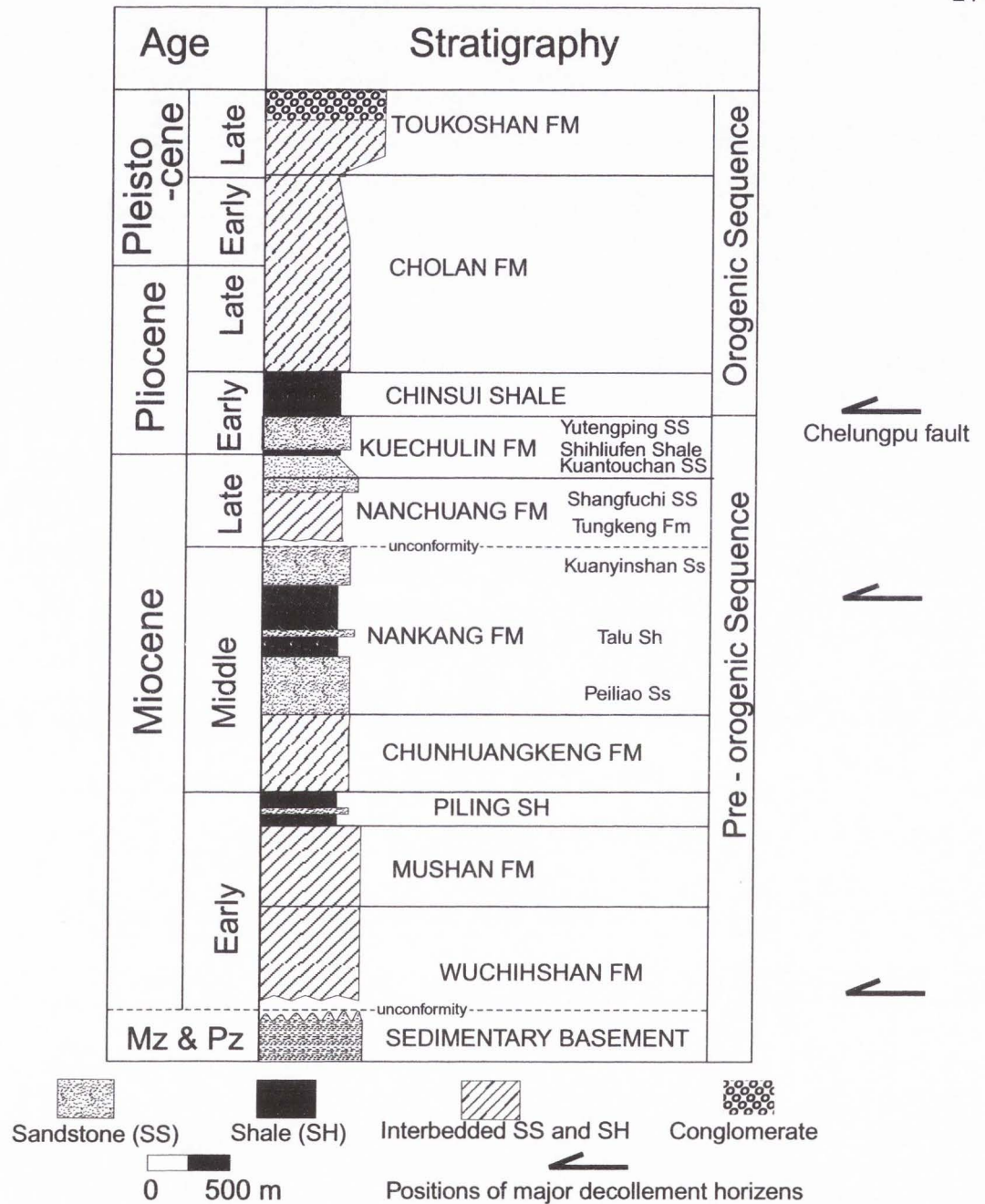


Figure 1-6. Stratigraphic column of the Western Foothills fold-and-thrust belt from the Chuhuangkeng oil and gas field, approximately 20 km north of the termination of the Chelungpu fault rupture. This column shows the typical units in the study area and the interpreted major decollement horizons. Adapted from Hung and Wiltschko (1993).

CHAPTER 2  
CONTROLS ON FAULT SLIP AND GROUND MOTION DURING THE  
1999 RUPTURE OF THE CHELUNGPU FAULT, TAIWAN<sup>1</sup>

Abstract

The Chelungpu fault, Taiwan, ruptured in a  $M_w$  7.6 earthquake on 21 September, 1999, producing a 90 km-long, dominantly thrust-type surface rupture trace. Displacement was greatest (11.5 m) near the northern end of the rupture, where high-frequency ground motion was minimal. By contrast, high-frequency ground motion was greatest near the epicenter where displacements were relatively small (2-4 m average). These differences in earthquake characteristics are attributed to a changing fault structure between the northern and southern regions. The fault in the northern region was investigated from a 450-m-long, inclined ( $50^\circ$ ) borehole through the fault, as well as two surface exposures of the fault trace. The results indicate that the fault consists of a narrow ( $<20$  cm), gouge zone along a bed-parallel surface within the Miocene Kueichulin Formation and/or Pliocene Chinsui Shale beds that dip  $50$ - $60^\circ$  within at least 250 m of the surface. Detailed structural analysis of the fault rocks in the northern region indicates that slip was likely localized in 50-300  $\mu\text{m}$  thick zones, uniquely confined to the narrow gouge zone, and that very minimal slip and/or shear were accommodated outside the fault gouge. The northern region has a flat-on-flat geometry, and the fault is localized along existing bedding planes. Fracture density increases in the hanging wall towards the fault, but decreases abruptly in the footwall below the fault, forming an asymmetric damage zone in the hanging wall. We propose that highly localized slip in the northern region occurred by the combination of 1) extreme deformation of micron-size particles within the existing clay-rich gouge, 2) slip along optimally oriented bedding planes, 3) slip on a relatively young fault segment. These factors produced the larger displacements and lower frequency strong ground

---

<sup>1</sup> Co-authored by R. V. Heermance, Z. K. Shipton, and J. P. Evans.

motion in the northern region. In contrast to the northern region, analysis from two localities in the southern region of the fault indicates a large, 20-70 m thick zone of intensely foliated shale and multiple clay-gouge zones characterizes the fault. The fault in the southern region dips 20-30° and contains a footwall ramp structure placing Pliocene and Miocene siltstone and shale on flat-lying Pleistocene sediments. The footwall ramp geometry and older fault segment in the southern region produced a wide, dispersed fault zone that produced less displacement but more high-frequency ground motion during the earthquake. These data demonstrate a correlation between fault structure and earthquake characteristics such as displacement and ground-shaking. This correlation may be useful when determining the hazard potential for future earthquakes on thrust faults.

### Introduction

The  $M_w$  7.6, 9/21/99 Taiwan earthquake lasted 45 seconds and ruptured along the Chelungpu fault. The Chelungpu fault is a west-vergent thrust fault along the boundary between the central mountains and the Taichung basin in central Taiwan (Fig. 2-1). The Chelungpu fault makes up the middle of 3, north-south trending thrust faults that form the active fold-and-thrust belt in central-western Taiwan. The 1999 earthquake caused over 2400 deaths and produced steep, often high (<12 m), fault scarps along an approximately 90-km-long, north-south, trace.

Seismic and rupture characteristics of the 1999 earthquake varied along strike. The change in rupture magnitude and strong-motion along the fault trace has been well documented (W. S. Chen et al., 2001; Dalguer et al., 2001; Lin et al., 2001; Ma et al., 2000, 2001). Slip and displacement increased towards the northern end of the rupture, while the greatest amounts of high-frequency ground acceleration occurred in the southern region near the epicenter. Rupture style changed from pure thrust near the epicenter (Dalguer et al., 2001), to thrust displacement with a significant left-lateral component (4-5 m) at the northern end of the fault trace (C.G.S., 2002; Y. G. Chen et al., 2001; Lin et al., 2001). Typical vertical displacements of 5-7 m (4 m average) in the northern region reached a maximum of 12-15 m at the Shihkang Dam on the Tachia River (Fig. 1-2) (Y. H. Lee et al.,

2001; W. S. Chen et al., 2001). Horizontal displacements in the northern region averaged 7 to 9 m and reached a maximum of 11.1 m (Lin et al., 2001; W. S. Chen et al., 2001). Slip vectors here were 320-330° based on surface rupture piercing points and GPS data, indicating oblique thrust motion (W. S. Chen et al., 2001; Yu et al., 2001). In contrast, the southern region had vertical and horizontal displacements of approximately 2 m. Slip vectors were 270-290° along a 20-30° dipping fault plane (J. C. Lee et al., 2001), indicating almost pure thrust movement in the southern region (Lin et al., 2001; W. S. Chen et al., 2001). Maximum subsurface slip was 15 m and averaged 9 m in the northern region, while average subsurface slip in the southern region was approximately 1-3 m (Ma et al., 2001).

The dip of the fault also changed along strike. Dips from the fault scarp in the northern region measured 50-80° east (Lin et al., 2001). Dips on the fault scarp in the southern region measured 25-35°. Focal mechanism solutions from the 1999 earthquake indicate that the fault ruptured along a 20-30°, east-dipping fault between 5-10 km depth (Wang et al., 2000; Kao and Chen, 2000; Ma et al., 2001).

The Chelungpu fault was divided into two regions for this investigation - northern and southern (Fig. 2-1) - based on rupture and seismic characteristics from the earthquake. Analysis of the fault was completed at three locations in the northern region and two locations in the southern region (Fig. 2-1). Additionally, core data from 3 sites (Y. H. Lee, pers. comm., 2002; Liao et al., 2002), outcrop analysis (Lin et al., 2001), and seismic reflection profiles (Chang, 1971; Wang et al., 2000) from other investigations were reviewed to examine the hypothesis that the fault structure changes from the north to the south.

Structural data from the northern region was collected from a 450 m, 50° inclined borehole to a total vertical depth (T.V.D.) of 345 m through the fault just east of Fengyuan city (Fengyuan drill site) (Fig. 2-1). This data was combined with detailed analysis from a surface exposure of the fault through the Tali River, 6 km south of the drill site near the town of Takeng. The fault was also

described at the fault scarp through the Tachia River, 5 km north of the Fengyuan drill site in the northern region (Fig. 2-1).

Structural data from the southern region were collected from a vertical drill hole immediately southeast of Nantou city, as well as from a surface exposure of the fault at the southern terminus of the fault trace near the Tungtou Bridge along the Chingshui River (Fig. 2-1). The structural data collected from the study sites were used to evaluate the relationship of the fault structure in each region to the rupture characteristics observed during the earthquake.

Drilling was completed as part of the Chelungpu Fault Drilling Project, funded by the Japanese Marine Science and Technology Center (J.A.M.S.T.E.C.). Drilling into recently ruptured faults can reveal significant insight into their composition and structure (Ohtani et al., 2000). The core not only provides samples of the fault zone at depth, but also allowed a determination of fault dip to at least a total vertical depth (T.V.D.) of 250 m from the surface. Determination of fault dip is otherwise difficult due to the bed parallel geometry of the fault, because seismic reflection would show bedding plane reflections similar to fault plane reflections, making differentiation difficult. But determination of the fault dip in the upper few hundred meters of the surface is important to understand the fault geometry, such as any bending or listric properties of the fault.

Analysis of fault zone structure may provide answers to the observed variation in the 1999 earthquake seismology. It is vital to determine whether slip is localized in a narrow zone, or is it dispersed over a wide area. Why is the largest offset at the northern end of the rupture and not near the epicenter? What are the causes of the spatial variation in slip and surface displacement along strike? How does the geology within the upper few hundred meters of the surface affect fault rupture? Several models explain how energy is dissipated near the earth's surface during the earthquake (Wald and Heaton, 1994; Brune and Anooshehpour, 1998), but few data have been collected to determine which model best explains the distribution of slip along the fault. Models of fault dynamics (Kanamori and Heaton, 2000; Brodsky and Kanamori, 2001; Ma et al., 2002) rely on understanding the thickness and roughness of fault surfaces. These models suggest that the

Chelungpu fault zone may act as a pressurized, viscous fluid. Additionally, models of the Chelungpu fault by Oglesby and Day (2001) and Oglesby et al. (2000) suggest that the near surface structure affects the displacement and ground motion at the surface. By studying the drilled transects through the active Chelungpu fault, and combining this data with detailed surface analysis of the fault, our investigation reveals fault width, dip, hanging wall and footwall geology, and deformation traits of the fault zone along strike. These characteristics are then related to questions on co-seismic slip on the fault, and how these factors influenced the rupture properties observed during the 1999 earthquake.

### Geologic Setting

Taiwan lies at the active tectonic boundary between the Eurasian plate and Philippine Sea plate. The Philippine Sea plate is converging northwesterly at a relative rate of approximately 7 cm per year (Seno et al., 1993). Shortening of between 150 and 200 kilometers has occurred in the Western Foothills geologic province of Taiwan since the Pliocene (Suppe, 1980). The Western Foothills consists of a thin-skinned fold-and-thrust belt located between the central mountains and foreland basin (Western Coastal Plain) in Taiwan. The Western Foothills make up the westward-propagating toe of the Taiwan accretionary wedge (Davis et al., 1983). Total displacement on the Chelungpu fault is estimated between 10-15 km since approximately 1.1 Ma, based on balancing of regional cross sections (Fig 2-2) (J. C. Lee et al., 2001; Suppe, 1980). An approximate long-term slip rate of 10-15 mm/yr can be calculated for the Chelungpu fault from these data (J. C. Lee et al., 2001). The Chelungpu fault places Pliocene and Miocene sandstone and shale from the Western Foothills over Pleistocene and Holocene Quaternary deposits in the Taichung basin (Fig. 2-2).

The northern region of the Chelungpu fault ruptured in the hanging wall of an old Chelungpu fault trace (old Chelungpu fault), which is buried beneath Holocene alluvium and late Pleistocene terrace surfaces ~1 km west of the 1999 earthquake rupture (Fig. 2-1) (Ho and Chen, 2000). The Chelungpu fault in the northern region is considered a bed-parallel thrust that ruptured

along the western flank of the south plunging Toukoshan syncline along 30-70° east-dipping beds in the northern region (Hung and Wiltschko, 1993; Lo et al., 1999; Lee et al., 2002). The Chelungpu fault is structurally above and east of the frontal thrust of the fold-and-thrust belt, the Changhua fault, which is located in the western coastal plain approximately 10 km west of the Chelungpu fault (Figs. 2-1, 2-2a). Thus, the recent earthquake was an out-of sequence event in the fold-and-thrust belt (Morley, 1988; Kao and Chen, 2000; Wang et al., 2000; Y. G. Chen et al., 2001).

Surface geology in the northern region consists of the Pliocene Chinsui Shale and the Miocene Kueichulin Formation in the hanging wall placed over Pliocene Chinsui Shale or Miocene Kueichulin Formation in the footwall along a bed-parallel fault (Fig. 2-2) (Ho and Chen, 2000; Chang, 1994). The footwall often has up to 70 m of Quaternary alluvium overlaying the bedrock, constrained by shallow (<100 m) drilling through the alluvium into Miocene/Pliocene bedrock (Y. H. Lee, pers. comm., 2002). Further west, in the footwall of the older Chelungpu fault thrust, the Quaternary deposits are over 1500 m thick (Hung and Wiltschko, 1993) (Fig. 2-2a). Therefore, the older Chelungpu fault has a footwall ramp geometry, whereas the recent rupture on the Chelungpu fault has a footwall flat geometry. Bedding strikes due north and dips range from 30-76° within 1 km of the fault. Average dip of bedding near the Fengyuan drill site of 56° (Fig. 2-3). Bedding dips gently (20-40°) eastward away from the fault trace towards the axis of the Toukoshan syncline (Fig. 2-1) (Lo et al., 1999). Near-surface outcrops in the northern region define a steeply dipping (45-80°) fault, parallel to bedding, that ruptured with oblique left lateral thrust motion (W. S. Chen et al., 2001; Lin et al., 2001; this chapter).

The southern region displays similar bedrock to the northern region, where the Pliocene Chinsui Shale and Miocene Kueichulin Formations are placed over a thick sequence of Quaternary alluvial deposits. The geometry is similar to the old Chelungpu fault in the northern region (Fig. 2-2). Bedding strikes due north and dips 20-40° east. Outcrops and seismic profiles in the southern region indicate the fault dips 20-30° (Ho and Chen, 2000; Chang, 1971). Miocene and Pliocene bedrock do



not outcrop in the footwall, and Quaternary deposits are estimated between 2000 and 3000 m in the southern region (Chang, 1971; J. C. Lee et al., 2001). The fault therefore has a footwall ramp geometry in this region (Fig 2-2).

Focal mechanism solutions from the 1999 earthquake indicate that the fault is a thrust fault that ruptured on a 15-30°, east-dipping fault between 5-10 km depth (Hung and Suppe, 2000; Kao and Chen, 2000; Wang et al., 2000; Ma et al., 2001). Near-surface outcrops in the northern region define a steeply dipping (45-80°) fault (Lin et al., 2001; this work). This disparity in dips implies that the fault must bend in the subsurface (Fig 2-2). Surface ruptures in the southern region show a 25-35° dipping fault, that aligns with the subsurface dip, indicating the fault may be planar from the hypocenter in that region (J. C. Lee et al., 2001) (Fig. 2-2).

#### Study Locations

##### Northern Region: Fengyuan Drill Site

A 450 m-long core was drilled through the fault near the city of Fengyuan from November, 2000 through January, 2001 (Fig. 2-1). Logging from 0 to 350 m (268 m true vertical depth (T.V.D.)) of the core was logged on the drill site during drilling. Logging of the core from the 350 to 450 m depth (268-345 m T.V.D.) interval was completed in the laboratory after the completion of drilling. Groundmat Construction Co. Ltd. from Taipei, Taiwan performed the drilling using a triple tube coring system. Core was taken directly from the core-barrel, and logged using a standardized logging sheet. Logging recorded the lithology, structures (depth, fracture type, width, orientation relative to core axis, fracture density, fracture fill, and other notes) and relevant drilling activities (driller comments on hardness, speed of drilling, fluid circulation or loss, etc). Core dimensions measured 1.5 m in length and 6.3 cm in diameter. All logs recorded depths of structures in the core to within 0.01 m. Depths were based on the surface of the drill-hole (0 m) and calibrated to drillers depths during drilling.

The borehole plunged 50° west and therefore the core depth is greater than the true vertical depth (T.V.D.) beneath the ground surface (Fig. 2-4a). Core recovery was excellent with the exception of two, 5 m-long, sections at 130 m and 230 m core depth, which were lost. These sections consisted of well-sorted, fine-grained, poor/moderately lithified sandstone that liquefied during drilling and therefore was not recoverable. The core was usually saturated with drilling fluids, so water content was not recorded as an in-situ observation of fault properties.

The core was oriented by aligning bedding in the core with surface outcrops (Fig. 2-4a, 2-4b). Bedding dips in the core (average: 58°) correlated well with hanging wall (average: 56°±20°) and footwall (average: 53°±6°) dips, indicating that bedding dips were consistent to at least 345 m vertical depth. Because the borehole was drilled at 274° (approximately perpendicular to regional strike of 0°) with a 50° dip west, the core provided a nearly true thickness view through the fault (± 20°) (Fig. 2-5).

The drilled core sampled mudstone and sandstone typical of the Chinsui Shale and Kuechulin Formation respectively (Figs. 2-3, 2-5). Both units are interpreted as shallow marine facies (Covey, 1984). Mudstone and sandstone in the core is damp to wet, moderately consolidated, moderately hard and weak. The mudstone is dark gray with intense bioturbation. Sandstone beds are yellow to tan, fine-to-medium-grained, and generally less consolidated than the mudstone. The contact between the formations is gradational, and was interpreted at approximately 220 m core depth by a change from massive mudstone above (Chinsui Shale) to interbedded mudstone and sandstone below (Fig. 2-5) (Kuechulin Formation). Hung et al. (2001) determined this same contact using biostratigraphy markers in the core. Sandstone and mudstone are often interbedded with <1 cm laminations (Fig. 2-6a). Cross-beds, bioturbation, coal, and shell fragments are typical. The sandstone beds and burrows are often calcareous, but the massive mudstone units are generally not. Thin sections show the sedimentary and structural features of the formations within the core (Fig. 2-7a-d). The Kuechulin Formation consists of interbedded mudstone and fine sandstone with intense

bioturbation (Fig. 2-7a), minor cross-bedding, and some imbrication of clasts along bedding planes. The sandstone and mudstone contain sub-angular clasts (immature) that are matrix supported. This matrix makes up 20-30% of the rock based on qualitative analysis of the thin sections. Compositionally, the rocks are quartz rich with less than 5% mafic fragments.

Fractures in this analysis are defined as any rupture, joint, break or fault in the core that cuts across bedrock. Some breaks in the core are drilling induced, but these make up less than 5 % of the fractures observed. They have a very different appearance from the in-situ fractures, and are distinguished by their irregular (not planar) boundaries and lack of fracture fill. In-situ fractures include brecciated zones that are greater than 4 cm in width (along core), and contain angular siltstone clasts up to 4 cm in maximum diameter suspended in light-gray, clay-silt matrix (Fig. 2-6d). Fracture fill consists of massive, clay-rich mudstone with no sedimentary structures (Fig. 2-7c,d). This fill is 75% matrix with 25% silt and sand grains incorporated from the protolith. Some minor foliation is apparent in the matrix, but generally the silty clay in the fractures shows random grain sorting and alignment (Fig 7 b, c, d). Brecciated clasts are sub-angular, show little rotation (Fig. 2-7b,c), are calcite cemented, and display sharp boundaries with the fracture matrix. There is very little evidence for shear in the brecciated zones, though small (<1 cm) offsets are apparent across some fractures. Clasts of mudstone are rare in the brecciated zones, implying the sandstone may be stronger in order to exist as individual clasts, unlike the mudstone. Fractures vary from irregular to planar, <0.001 m to 1.5 m in width and are filled with dark to light gray clay or silt with brecciated clasts (Fig. 2-6b, 2-6c). Clasts make up approximately 10-50% of the brecciated zones, and clast size scales up with fracture width. That is, smaller clasts are found in smaller-width brecciated zones. Silt and clay within the fractures are very soft, moderately plastic and usually very wet relative to the host rock. Fractures, including brecciated zones, frequently occur parallel to bedding (Fig. 2-6d). The amount of slip, if any, across the fractures is difficult to determine. Though the fractures are texturally distinct from the protolith, x-ray diffraction analysis (next section) of the core samples indicates that the fractures are compositionally indistinct from the protolith.

The density of fractures varies along the linear transect formed by the drilled core through the fault zone. Fracture density in the core is determined using two different methods. Method A involves determining the spatial percentage of a 5 m section of core taken up by fractures. These percentages are then plotted for the 5 m bin size for the entire core length (Fig. 2-8a). All fractures encountered in the core are used in this method. Method B quantifies the density of all fractures greater than 4 cm width per 5 m bin size. Four cm width is chosen arbitrarily for our analysis to eliminate any bias that might be introduced by including smaller fractures in the histogram. Smaller fractures, though in some places abundant, do not cumulatively represent large damage areas in the core. Both methods produce similar results, with the largest density of fractures occurring immediately above 327 m (Fig. 2-8 a, b). Method A shows that fracture density increases at 150 m, 300 m, and 400 m in the core. All three zones are associated with brecciated zones greater than 0.5 m thick at their base. Method B shows abrupt increases in the density of fractures at 150 m, 250 m, 300 and 400 m depth in the core. The zones of high fracture density are defined as fault-related damage zones (Caine et al., 1996; Chester and Logan, 1986) in the core. They occur consistently above the widest fractures (>0.5 m thick), and abruptly drop off below these fractures. This asymmetry of fracture density is observed around the four largest fractures in the core.

At 327.6 m core depth (250 m T.V.D.), a 1.5 m thick brecciated zone is encountered that corresponds to the base of a zone with the highest fracture density (Fig. 2-9). Additionally, an anomalous, thin (7 mm), dark gray, plastic, striated clay zone is present at the base of this 1.5 m thick brecciated zone. The clay zone was located along a naturally parted surface in the core. Slickenlines on the surface indicate a 40° rake down from the south, consistent with left-lateral movement in addition to thrusting in the region. This dip and slickenline data correspond with surface rupture data from the area (Lin et al., 2001; C.G.S., 2002). The parted surface with striations is unique within the core, is associated with the largest damage zone (30-50 m thick), and is associated with the highest fracture density in the core. For the above reasons, we interpret the rupture at 327.6 m as the primary fault surface of the 1999 earthquake.

The primary rupture surface of the fault was confined within the Kuechulin Formation, based on biostratigraphy (Hung et al., 2001). No age dating has been completed on the core, but it appears that the interbedded sandstone and shale in the hanging wall are younger than the Kuechulin Fm. rocks in the footwall, indicating the rocks are in normal stratigraphic sequence. If this is true, then the fault is bed parallel, and is probably a very young fault. Otherwise we would expect an unconformity across the fault.

Surface observations near the Fengyuan drill site indicate net surface displacement of 9.5 m (J.C. Lee, personal communication, 2000). GPS data from a station approximately 1.75 km SSE of the drill site indicated 3.97 m of vertical and 9.09 m of horizontal displacement in the direction of  $340^\circ$  (C.G.S., 2002). Slickenlines and fault trace measurements near the Fengyuan drill site show that the fault ruptured obliquely with thrust and left-lateral motion along a steeply dipping fault ( $45\text{-}80^\circ$ ) (Lin et al., 2001). The 1999 earthquake rupture trace is obscured on the hillside west of the Fengyuan drill site by earthquake-induced landslides and steep colluvial slopes (Fig. 2-3). Well-developed scarps from the 1999 rupture were apparent in river banks northwest and southwest of the northern drill-site. Therefore, the fault trace location directly west of the drill-site was calculated from structural contours of the fault plane, that are constrained by the two surface traces and fault position in the borehole. The scarp was then aligned with the fault surface in the Fengyuan drill core to determine a fault dip of  $52^\circ$  to at least 250 m T.V.D. in the northern region. Structural analysis of the core combined with geologic mapping around the drill site allows us to conclude that the Chelungpu fault dips between  $52^\circ$  and  $60^\circ$  east, along a narrow,  $< 1$  cm, bed-parallel surface.

#### Northern Region: Takeng Site

The fault zone was investigated in detail at a temporarily excavated locality near the town of Takeng in the Tali River, just north of Taichung City and 6 km due south of the Fengyuan drill site (Fig. 2-1). Here, the fault is oriented  $320^\circ$  and dips  $48^\circ$  east across a river channel, sub-parallel to

bedding (strike: due N, dip: 40°-66° E) (Fig. 2-10). Net displacement at this location reached 7.3 m during the earthquake (Lin et al., 1999). The fault juxtaposes siltstone (Miocene Kuechulin Formation or Pliocene Chinsui Shale) in the hanging wall with unconsolidated Quaternary fluvial gravel deposits in the footwall. These gravel deposits are approximately 70 m thick (Y-H. Lee, personal communication, 2002), and overlie siltstone similar to that in the hanging wall. This suggests that the fault plane be confined within the Miocene Kuechulin Formation and/or Pliocene Chinsui Shale to very near the surface, possibly along a bed-parallel, footwall flat surface similar to that seen at the Fengyuan drill site.

The excellent fault exposure at Takeng was mapped and samples collected during December 2000. A distinctive, 20 cm-thick, dark gray clay gouge lies at the faulted siltstone/conglomerate contact (Fig. 2-10). The gouge changes across a sharp contact from dark-gray (derived from shale) to reddish brown (derived from conglomerate) at approximately 15 cm into the gouge from the hanging wall (Fig. 2-11a). The siltstone in the hanging wall within approximately 30 m of the gouge is intensely fractured, and bedding is indistinguishable. This is interpreted as the damage zone of the fault that may record the effects of accumulated slip over much of the fault history (Caine et al., 1996; Chester and Logan, 1986). Beyond this zone, fracture density decreases and bedding is apparent. At least two synthetic faults with < 1 m vertical displacement are apparent in the hanging wall. Very little deformation is apparent in the footwall. The sub-parallel geometry of the fault to the hanging wall bedding implies that bedding planes may have acted as a guide for the rupture in the near surface, contributing to the large offsets in the northern region.

Microstructural analysis across the fault zone at the Takeng site reveals the deformation mechanisms and fabrics associated with the localized zone of slip. The protolith in the hanging wall consists of well sorted, rounded, quartz and feldspar grains in a clay matrix (Fig. 2-11b). At 20 cm from the fault gouge, the fine-grained quartz-clay siltstone of the hanging wall has few deformation-related microstructures. A faint foliation is defined by the clay matrix, but undeformed foraminiferid fragments and no indication of shear around these fossils (Fig. 2-11c) document the small amount of

deformation. Samples from the clay gouge at the fault contact reveal a foliated, clay-dominated fabric (Fig. 2-11d) in which dark zones <0.1 mm thick cut the clay fabric. Irregularly shaped zones defined by color variations (Fig. 2-11e) are interpreted as porphyroclast rotation, isoclinal folds, and mullion structures. Sub-parallel, parted surfaces are found only in the 20 cm fault gouge zone and these appear to be associated with the narrow slip surfaces developed within the slip zone (Fig. 2-11a, d). These surfaces are interpreted as the slip planes within the gouge.

Back-scattered scanning electron microscopy of the fault contact further clarifies the narrow thickness of the 1999 rupture. Images of the fault surface (Fig. 2-12) reveal that the fault zone consists of a zone 50 to 300  $\mu\text{m}$  thick that is composed of disrupted and brecciated clay-rich gouge. Intra-and-intergranular fractures and a random fabric characterize the zone, whereas rocks in the hanging wall have a well-defined clay-rich foliation. The material within the slip zone consists of micron to submicron-sized grains of clay and rounded to sub-rounded quartz grains. Quartz grains outside the fault zone are 100-300  $\mu\text{m}$  (Fig. 2-12) similar to the grain sizes of protolith well away from the fault surface (Fig. 2-11b, c). Clay grains define a foliation within the fault zone (Fig. 2-12) but at high magnification much of the clay-rich gouge consists of amorphous grains.

X-ray diffraction (XRD) analysis of fault rocks indicates a change in clay-mineralogy between the fault-related rocks and undeformed siltstone away from the fault gouge in the hanging wall. The siltstone 100 m into the hanging wall from the fault gouge contained primarily smectite, illite, amesite and kaolinite (Fig. 2-13b). Within the damage zone (<30 m from fault gouge), and in the fault core, the dominant clay minerals are vermiculite, illite, amesite and kaolinite (Fig. 2-13b). Other than this clay variability, the rocks from the undeformed protolith and the fracture fill (matrix and siltstone clasts) near the fault show identical bulk mineralogy (Fig. 2-13a). The compositional signature of decreasing smectite towards the fault is consistent with other localities along the Chelungpu fault (Liao et al., 2002) and indicates a fault genesis for the clay. Similar signatures showing a decrease in smectite towards fault zones have been observed in thrust faults in the

Canadian fold-and-thrust belt (Vrolijk and Van der Pluijm, 1999; Van der Pluijm, 2001) and the Barbados accretionary prism (Vrolijk et al., 1999; Bekins et al., 1994). These studies indicate the change in clay mineralogy may be attributable to fluid flow in the fault zone inducing a smectite-illite conversion along the fault, and this change may facilitate slip localization in zones of clay alteration (Vrolijk and Van der Pluijm, 1999).

The structure of the Chelungpu fault at the Takeng site appears similar to the structure observed at the Fengyuan drill site. The narrow, dark-gray gouge zones, associated damage zones, and bed-parallel, footwall flat geometry are all very similar. Unfortunately, the 7 mm gouge from the drill site could not be sampled, but the observations from the Takeng site are probably what we would have observed in the gouge from the drill site. Therefore, we hypothesize that the fault structure observed exists to at least 250 m T.V.D. in the northern region of the fault.

#### Northern Region: Tachia River Site

The 1999 earthquake scarp was studied at the Tachia River, 5 km north of the Fengyuan drill site, where the vertical offset on the fault created a 6-m-high waterfall through the river. The Chinsui Shale is exposed in the hanging wall and strikes approximately  $45^\circ$ . The Kueichulin Formation is exposed near the fault trace in the footwall, and parallels the hanging wall bedding. Dips vary between  $30^\circ$  and  $55^\circ$  in the hanging wall and the footwall. Bedding is very distinct, and appears to be in stratigraphic sequence across the fault despite the fault scarp that ruptured parallel to bedding. A thin cover of  $<1$  m of alluvium covers the footwall bedrock in the river channel within 50 m of the fault. One brecciated zone, 20 cm in width, was observed approximately 2 m from the rupture surface. Lee et al. (2002) documented 3 subsidiary faults, parallel to bedding, in the hanging wall, but these faults showed cumulative displacement of less than 1 m vertically, which accounts for  $<10\%$  of the total displacement during the earthquake. These faults are therefore not considered significant when considering slip in the fault zone during the earthquake. Jointing and fracturing are apparent in the hanging wall and footwall bedrock, but the fracture density is not higher than 1 fracture per 3 cm



(low damage). The primary fault surface from the 1999 rupture was not observed as it was below the water level. The evidence from this site supports a localized fault zone where most of the slip is accommodated along the primary fault surface. The relatively little deformation observed, intact stratigraphic sequence from the footwall into the hanging wall, and lack of footwall alluvium are evidence that this fault is bed-parallel, and may be very young with little historic slip.

#### Southern Region: Nantou Drill Site

A vertical hole was cored through the Chelungpu fault a few kilometers southeast of Nantou City as part of the Chelungpu fault drilling project-the same project that drilled the Fengyuan hole (Fig. 2-1). This hole penetrated the fault at approximately 180 m. The hanging wall consisted of Pliocene Chinsui Shale, while the footwall was the Quaternary Toukoshan Formation conglomerate. The Toukoshan Formation is relatively flat-lying and is interpreted to be 2000-3000 feet thick in the area (Chang, 1971; J. C. Lee et al., 2001). Outcrops of the Chinsui shale in the hanging wall indicate the bedding strikes  $0^{\circ}$  and dips  $30-40^{\circ}$  east, parallel to the fault trace. Fault dip is estimated at  $\sim 35^{\circ}$  in this region of the fault (J. C. Lee et al., 2001), and surface displacement was  $\sim 2$  m in the area.

The fault zone observed in the core is characterized by a 20 m section of intensely foliated shale. This segment included approximately 50 % (10 m) of discontinuous brecciated zones. Bedding was indistinguishable within 20 m of the fault. The contact with the Toukoshan conglomerate was observed at 177 m, but the fault anastomoses into the underlying conglomerate, and 1 m of foliated shale is observed at 180 m. Structures observed include wavy foliation parallel to fault dip, and rotated, sub-rounded sandstone clasts in a foliated, muddy matrix. No distinct gouge zone was observed in the core, but more than 5 brecciated zones with greater than 30 cm widths were observed between 120 m and 180 m. Within 70 m of the Toukoshan Formation contact, the bedrock was usually intensely deformed by foliation and fracturing. There was less than 15 m of "undeformed (less than 1 fracture per 3 cm)" Chinsui Shale in the 70 m above the fault. The

footwall was only cored for approximately 6 m due to poor recovery of the conglomerate, so the deformation in the footwall was not observed.

The fault zone in this core is clearly a diffuse zone, where shear has been distributed over a wide (>20 m) area. The presence of a thick Quaternary package in the footwall implies a long history of displacement and a large cumulative slip on this fault. The fault geometry is a footwall ramp, in contrast to the fault trace from the northern region.

#### Southern Region: Tongtou Bridge Site

The Chelungpu fault outcrop was studied in the Chingshui River at the Tungtou Bridge near the southern termination of the 1999 fault trace (Fig. 2-1, 2-14). The fault is interpreted to dip  $\sim 30^\circ$  in this area (Liu and Lee, 1998). Two m of strike-slip and 0.4 m of vertical displacement occurred during the 1999 earthquake (Lin et al., 1999). The footwall consists of the Quaternary Toukoshan Formation. Bedrock in the hanging wall consists of the Miocene Kueichulin Formation that strikes northeast and dips steeply  $70\text{-}80^\circ$  southeast near the fault. This steep dip in the hanging wall only exists along the southernmost 5-10 km of the fault trace, from the point where the fault bends to the southeast just south of Chushan (Fig. 2-1), and is interpreted as folding in the hanging wall above the fault (Liu and Lee, 1998). The steep dip at this southern termination of the Chelungpu fault is not typical of the southern region in general, where the bedding typically dips  $20\text{-}40^\circ$  east, sub-parallel to the fault.

An  $\sim 60$  m wide region of intensely foliated shale with numerous (>20) gouge zones characterizes the fault in this region (Fig. 2-14). The gouge zones consist of sheared, foliated shale sub-parallel to bedding. Fault geometry is a footwall ramp, corresponding to the rest of the southern region.

### Southern Region: Peikou Stream

Ho and Chen (2000) discuss the Chelungpu fault properties from the Peikou Stream in the southern region (Fig. 2-1). Their observations indicate the fault zone consists of a 20 m shear zone with a dip of 25° east. These observations are consistent with a wide, diffuse shear zone and gently dipping (20-30°) fault in the southern region.

### Discussion

The 1999 rupture of the Chelungpu fault in Taiwan provides an ideal opportunity to study the structure of an active thrust fault, how this structure has evolved, and how the structure relates to displacement during a single earthquake event. Data collected in the northern region indicates that the fault is confined to a narrow (0.7-20 cm) gouge zone. The widening of the gouge towards the free surface could be due to a greater lithostatic pressure at 250 m depth than at the surface, that would act to confine the region that slip can occur. Within 50 m of the surface, the lithostatic load is quite low, and the fault can form a wider zone. Microstructural petrography and scanning electron microscopy indicate that slip was accommodated on extremely thin (50-300  $\mu\text{m}$ ) surfaces within the narrow, clay-rich, gouge zone. The narrow gouge was unique in the fault zone and only found aligned with the fault scarp, indicating that the gouge is located at the location of maximum slip and displacement during the earthquake. The subsurface slip values (9 m avg.) modeled by Ma et al. (2000) almost equal the net surface slip in the northern region, indicating that all slip was confined to the narrow zone that produced the fault scarps during the earthquake. Other fault structures identified in the northern region include an increase in fracture density near the fault gouge, and specifically the presence of large (.04-1.5 m width) brecciated zones. Smaller faults are apparent, but their slip appears to be inconsequential to the total displacement along the Chelungpu fault, based on fault scarp preservation and the accumulation of alluvium only in the footwall of the primary slip-surface. Otherwise, we would expect alluvium to accumulate in the footwall of any scarp with

significant historical displacement ( $>10$  m). The fault structure observed in the southern region consists of a large (20-150 m), diffuse shear zone that is very different from the localized zone observed in the northern region. There are abundant gouges and shear zones associated with the fault in the southern region, and slip is not localized in a single, narrow zone.

The Chelungpu fault is located along a footwall flat surface (Wang et al., 2000) in the Kueichulin Formation or Chinsui Shale to within 70 m of the surface in the northern region. In contrast, the southern region fault geometry contains a footwall ramp juxtaposing Kueichulin Formation or Chinsui Shale with unconsolidated conglomerate for at least 2 km in the near surface (J. C. Lee et al., 2001). Total displacement on the Chelungpu fault is estimated between 10-15 km since the late Pliocene, based on balancing of regional cross sections (Fig. 2-2) (Suppe, 1987; J. C. Lee et al., 2001). The bed-parallel fault geometry in the north may have facilitated slip localization by orienting slip along existing planes (bedding) of weakness. The flat east-dipping siltstone and flat-lying conglomerate in the south may have inhibited slip localization but increased high-frequency ground motion, by accommodating slip and earthquake energy in a wide zone.

Thrust faults near the surface can display either localized or diffuse fault zones (Carver and McCaig, 1996). Where slip is localized on a discrete, narrow zone, the surface displacements on an individual fault trace are usually large. Conversely, diffuse fault zones normally do not produce steep fault scarps, and generally form gentle, up-warped scarp surfaces, sometimes manifested in fault-related folding. The northern region of the Chelungpu fault behaves as a localized zone with a single, large-displacement surface offset and a discrete fault plane beneath the surface, as evidenced by the core logging and outcrop mapping. Fault related-folding was documented near Wufeng in the southern region, where the fault is a diffuse zone (J. C. Lee et al., 2001).

The dip of the Chelungpu fault to 250 m T.V.D. was determined by aligning the surface trace with fault gouge in the core. The dip of approximately  $52^\circ$  correlates well with the dip measured on the fault at Takeng ( $48^\circ$ ) and bedding in the hanging wall (avg.  $56^\circ \pm 20^\circ$ ) and footwall

(avg.  $53^{\circ} \pm 4^{\circ}$ ) near the Fengyuan drill site. Dips measured near the drill site on the scarp indicate a near-surface fault dip of  $50-80^{\circ}$  (Lin et al., 2001). Additional constraints on the dip of the fault are provided by data collected from a  $\sim 100$  m deep borehole (BH-2) approximately 0.5 km northwest of the Fengyuan drill site from this investigation. BH-2 was drilled by C.T. Lee from National Central University in Taiwan and showed that the fault has a dip of approximately  $60^{\circ}$  (Fig. 2-3, 2-5) (C. T. Lee, pers. comm.). Focal mechanisms for the main shock and immediate aftershocks for the 1999 earthquake constrain the fault dip between  $25-30^{\circ}$  east at 5-10 km depth (Fig. 2-2) (Hung and Suppe, 2000; Kao and Chen, 2000; Wang et al., 2000; Ma et al., 2001; Shin and Teng, 2001; Lee et al., 2002;). This value aligns with fault dips measured in the southern region, indicating a planar ramp from the epicenter to the surface (J. C. Lee, 2001). But the fault clearly steepens in the northern region, indicating there must be a bend in the fault.

Bedding in the northern region dips steeply ( $45-60^{\circ}$ ) parallel to the fault. This bedding was tilted into its current position prior to the 1999 fault rupture. This tilting may have occurred from folding in the hanging wall of a different, older strand of the Chelungpu fault, located  $< 1$  km west of the 9/21/99 trace (Fig 2a) (Ho and Chen, 2000). The most plausible explanation for the steep dip of bedding is that they were carried into their position above a listric footwall ramp of the older strand of the Chelungpu fault (Fig. 2-2a).

#### Brecciated Zone formation

The origin of the asymmetry in the damage zones is uncertain. GPS data indicates that 90% of the co-seismic movement during the earthquake occurred in the hanging wall (Yu et al., 2001; Lin et al., 2001), implying that the footwall was nearly fixed in an absolute reference frame. Brune (2001) has provided evidence for similar asymmetry of damage in thrust faults in southern California, due to larger ground-motion in the hanging wall than in the footwall. The damage would be mainly co-seismic or perhaps aftershock related.

Alternatively, the damage zone could be an inherited aspect of the fault zone, formed deeper in the crust where the hanging wall was deformed as it moved from a flat to a ramp. At a flat-ramp "corner," there would be localized shortening in the hanging wall. The brecciated zones that define the damaged areas may have formed in the hanging wall at such corners, and then would have been carried up the fault in the hanging wall during subsequent earthquakes. This process would also result in an asymmetric damage zone with the fault at the base of this damage zone.

A third alternative is that the brecciated zones form "passively" from fluid flow in areas of increased fracture density. Fluid flow through fractures causes disintegration of the host rock around the fractures. This widens the fractures, until the widening fracture network isolates clasts of the protolith (Regenfuss et al., 1999). These clasts "fall" into the fracture that is filled with a matrix composed of the disintegrating protolith rock. This hypothesis works well for the brecciated zones in the Chelungpu fault. Fracture density is increased near the fault, and the muddy matrix in the zones is compositionally indistinct from the protolith. There is evidence for fluid flow through the fractures, and there is no evidence for shearing in the brecciated zones. All these characteristics would work in this "passive" method of brecciated zone formation.

### Rupture Properties

Fault zones may exhibit variations in thickness and slip distribution along strike and down dip (Evans, 1990; Imber et al., 2001). Observations made from the Fengyuan core combined with surface observations from Takeng suggest slip localization on a narrow gouge zone to depths of at least 250 m. We suggest that extreme slip localization in the near surface reflects the presence of a narrow slip surface at depth, and that the fault is parallel to and guided by bedding. The presence of this very narrow (50-300  $\mu\text{m}$ ), clay rich, slip surface supports fault models (Kanamori and Heaton, 2000; Brodsky and Kanamori, 2001) in which narrow, lubricated fault zones may have reduced coefficients of dynamic friction during faulting. Slip constrained to such narrow slip planes may have reduced high-frequency energy radiation ( $>1$  Hz) during a large-magnitude earthquake, as occurred

during the 1999 event. The observations of high displacement and relatively low frequency ground motion along the northern region of the Chelungpu fault can therefore be explained by this fault structure.

Thin fault surfaces have been documented for other large-displacement thrusts, such as the Lewis thrust, Canada (see Price, 1988), the McConnell thrust, Canada, the Muddy Mountain thrust, Nevada, the Glarus thrust, Switzerland (Gretener, 1972, 1977), and the Keystone thrust, Nevada (Brock and Engelder, 1977). These observations and those described here indicate that the extremely narrow, "knife-edge" nature of these faults may extend from the surface to considerable depth.

Lithology variation along strike may have also contributed to the observed large displacement and strong ground-motion variations along the Chelungpu fault. Displacement in the northern region along a bedding plane between similar siltstone or shale lithologies would act as a relatively low-friction surface for slip. The result may be a "smooth," low-frequency rupture with large displacement. In contrast, displacement between flat-lying conglomerate and 30° dipping siltstone would act as a relatively high-friction surface, resulting in less displacement but higher-frequency ground motion. Therefore, lithology and structure controlled the rupture characteristics along the northern part of the Chelungpu fault during the 9/21/99 earthquake.

Slip on the Chelungpu fault was accommodated primarily on the narrow, sheared clay surface at the base of the largest brecciated zone in the drilled core. The surface displacements that almost equal the displacements inverted from the seismic models (Ma et al., 2001; W. S. Chen et al., 2001; Lin et al., 2001) support this conclusion. Narrow slip-surfaces have been documented along exhumed strike-slip fault zones (Chester and Chester, 1998), on in situ faults that slipped seismically (Gay and Ortlepp, 1979), and in naturally occurring thrust faults (Gretener, 1972, 1977; Brock and Engelder, 1977). These surfaces may form early in the growth of a fault system and accommodate much of the slip in a fault zone (Shipton and Cowie, 2001), or they may be the result of slip localization after the formation of the damaged zone (Brock and Engelder, 1977). Narrow slip zones are also consistent with thermodynamic models of co-seismic faulting events (Kanamori and Heaton,

2000; Brodsky and Kanamori, 2001). Factors such as structure and geometry are readily identifiable prior to rupture, and should be considered when determining earthquake hazard potential near active thrust faults. This investigation clearly demonstrates an association between a narrow, localized slip surface with a large-displacement surface rupture.

### Conclusions

By combining core logging, structural analysis, and field mapping, we have identified the different structures of the northern and southern regions of the Chelungpu fault. The northern region of the Chelungpu fault dips  $\sim 52^\circ$  to at least 250 m, and has a flat-on-flat geometry. The bed-parallel geometry has resulted in a narrow fault gouge where slip is localized in 50-300  $\mu\text{m}$  zones. The data presented in this paper suggest that the existence of a narrow slip-surface causes slip localization, large displacements and less high-frequency ground motion during an earthquake. High-frequency ground accelerations were 50-70% lower in the northern region than near the epicenter, but surface displacement was 200-300% greater, due to a narrow fault zone (Ma et al, 2001; Lin et al, 2001). The 25-35 $^\circ$  dip in the southern region, where the fault has a footwall ramp geometry, produced a more diffuse fault zone that produced less surface displacement, but more high-frequency ground motion. The data collected on the structure and rupture characteristics from the active Chelungpu thrust fault provides insight into fault processes that can be applied to studies from older, exhumed thrust faults, as well as help us understand the characteristics of active faulting.

### References

- Bekins, B., A. M. McCaffrey, and S. J. Dreiss (1994). Influence of kinetics on the smectite to illite transition in the Barbados accretionary prism, *J. Geophys. Res.* **99**, 18,147-18,158.



- Brock, W. G., and T. Engelder (1977). Deformation associated with the movement of the Muddy Mountain overthrust in the Buffington window, southeastern Nevada, *Geol. Soc. Amer. Bull.* **88**, 1667-1677.
- Brodsky, E. E., and H. Kanamori (2001). Elastohydrodynamic lubrication of faults, *J. Geophys. Res.* **106**, 16357-16374.
- Brune, J. N. (2001). Shattered rock and precarious rock evidence for strong asymmetry in ground motions during thrust faulting, *Bull. Seism. Soc. of Amer.* **91**, 441-447.
- Brune, J. N., and A. Anooshehpour (1998). A physical model of the effect of a shallow weak layer on strong ground motion for strike-slip ruptures, *Bull. Seism. Soc. of Amer.* **88**, 1070-1078.
- Caine, J. S., J. P. Evans, and C. B. Forster (1996). Fault zone architecture and permeability structure, *Geology* **24**, 1025-1028.
- Carver, G. A., and J. P. McCalpin, (1996). Paleoseismology of compressional and tectonic environments, in *Paleoseismology*, J. P. McCalpin (Editor), Academic Press, California, 183-270.
- Central Geological Survey (2002). Ground ruptures of the September 21, 1999 Chi-Chi earthquake (II), Ministry of Economic Affairs, Taipei, R.O.C., scale 1:50,000.
- Chang, H. C. (1994). The geological map and explanatory text of Tachia, Taiwan, Central Geol. Surv., Ministry of Economic Affairs, R.O.C., scale 1:50,000.
- Chang, S. L. (1971). Subsurface geologic study of the Taichung Basin, Taiwan, *Petrol. Geol. Taiwan* **8**, 21-45.
- Chen, C. H., H. C. Ho, K. S. Shea, W. Lo, W. H. Lin, H. C. Chang, C. S. Huang, C. S. Huang, C. W. Lin, G. H. Chen, C. N. Yang, and Y. H. Lee (2000). Geologic map of Taiwan, Central Geol. Surv., Ministry of Economic Affairs, R.O.C., scale 1:500,000.
- Chen, W. S., B. S. Huang, Y. G. Chen, Y. H. Lee, C. N. Yang, C. H. Lo, H. C. Chang, Q. C. Sung, N. W. Huang, C. C. Lin, S. H. Sung, and K. J. Lee (2001). 1999 Chi-Chi earthquake: a case study on the role of thrust-ramp structures for generating earthquakes, *Bull. Seismol. Soc. Am.* **91**, 986-994.

- Chen, Y. G., W. S. Chen, J. C. Lee, Y. H. Lee, C. T. Lee, H. C. Chang., and C. H. Lo (2001). Surface rupture of 1999 Chi-Chi earthquake yields insights on active tectonics of central Taiwan, *Bull. Seismol. Soc. Am.* **91**, 977-985.
- Chen, Y. G., W. S. Chen, Y. Wang, P. W. Lo, T. K. Liu, and J. C. Lee (2002). Geomorphic evidence for prior earthquakes: lessons from the 1999 Chichi earthquake in central Taiwan, *Geology* **30**, 171-174.
- Chester, F. M., and J. S Chester (1998). Ultracataclasite structure and friction processes of the Punchbowl fault, San Andreas system, California, *Tectonophysics* **295**, 199-221.
- Chester, F. M., and J. M. Logan(1986). Implications for mechanical properties of brittle faults from observations of the Punchbowl fault zone, California, *Pure and App. Geophys.* **124**, 79-196.
- Covey, M. (1984). Lithofacies analysis and basin reconstruction, Plio-Pleistocene western Taiwan foredeep, *Petrol. Geol. Taiwan*, **20**, 53-83.
- Dalguer, L. A., J. D. Irikura, J. D. Riera, and H. C. Chiu (2001). The importance of the dynamic source effects on strong ground motion during the 1999 Chi-Chi, Taiwan, earthquake: brief interpretation of the damage distribution on buildings, *Bull. Seismol. Soc. Am.* **91**, 1112-1127.
- Davis, D., J. Suppe, and F. A. Dahlen (1983). Mechanics of fold-and-thrust belts and accretionary wedges, *J. Geophys. Res.* **88**, 1153-1172.
- Evans, J. P. (1990). Thickness-displacement relationships for fault zones, *J. Struc. Geol.* **12**, 1061-1066.
- Gay, N. C., and W. D. Ortlepp (1979). Anatomy of a mining-induced fault zone, *Geol. Soc. Amer. Bull.* **90**, 47-58.
- Gretener, P. E. (1972). Thoughts on overthrust faulting in a layered sequence, *Bull. Can. Pet. Geol.* **20**, 583-607.
- Gretener, P. E. (1977). On the character of thrust faults with particular reference to the basal tongues, *Bull. Can. Petrol. Geol.* **25**, 110-122.

- Ho, H. C., and M. M. Chen (2000). The geologic map and explanatory text of Taichung, Taiwan, sheet 24, Central Geol. Surv., Ministry of Economic Affairs, R.O.C., scale 1:50,000.
- Hsieh, M. L., Y. H. Lee, T. S. Shih, S. T. Lu, and W. Y. Wu (2001). Could we have pre-located the northeastern portion of the 1999 Chi-Chi earthquake rupture using geological and geomorphic data? *Terr., Atm. and Oceanic Sci.* **12**, 461-484.
- Hung, J. H., and D. V. Wiltschko (1993). Structure and kinematics of arcuate thrust faults in the Miaoli-Cholan area of western Taiwan, *Petrol. Geol. Taiwan* **28**, 59-96.
- Hung, J. H., and J. Suppe (2000). Subsurface geometry of the Chelungpu fault and surface deformation style, *Int. Workshop Annual Commem. Chi-Chi Earthquake* **1**, 133-144.
- Hung, J. H., S. T. Huang, and J. C. Wu (2001). Lithofacies and biostratigraphy of the core from the boreholes drilled through the Chelungpu fault, in *meeting notes from the 2nd anniversary of the Chichi earthquake, September, 2001, Taiwan*, sponsored by International Continental Drilling Program and the International Symposium of Eastern Asian Tectonics.
- Imber J., R. E. Holdsworth, C. A. Butler, and R. A. Strachan (2001). A reappraisal of the Sibson-Scholz fault zone model; the nature of the frictional to viscous ("brittle-ductile") transition along a long-lived, crustal-scale fault, Outer Hebrides, Scotland, *Tectonics* **20**, 601-624.
- Kanamori, H., and T. H. Heaton (2000). Microscopic and macroscopic physics of earthquakes, in: geocomplexity and the physics of earthquakes, *Am. Geoph. Un. Mono.* **120**, 147-161.
- Kao, H., and W. P. Chen (2000). The Chi-Chi earthquake sequence: active, out-of-sequence thrust faulting in Taiwan, *Science* **288**, 2346-2349.
- Lee, J. C., H. T. Chu, J. Angelier, Y. C. Chan, J. C. Hu, C. Y. Lu, and R. J. Rau (2002). Geometry and structure of northern surface ruptures of the 1999 Mw=7.6 Chi-Chi, Taiwan earthquake: influence from inherited fold belt structures, *J. Struc. Geol.* **24**, 173-192.
- Lee, J. C., Y. G. Chen, K. Sieh, K. Mueller, W. S. Chen, H. T. Chu, Y. C. Chan, C. R. Rubin, and R. Yeats (2001). A vertical exposure of the 1999 surface rupture of the Chelungpu fault at Wufeng,

- western Taiwan: structural and paleoseismic implications for an active thrust fault, *Bull. Seismol. Soc. Am.* **91**, 914-929.
- Lee, Y. H., W. Y. Wu, T. S. Shih, S. T. Lu, M. L. Shieh, and H. C. Cheng (2001). Deformation characteristics of surface ruptures of the Chi-Chi earthquake, east of the Pifeng bridge, *Central Geol. Surv. Spec. Issue* **12**, 27-40 (in chinese).
- Liao, C.F., Hung J. H., and Lee, C. T. (2002). Analysis of clay minerals and fractures from cores of Chelungpu fault zone (abstract), in *Geol. Soc. of China, Annual Meeting*.
- Lin, A., T. Ouchi, A. Chen, and T. Maruyama (2001). Co-seismic displacements, folding and shortening structures along the Chelungpu surface rupture zone occurred during the 1999 Chi-Chi (Taiwan) earthquake, *Tectonophysics* **330**, 225-244.
- Lin, C. C., and 67 others (1999). Map of surface ruptures along the Chelungpu Fault during the Chi-Chi earthquake, Taiwan, Central Geologic Survey, Ministry of Economic Affairs, R.O.C., scale 1:25,000.
- Liu, H. C., and J. F. Lee (1998). The geological map and explanatory text of Yun Lin, Taiwan, Central Geol. Surv., Ministry of Economic Affairs, R.O.C., scale 1:50,000.
- Lo, W., L. C. Wu, and H. W. Chen (1999). The geological map and explanatory text of Kuohsing, Taiwan, Central Geol. Surv., Ministry of Economic Affairs, R.O.C., scale 1:50,000.
- Ma, K. F., E. E. Brodsky, J. Mori, C. Ji, T. R. A. Song, and H. Kanamori (2002). Evidence for fault lubrication during the 1999 Chi-Chi, Taiwan, earthquake ( $M_w$  7.6), *submitted*.
- Ma, K. F., J. Mori, S. J. Lee, and S. B. Yu (2001). Spatial and temporal distribution of slip for the the 1999 Chi-Chi, Taiwan, earthquake, *Bull. Seism. Soc. Amer.* **91**, 1069-1087.
- Ma, K. F., T. R. A. Song, S. J. Lee, and H. I. Wu (2000). Spatial slip distribution of the September 20, 1999, Chi-Chi, Taiwan, earthquake ( $M_w$  7.6) --Inverted from teleseismic data, *Geophys. Res. Lett.* **27**, 3417-3420.
- Morley, C. K. (1988). Out of sequence thrusts, *Tectonics* **7**, 539-561.

- Oglesby, D. D., R. J. Archuleta, and S. B. Nielson, (2000). The three-dimensional dynamics of dipping faults, *Bull. Seism. Soc. Am.* **90**, 616-628.
- Oglesby, D. D., and S. M. Day (2001). The effect of fault geometry on the 1999 Chi-Chi (Taiwan) earthquake, *Gephys. Res Let.* **28**, 1831-1834.
- Ohtani, T., K. Fujimoto, H. Ito, H. Tanaka, N. Tomida, and T. Higuchi (2000). Fault rocks and paleo-to-recent fluid characteristics from the borehole survey of the Nojima fault ruptured in the 1995 Kobe earthquake, Japan, *J. Geophys. Res.* **105**, 16161-16172.
- Price, R. A. (1988). The mechanical paradox of large overthrusts, *Geol. Soc. Amer. Bull.* **100**, 1898-1908.
- Regenfuss, S. M., J. M. Strickland, and J. D. Cooper (1999). Late Ordovician breccias in a Middle Ordovician orthoquartzite, southern Great Basin; evidence for unusual paleokarst, *Geol. Soc. Amer. Abstracts with Programs* **31**, 99.
- Seno, T., S. Stein, and A. Gripp (1993). A model for the motion of the Philippine sea plate consistent With NUVEL-1 and geological data, *J. Geophys. Res.* **98**, 17941-17948.
- Shin, T. C., and T. Teng (2001). An overview of the 1999 Chi-Chi earthquake, *Bull. Seism. Soc. Am.* **91**, 895-913.
- Shipton, Z. K. and P. A. Cowie (2001). Damage zone and slip-surface evolution over  $\mu\text{m}$  to km scales in high-porosity Navajo sandstone, Utah, *J. Stuc. Geol.* **23**, 1825-1844.
- Suppe, J. (1980). A retrodeformable cross section of northern Taiwan, *Proceed. Geol. Soc. China* **23**, 46-55.
- Suppe, J. (1987). The active Taiwan mountain belt in *Anatomy of Mountain Chains* (Princeton Univ Press, eds. Schaer, J. P. & Roger, J.) 277-293.
- Van der Pluijm, B. A., C. M Hall, P. J. Vrolijk, D. R. Pevear, and M. C. Covey (2001). The dating of shallow faults in the Earth's crust, *Nature* **412**, 172-175.
- Vrolijk, P., A. Fisher, and J. Gieskes (1991). Geochemical and geothermal evidence for fluid migration in the Barbados accretionary prism (ODP leg 110), *Geophys. Res. Letters* **18**, 947-950.

- Vrolijk, P. and B. A. Van der Pluijm (1999). Clay gouge, *J. Struc. Geol.* **21**, 1039-1048.
- Wald, D. J., and T. H. Heaton (1994). Spatial and temporal distribution of slip for the 1992 Landers, California, earthquake, *Bull. Seism. Soc. Am.* **84**, 668-691.
- Wang, C., T. H. Huang, I. C. Yen, S. L. Wang, and W. B. Cheng (2000). Tectonic environment of the 1999 Chi-Chi earthquake in central Taiwan and its aftershock sequence, *Terr., Atm. and Oceanic Sci.* **11**, 661-678.
- Yu, S. B., L. C. Kuo, Y. J. Hsu, H. H. Su, C. C. Lui, C. S. Hou, J. F. Lee, T. C. Lai, C. C. Liu, C. L. Liu, T. F. Tseng, C. S. Tsai, and T. C. Shin (2001). Preseismic deformation and coseismic displacements associated with the 1999 Chi-Chi, Taiwan, earthquake, *Bull. Seism. Soc. Amer.* **91**, 995-1012.

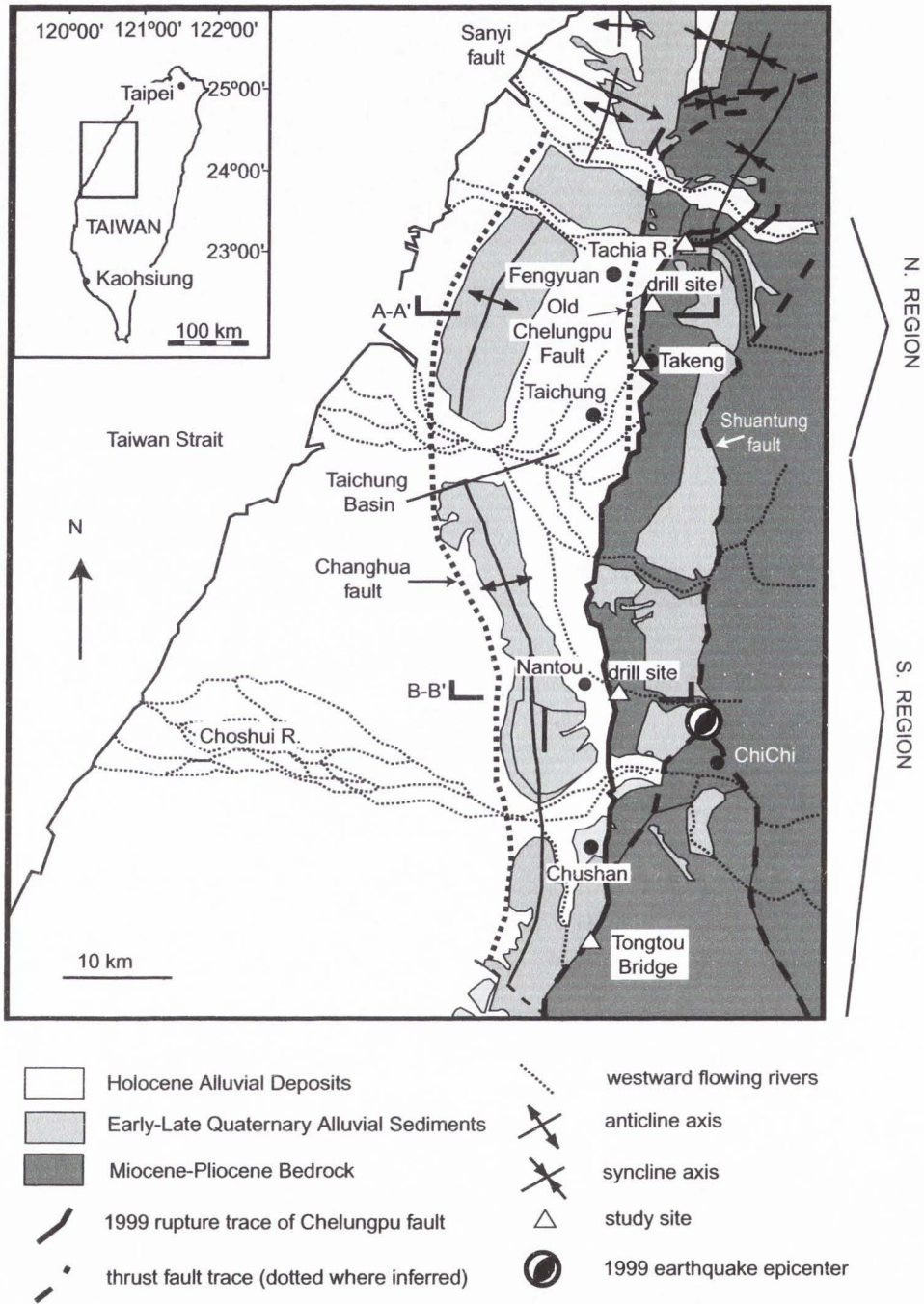


Figure 2-1. Location map of the Chelungpu fault rupture and generalized geologic map of the Chelungpu/Sanyi fault region. Mapping based off of C. H. Chen et al. (2000), Hsieh et al. (2001), and Y. G. Chen et al. (2002). Cross section A-A' and B-B' are indicated. Epicenter position from Shin and Teng (2001). All faults are west vergent thrust faults.

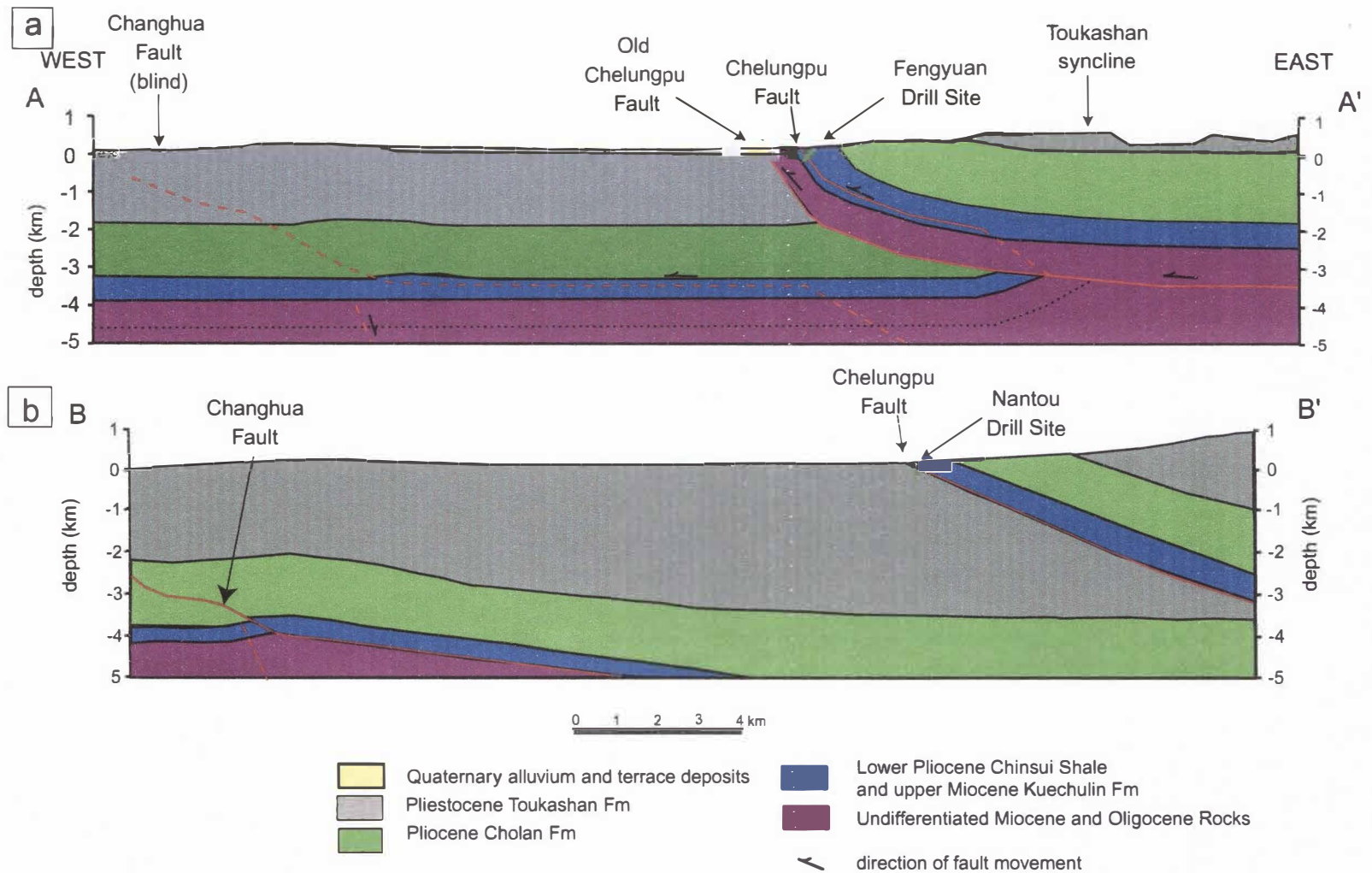


Figure 2-2. Cross-section A-A' (a) and B-B' (b) through the northern and southern regions of the Chelungpu fault. Drill holes are shown in green. The Chelungpu Fault indicates the 1999 rupture trace. The Old Chelungpu refers to the mapped trace that did not rupture during the 9/21/99 earthquake. Cross sections are based on field mapping, seismic data from Chang (1971) and mapping by Ho and Chen (2000) and Lo and Wu (1999). Section A-A' modified after Y. H. Lee et al. (2001).



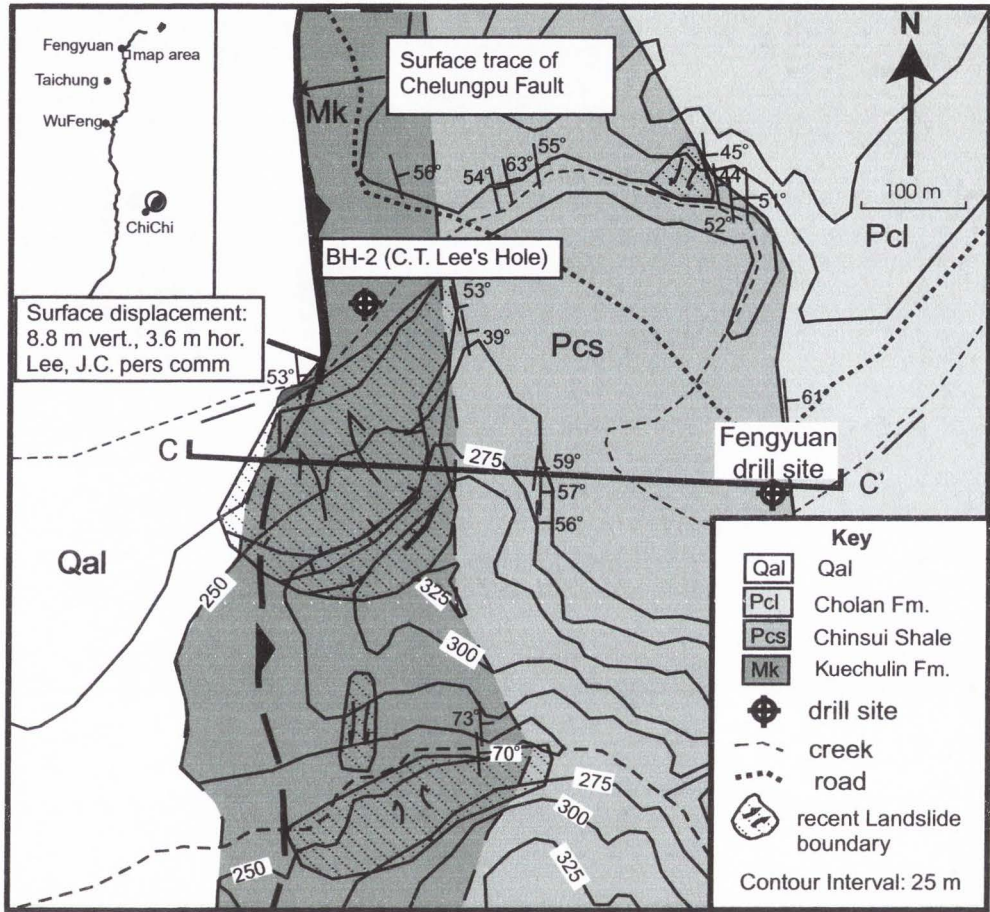


Figure 2-3. Geologic map of the northern drill site showing local stratigraphy. Inset sketch at upper right shows location of map on 90 km-long fault trace. Strike and dip of local outcrops are shown. Rupture trace of 1999 earthquake is the thick black line, dashed where approximate. Teeth are on the hanging wall. Local earthquake-induced landslides are also shown.

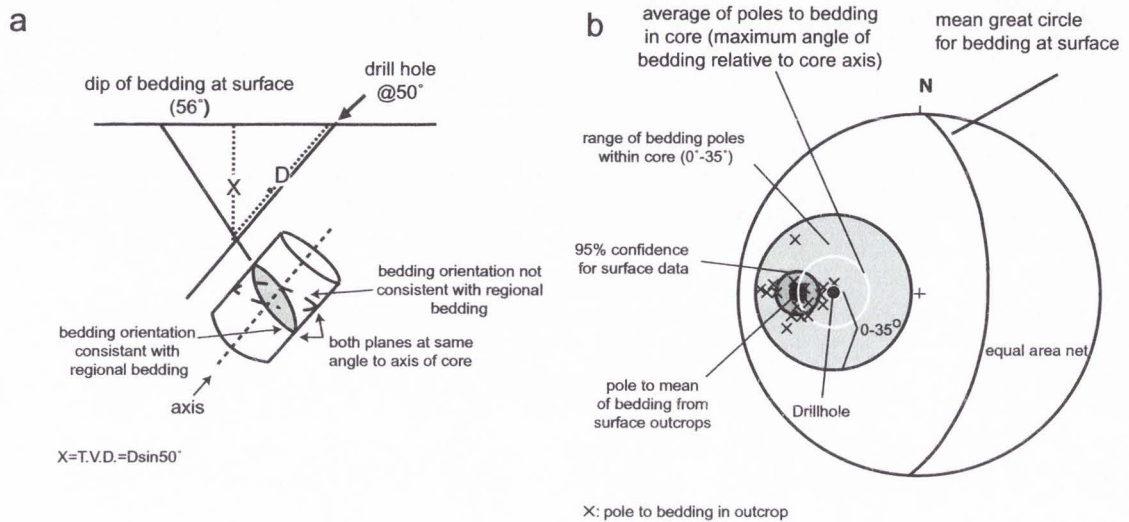


Figure 2-4. Determination of bedding dips within the core. a) Bedding angle ( $<90^\circ$ ) was measured relative to the core axis. Because strike of bedding is known from surface outcrops, and drilling was perpendicular to regional bedding strike, the bedding measured in the core represented 2 possible dips at the surface. The correct dip is determined (shaded ellipse) in the core by correlating with the surface outcrops. b) The stereonet shows the range of poles to bedding in the core as measured relative to the core axis ( $0\text{-}35^\circ$  shown by grey circle). Poles to bedding in outcrop (black x's) are plotted over the core results. The outcrop data aligns with the bedding in the core with the core oriented in only one, unique position. The average pole to bedding in the core (95% confidence range) indicates the core dips correlate only with steeply dipping bedding ( $\sim 56^\circ$ ), giving the bedding dip in the core. Surface outcrop dips ranged from  $39^\circ\text{-}76^\circ$  with an average of  $56^\circ$  and standard deviation of 9.8. Bedding in the core ranged from  $55^\circ\text{-}90^\circ$ , with an average of  $71^\circ$  and a standard deviation of  $7.8^\circ$ .

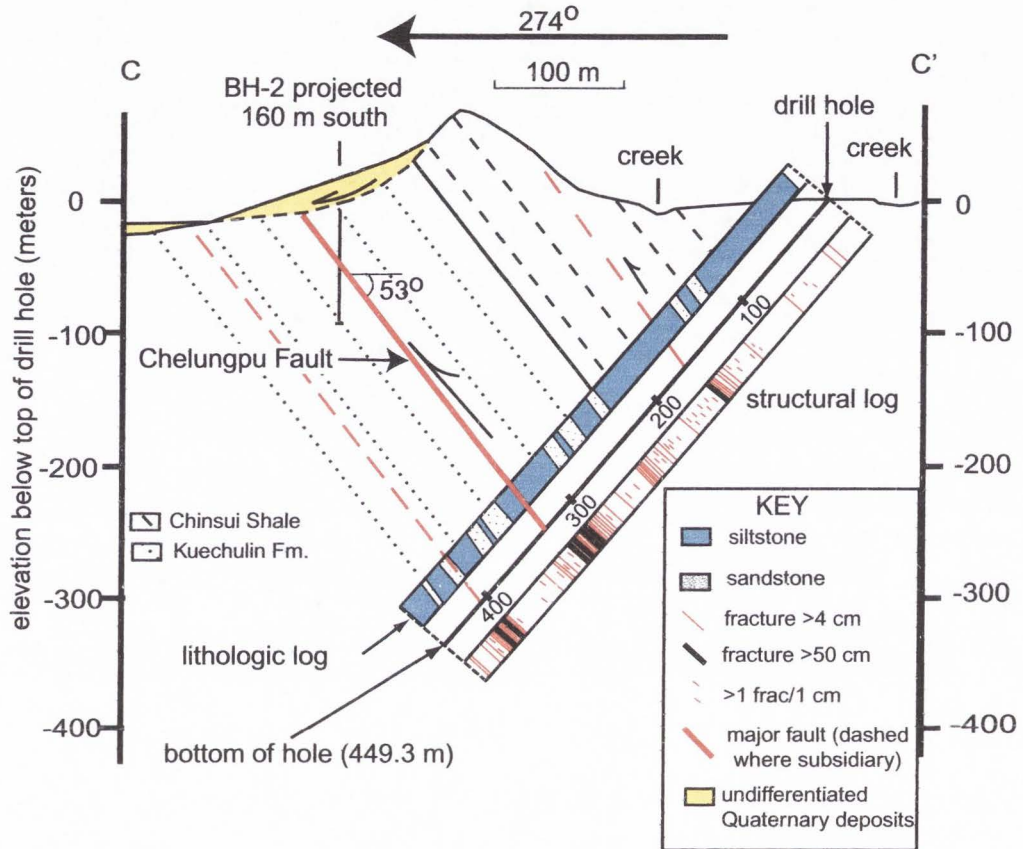


Figure 2-5. Cross section C-C' through the Fengyuan drill site. The structural log indicates the location of fractures within the core. The bold black lines in the structural log indicate fractures >50 cm in width. The thin red lines within the structural log indicate fractures >4 cm, and red dashes indicate zones of high fracture intensity (>1 fracture per 3 cm in core). These were extrapolated as subsidiary faults to the surface along bedding (dashed red lines). The primary rupture surface (bold red line) was aligned with the surface trace determined from structural contours on the local fault trace. The lithologic log shows the depth of siltstone and sandstone within the core at their appropriate dip determined from core and outcrop data. Solid black lines indicate approximate formation boundaries.

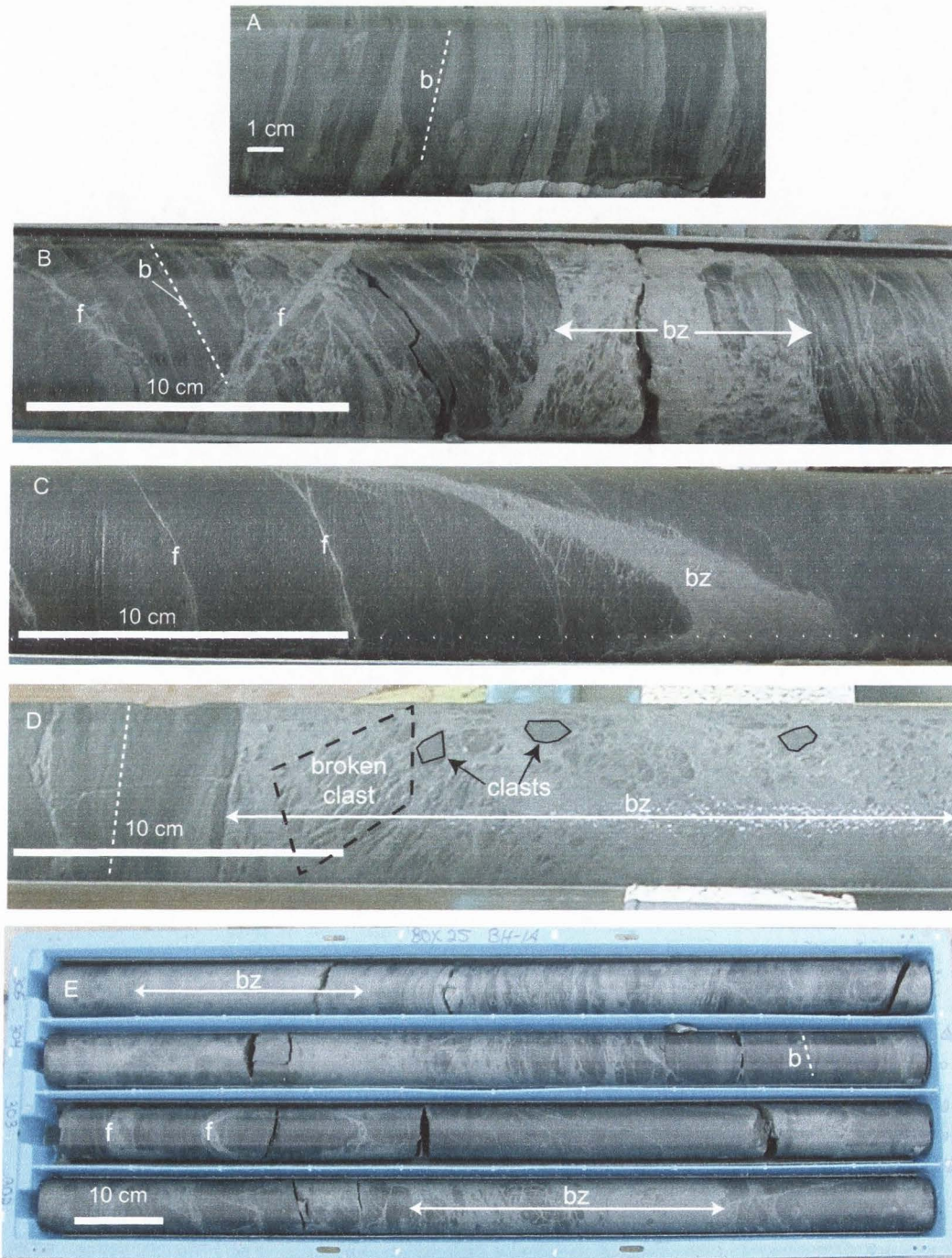


Figure 2-6. Typical core lithology and structures. b=bedding (dashed lines indicate dip in core), f=fracture, bz=brecciated zone, some clasts are outlined. A) Thinly laminated, bioturbated mudstone within the Cholan Fm at 234 m. B) Intense fracturing cutting beds in the Chinsui Shale at 221.5 m. C) Fractured Chinsui Shale at 283 m in core. D) Upper end of 30 cm brecciated zone from 239 m in core. The fracture contact is sharp and bed parallel. Clasts are outlined in black, and the dashed black line indicates a clast that is currently breaking up. E) Core box from 301-305 m in core, showing fractures, brecciated zones and undeformed Chinsui Shale.

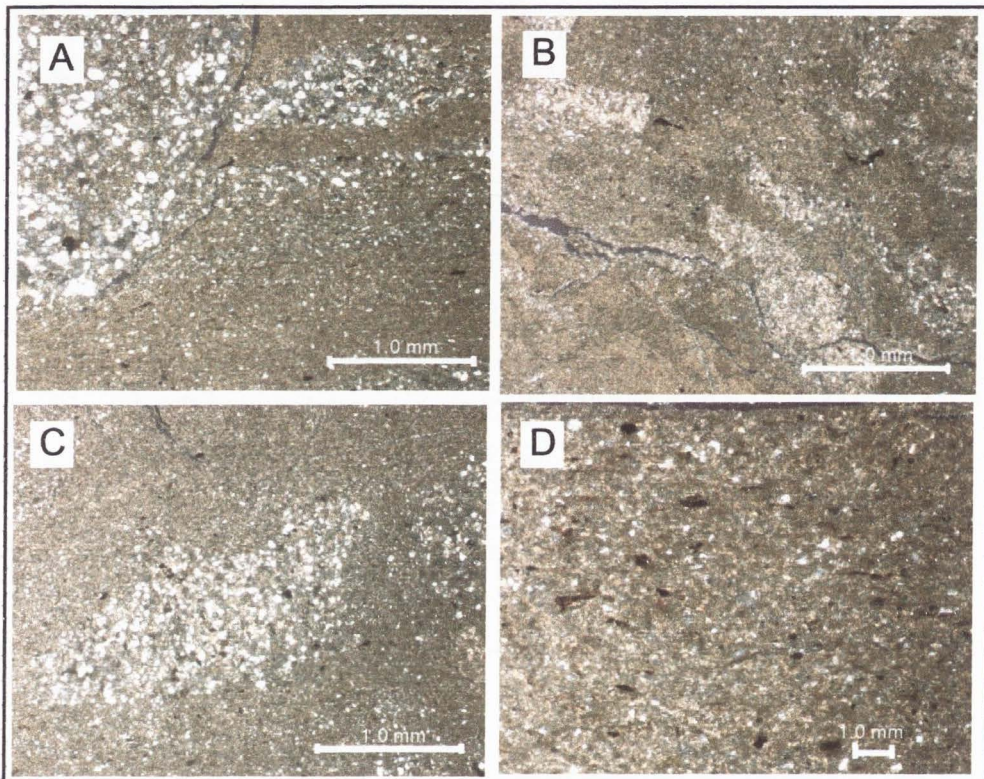


Figure 2-7. Thin section photomicrographs of core samples: a) Typical laminated mudstone and siltstone protolith of core. This is from the Kuechulin Formation at 328 m core depth, less than 2 m into the footwall of the primary rupture surface. There is very little deformation in the sample. Top of photo is up. The massive sandstone in the upper right is an undeformed, sand-filled burrow, and is lithologically typical of the sandstone encountered in the core. b) Breccia clasts in clay-rich mudstone matrix from a 6 cm fracture (brecciated zone) at 321.4 m. There are very few structural textures. c) Brecciated sandstone clast from a 28 cm brecciated zone at 322.55 m. Notice the lack of foliation in surrounding clay-rich matrix. d) Typical matrix in a 1.5 m brecciated zone at 326.45 m in the core, 20 cm above the primary rupture. The matrix consists of massive clay-rich mudstone with <15% silt clasts. Minor foliation but no sedimentary structures are apparent.

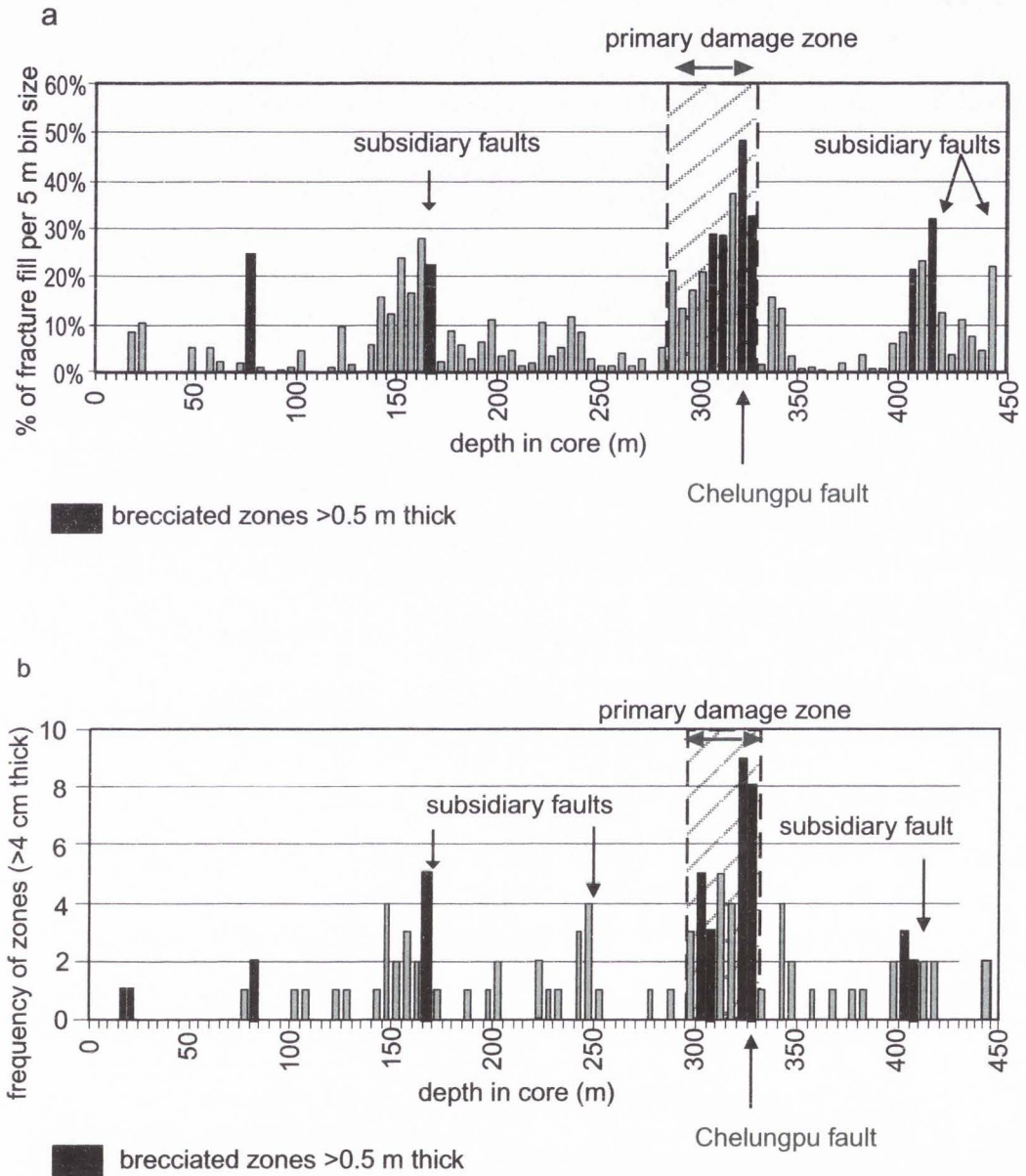


Figure 2-8. Histograms showing the fracture density in the core and their relation to the largest fractures. Location of primary rupture surface is indicated. a) Method A showing the percentage of fracture fill per 5 m core length. b) Method B showing the frequency of gouge zones > 4 cm thick within the core.

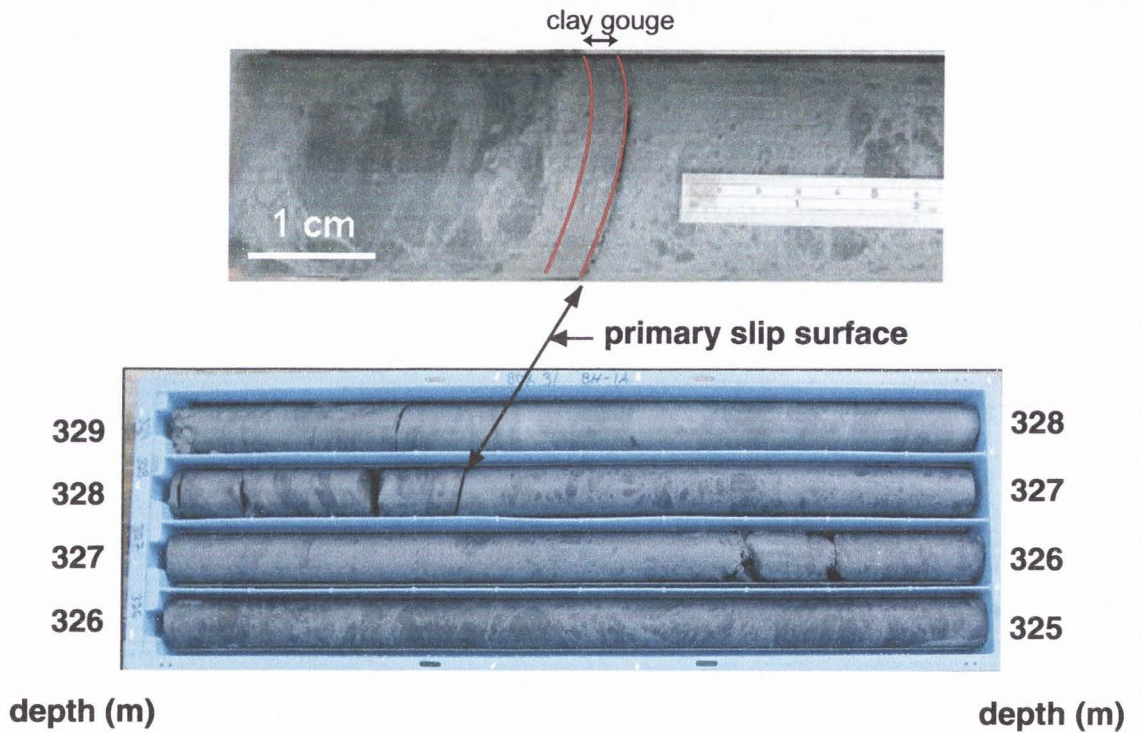


Figure 2-9. Photo of the core box from 325-329 m. The close up shows the primary slip surface of the 1999 rupture. This thin, 7-mm, dark gray, planar, sheared clay contained striations on the parted surface corresponding to surface displacement vectors.

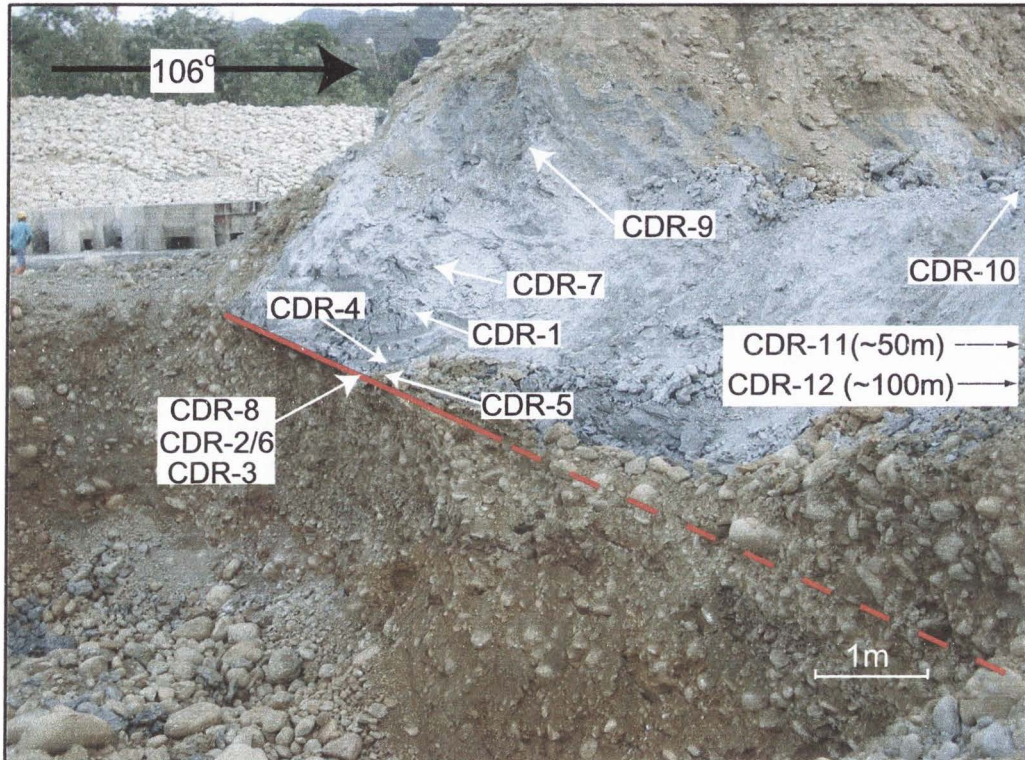


Figure 2-10. Oblique photo of the Chelungpu fault in the Tali River near Takeng City. The fault strikes  $300^{\circ}$  and dips  $48^{\circ}$  east. Pliocene or Miocene siltstone and mudstone (probably Chinsui Shale or Kuechulin Fm.) placed over Quaternary alluvial deposits. Sample locations are indicated. Siltstone within 20 m of the fault is intensely fractured and determined to be the damage zone related to the primary rupture trace. Fault gouge is 20 cm thick and shown as the red line on the photo, dashed where inferred. This gouge was unique in the 200 m long outcrop.



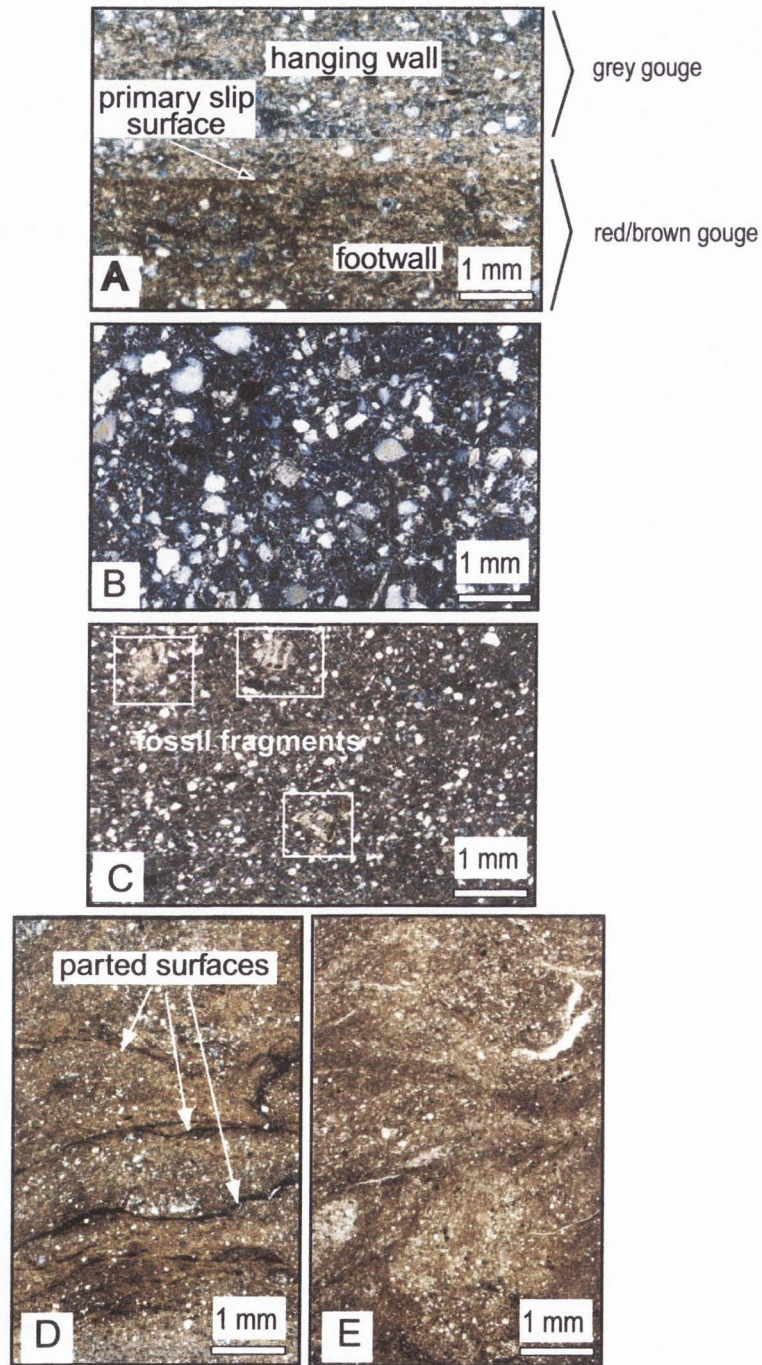


Figure 2-11. Cross-polarized photomicrographs from the 1999 rupture surface of the Chelungpu fault and hanging wall rocks. Sample locations are shown in Figure 2-10. A) The 1999 rupture surface, CDR-8, with hanging wall siltstone and footwall Quaternary alluvial deposit. The trace of the 1999 rupture is a 1-2 mm thick horizon in the center of the photo. B) Protolith sample CDR-11, 55 m from the slip surface shows texturally mature Pliocene siltstone with no evidence of deformation. C) Hanging wall sample CDR-5, from 20 cm above the slip-surface exhibits a faint, fault-parallel foliation and undeformed foraminiferid fragments. D) Sample CDR-2/6, 5 cm above slip-surface with narrow faults marked by very fine grained dark horizons. E) Foliated fabrics from sample CDR-8 of clay gouge adjacent to the slip-surface.

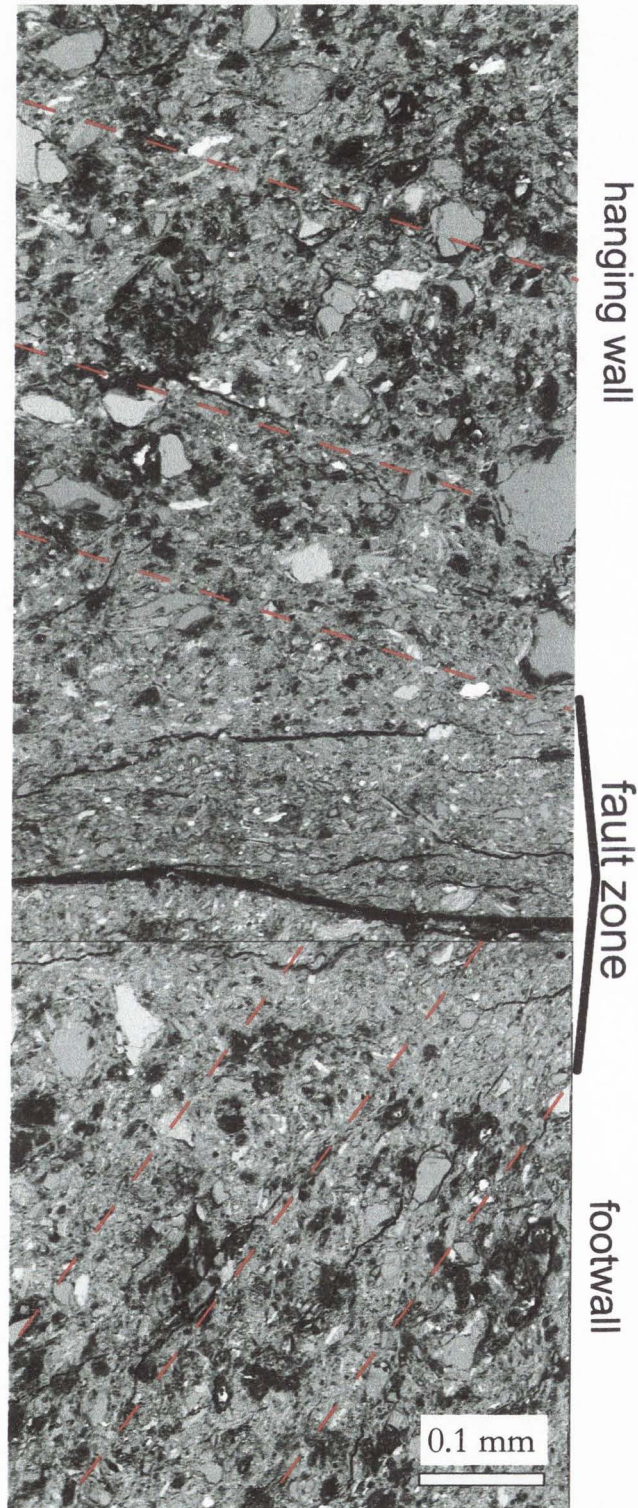


Figure 2-12. Scanning electron microscope image of the Chelungpu fault slip-surface from sample CDR-8. Intra- and intergranular fractures and a random fabric characterize the fault zone, whereas rocks in the hanging wall and footwall have a well-defined clay-rich foliation (dashed red lines). Sense of shear is unknown, but probably oblique with hanging wall to left.

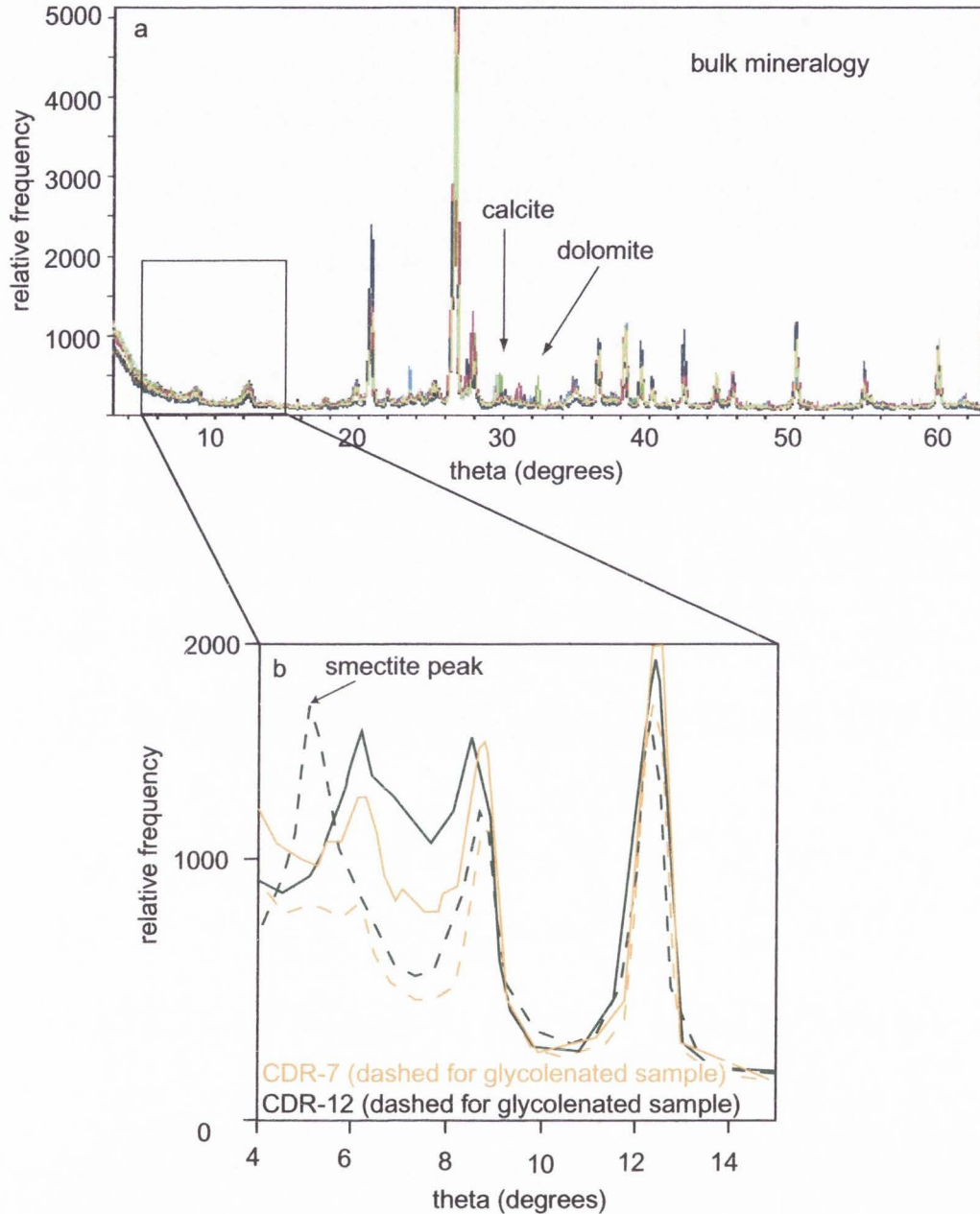


Figure 2-13. XRD analysis of samples from the Takeng fault outcrop. a) Bulk mineralogy of all samples collected in a 100 m transect through the hanging wall into the fault. Sample locations are shown on Figure 2-10. Analyses indicates the bulk mineralogy of the samples remains the same along a transect into the fault zone. b) Close-up of clay mineralogy for samples CDR-7 (~1 m from fault gouge) and CDR-12 (~100 m from fault gouge). This shows that smectite is a dominant clay mineral in the protolith, but smectite is not apparent in the samples near the fault.

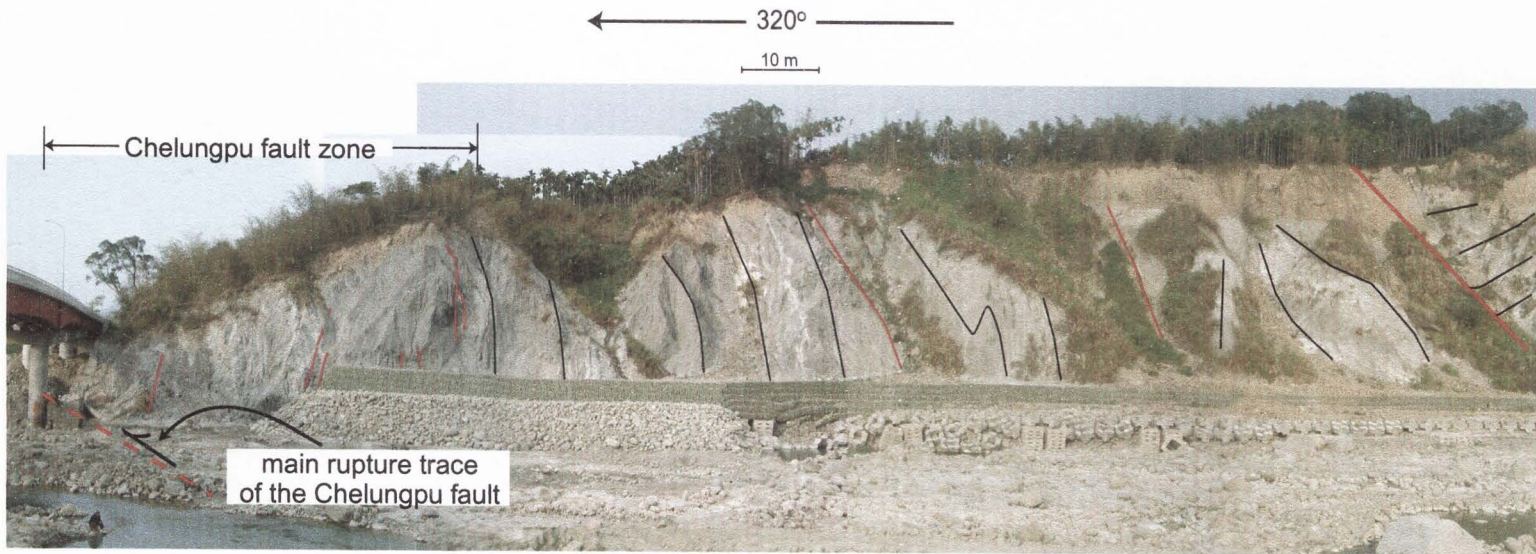


Figure 2-14. Oblique view of Chelungpu fault outcrop exposure in the Chingshui River at the Tungtou Bridge. Red lines indicate fault gouge zones, 10-50 cm-thick (dashed where inferred). Black lines indicate approximate bedding traces. The Chelungpu fault is dashed beneath the Tungtou bridge on the right. Bedding is indistinguishable in the Chelungpu fault zone. This zone consists of foliated shale and many gouge zones. Bedding southeast of the fault zone consists of the Kuechulin Fm. (Liu and Lee, 1998), generally dipping steeply southeast and is folded in places. Photo taken towards northeast.

## CHAPTER 3

GEOMETRIC EVOLUTION OF THE SANYI/CHELUNGPU FAULT  
AND THE EFFECTS OF RAMPS ON FAULT STRUCTURE

## Abstract

Investigation into the Chelungpu/Sanyi fault in central Taiwan indicates that its geometry changes from a footwall ramp geometry in the Sanyi and southern Chelungpu regions, to a footwall flat, bed-parallel geometry in the northern Chelungpu region. Deformation in fault rocks and stratigraphic offset indicate that in the northern region, where the fault is bed parallel, the Chelungpu fault is young (50-100 ka) whereas in the southern region the fault is ~1 Ma old. The northern-most part of the Chelungpu/Sanyi fault system consists of the Sanyi fault. The Sanyi fault dips ~20° east, north of the Tachia River, and ~50° east south of the Tachia River. The Sanyi fault has a ramp geometry and places east-dipping Miocene and Pliocene siltstone and shale over >1500 m of Quaternary sandstone and conglomerate. The Chelungpu fault northern region makes up the middle section of the Chelungpu/Sanyi fault system, and dips ~50° east but flattens to ~20° at depth. Terraces ~46 ka old in the hanging wall, uplifted 200 m above the correlative terraces in the footwall, attest to rapid slip on the Chelungpu fault. These relations suggest that active faulting has migrated into the hanging wall where it ruptured along fault-parallel, 40-60°, east-dipping bedding planes where the frictional resistance was less. The southern region of the Chelungpu fault is an ~30°, east-dipping, planar fault that places Pliocene Chinsui Shale over >2 km of Quaternary Toukoshan Formation. The northern region of the Chelungpu fault ruptured with the southern region during the 9/21/99 earthquake. Though the lithology, age and ramp geometry are the same in the southern Chelungpu region as in the Sanyi region, the fault did not migrate into its hanging wall in the southern

region. This is because the  $\sim 30^\circ$  dip provided the optimum angle for thrust-fault rupture, and therefore the frictional resistance did not overcome the resistance in the hanging wall. This investigation of the Chelungpu/Sanyi fault system indicates that hindward migration of an individual fault can occur simultaneous with foreland-progression of the fold-and-thrust belt. The implications of hindward migration into the hanging wall are a different fault geometry and fault width along strike, as observed on the Chelungpu fault.

### Introduction

The Chelungpu fault ruptured in a  $M_w$  7.6 earthquake on September 21, 1999. The earthquake produced a 90 km long rupture with vertical displacement up to 12 m (Y. H. Lee et al., 2001). The rupture displayed primarily thrust motion with oblique displacement at the northern and southern ends of the rupture (Lin et al., 2001). Though the 90 km long rupture was fairly continuous along the base of the foothills, where it separated the foothills from the Taichung basin to the west (Fig. 3-1), the rupture characteristics and fault structure varied significantly along strike. Investigation into the fault structure indicates a different geometry in the northern Chelungpu region than in the southern Chelungpu region (Fig. 3-2). The northern region ruptured along steep,  $50-80^\circ$  bedding to very near ( $<70$  m) the surface (chapter 2; Lin et al., 2001; Y. H. Lee, pers. comm., 2002). In contrast, the southern region ruptured along a  $20-30^\circ$ , east-dipping, footwall ramp that places east-dipping, Pliocene siltstone and shale above flat-lying, Quaternary deposits for at least 2 km at the surface (J. C. Lee et al., 2001).

The Chelungpu/Sanyi fault system includes the southern Chelungpu region, the northern Chelungpu region, and the Sanyi regions. The 9/21/99 rupture and recent geologic investigations suggest that the northern Chelungpu fault is an out-of-sequence thrust fault behind the Sanyi fault. The Sanyi fault has been abandoned, and the northern

Chelungpu fault is now continuous with the southern Chelungpu fault. This investigation addresses the question as to how and when these different fault regions developed, in hopes to provide insight into the development of active fold-and-thrust belts.

The different geometry in the northern region is attributed to eastward (hinterland) migration of the active fault segment (northern Chelungpu fault). The Sanyi fault and southern Chelungpu were probably one continuous fault strand for some time during the fault's history (Hung and Wiltschko, 1993; Meng, 1963). The 1999 rupture on the Chelungpu fault indicates that the active fault has migrated east, into the hanging wall of the older Sanyi thrust, leaving the Sanyi fault as a dormant fault strand (Y. G. Chen et al., 2001). South of the Tachia River the Sanyi fault trace is observed parallel to but approximately 1 km west of the northern Chelungpu fault (Fig. 3-1) (Ho and Chen, 2000). North of the Tachia River, the Sanyi fault is mostly obscured by Quaternary alluvium, but does outcrop at some locations where it places middle Miocene sandstone and shale over Quaternary sandstone and conglomerate (Hung and Wiltschko, 1993).

Structural properties of the Chelungpu fault addressed in this investigation include the geometry (ramp or flat), dip, and width of fault features (including gouge, fracture zones, brecciated zones). Analysis of the Chelungpu fault was undertaken through surface mapping, drilling through the fault zone, and review of previous work (Chang, 1971; Y. G. Chen et al., 2001; Hung and Wiltschko, 1993; J. C. Lee, 2001; Wang et al., 2000).

### Regional Geology

Taiwan has formed as the result of oblique convergence of the Philippine Sea Plate and Eurasian Plate since the early Pliocene (Chi et al., 1981; Hsieh, 1990). Plate convergence has resulted in structural thickening of sediments along the plate boundary and development of a fold-and-thrust belt in Taiwan. This fold-and-thrust belt is manifested in the southward propagating uplift of the mountains in Taiwan (Suppe, 1987). The Western Foothills consist

of Miocene through Quaternary sedimentary rocks accreted from the Eurasian margin that form the active fold-and-thrust belt in Taiwan (Ho, 1986; Chen et al., 2001).

The Chelungpu/Sanyi fault system comprises the middle of three, north-south striking, west-vergent thrust faults in the Western Foothills geologic province of central-western Taiwan (Fig. 3-2). The system runs for approximately 100 km N-NE along the margin of the foothills and the Taichung basin (Figs. 3-1, 3-2). The Shuangtung fault and blind Changhua fault roughly parallel the Chelungpu/Sanyi fault to the east and west, respectively (Fig. 3-2). These three faults make-up the westward-propagating toe of the accretionary wedge created from oblique convergence of the Philippine sea plate with the Eurasian continent (Davis et al., 1983; Ho, 1986).

The Chelungpu/Sanyi fault system can be divided into 3 regions based on structural properties and rupture properties from the 9-21-99 earthquake. These sections are 1) the Sanyi region, 2) the northern region of the Chelungpu fault, and 3) the southern region of the Chelungpu fault (Fig. 3-2). The northern Chelungpu fault is located in the hanging wall of the Sanyi thrust north of Taichung (Fig. 3-2, 3-3). The Sanyi and southern Chelungpu faults have total displacements of at least 8 km (Hung and Wiltschko, 1994; J. C. Lee et al., 2001), and cut a thick (>1500 m) section of Quaternary Toukoshan Formation (Fig.3-3).

### Sanyi Region

The Sanyi region of the Chelungpu/Sanyi fault system was described by Hung and Wiltschko (1993). The fault strikes N-NE and turns NE at its northern terminus, where slip is transferred to a series of north-south striking folds. The northern termination of the Sanyi fault consists of a complicated zone with a transverse ramp where fault displacement is decreased and shortening is accommodated by folding to the north (Hung and Wiltschko, 1993). North of the Tachia River, the fault dips 18-22° east. South of the Tachia River the fault steepens to >45° towards the surface in a listric fashion (Chang, 1994). Large



wavelength folding is evident in the footwall formations, but the Sanyi thrust fault nevertheless cuts up section along a footwall ramp in the Sanyi region (Fig. 3-4).

The Sanyi fault consists of a hanging wall flat (bed-parallel) over a footwall ramp that places late Miocene siltstone and shale (Tungkeng Fm. and Kuechulin Fm.) above Quaternary Toukashan Formation and Pliocene Cholan Formation in the footwall (Fig. 3-4) (Hung and Wiltschko, 1993). The Toukoshan Formation is a 1-2 km thick package of terrestrial sandstone and conglomerates (W. S. Chen et al., 2001). Paleomagnetic analysis of the Toukoshan Formation indicates that the lower section was deposited starting at approximately 1.1 ma (see Chen et al., 2001). Deposition of the Toukoshan Formation is interpreted to coincide with uplift in the Western Foothills fold-and-thrust belt. Therefore, the base of the Toukoshan Formation may be an approximate age for the initiation of the Western Foothills fold-and-thrust belt. We can place a maximum age of faulting on the Sanyi fault at  $\sim 1.1$  Ma. But the age is probably younger since the Sanyi fault most-likely initiated after the easternmost Shuangtung fault (Fig. 3-2) in an in-sequence development of the fold-and-thrust belt (Davis et al., 1983). There has been no historic activity on the Sanyi fault, but lateritic terraces north of the Tachia River are offset, indicating the fault has been active since  $\sim 46,000$  years before present (y.b.p.) (Fig. 3-2) (Liu, 1990).

#### Northern Region of the Chelungpu Fault

The northern region of the Chelungpu fault dips  $45-60^\circ$  east along a bed-parallel surface. This was determined by drilling through the fault at 250 m vertical depth, field mapping (Chapter 2), and seismic surveys (Wang et al., 2000) across the fault (Fig. 3-3). The hanging wall of the 1999 rupture trace consists of the Pliocene Cholan Formation, Pliocene Chinsui Shale (strike:  $0-45^\circ$ , dip:  $35-70^\circ$ E), and Miocene Kuechulin Formation sandstone and shale (Fig. 3-3). Bedding becomes gentler ( $20-40^\circ$ ) eastward away from the fault trace towards the axis of the Toukashan syncline (Lo et al., 1999), suggesting the fault follows

bedding of the syncline flank. The footwall consists of the Miocene Kueichulin Formation and the Pliocene Chinsui Shale, covered by a thin veneer (<100 m) of Quaternary alluvial deposits (Y. H. Lee, personal communication, 2001) (Fig. 3-3). Total displacement on the Chelungpu fault in the northern region is unknown, but is not more than 500 m based on the lack of Quaternary deposits in the footwall, and the relatively undeformed state of the protolith rocks surrounding the fault. Lateritic terrace surfaces can be correlated across the fault, from the top of the hanging wall to the top of the footwall. If this terrace surface represents the pre-faulting surface, then the age of the terrace provides a maximum age on the fault of ~46,000 years before present (y.b.p.) (Liu, 1990). The northern Chelungpu appears to be much younger than the southern Chelungpu or the Sanyi regions, based on relatively little deformation around the fault zone, and very little deposition in the footwall, indicating little total displacement. The Chelungpu fault may therefore be a young strand in the hanging wall of the older Sanyi thrust fault.

#### Southern Region of the Chelungpu Fault

The southern region of the Chelungpu fault shows a distinctly different structure than the northern region, but a similar structure to that of the Sanyi region. The fault in the southern region dips 30° east in the near surface (Y. G. Chen et al., 2001), and has a footwall ramp geometry that cuts across relatively horizontal beds of Pleistocene and Pliocene stratigraphy in the footwall (Fig. 3-5). Bedding in the hanging wall dips 20-36° east (Chapter 2), indicating a bed parallel, hanging wall flat geometry (Fig. 3-5) (Chang, 1971; Wang et al., 2000). Quaternary deposits of the Toukashan Formation in the footwall are estimated at approximately 2000-3000 m thick in this region (Chang, 1971; J. C. Lee et al., 2001). This suggests that the fault juxtaposes two different lithologies for a significant portion of its rupture length (2-4 km), and the rupture does not follow pre-existing bedding planes in the footwall, at least in the near surface (< 2 km).

## Geomorphology

Fluvial terraces can be used as geomorphic indicators that can provide evidence for recent faulting and uplift along the Chelungpu fault (Chen et al., 2002; Hsieh et al., 2001; Knuepfer and Long, 1996). This study will attempt to use relative terrace heights and ages, when known, to infer when fault activity occurred and the rate of uplift in different regions of the Chelungpu/Sanyi fault system. Correlation of terraces across the fault can provide maximum ages for fault activity, and possibly provide insight into when a new strand initiated in relation to an older strand.

The Chelungpu/Sanyi fault system contains many more terrace levels in the hanging wall than the footwall (Chen et al., 2001; Hsieh et al., 2001). Hsieh et al. (2001) relate the occurrence of multiple terrace levels in the hanging wall and not the footwall to rapid uplift in the hanging wall, causing base-level to drop in the footwall for rivers flowing across the fault. The rivers then quickly incise and abandon older terrace surfaces in the hanging wall.

Fault scarps can be traced through different terraces, providing maximum ages for the rupture, given that the terrace age is known. Scarps through terraces along the Chelungpu/Sanyi fault are all oriented north-south, parallel to the strike of the fault, and perpendicular to the east-west flow direction of the rivers. This indicates the scarps are tectonic (fault scarps) and not fluvial terrace risers, which would parallel the axis of the rivers (Hsieh et al., 2001).

Terraces in the Sanyi region are best described from the Taan River, 3-4 km north of the Tachia River, where the northern region of the Chelungpu bends towards the east (Fig. 3-2). Five to seven terrace levels are present, with five of these terraces containing lateritic soil horizons. The lateritized terraces range from 80 to 180 m above river level (Fig. 3-6) (Hsieh et al., 2001). These lateritic terraces are fill terraces up to 50 m in thickness (Fig. 3-7). The most prominent lateritic terrace is offset by a 50 m fault scarp trending NE (Hsieh

et al., 2001), and this scarp is interpreted as the Sanyi fault. The laterized terrace in the footwall dips gently downstream, whereas the terraces in the hanging wall are inclined southward perpendicular to the west-flowing Taan river. The presence of scarps cutting the terrace indicates that the fault has been relatively active since terrace formation.

Terrace levels in the northern region of the Chelungpu fault are best observed near the Tachia river, where the hanging wall was uplifted up to 12 m during the 1999 earthquake (Y. H. Lee et al., 2001). Twelve terrace levels have been identified in this area on the hanging wall side of the fault, whereas only one terrace is identified in the footwall (Hseih et al., 2001). Eight of these terraces are laterized, and range from 80 to 350 m above river level (Fig. 3-6). The lateritic terraces are fill terraces, and are preserved above an angular unconformity with the Cholan Formation (Fig. 3-7).

The southern region of the Chelungpu fault contains multiple terraces in the hanging wall, but only 1-2 terrace levels in the footwall of the fault. Chen et al. (2002) describe 4 and 5 terrace levels from 2 river locations respectively in the southern region. These terraces are truncated on their western edge by a fault scarp from the Chelungpu fault. These terraces are strath terraces that overlie folded bedrock in the hanging wall.

Soil development in terraces can be used to correlate surfaces (Birkeland, 1999). Lateritic terraces in Taiwan have been dated using radiocarbon dating, and provide a useful marker horizon to bracket ages on faulting. The lateritic terraces are distinctively reddish (Fig. 3-7) whereas other terraces in Taiwan are grayish and have less soil development (this study). Lateritic soil horizons are interpreted as developed over long periods of time under stable conditions where weathering is intense (Birkeland, 1999). Lateritic terraces have been dated in the northern part of the island near Taipei, 75 km north of the northern region of the Chelungpu fault, between 37,600-46,800 y.b.p. (Liu, 1990), and are generally assumed to be older than 30,000 years before present in Taiwan (Hseih et al., 2001). Though dating of these terraces is difficult within the coarse-grained, high-energy fluvial deposits, we feel

confident that a general correlation may be made based on soil development within these terraces. Therefore, the lateritic terraces observed in the Taichung region of Taiwan are considered to have ages similar to those observed near Taipei. The climatic variation is minimal between these areas, and the topography is similar, indicating similar weathering processes are probably taking place in both regions.

Lateritic terraces are preserved sporadically within the foreland basin coastal plain of Taiwan, generally on the west-side of the Chelungpu/Sanyi fault surface. Terraces in the hanging wall are 350 m above the river level while the maximum elevation for these terraces in the footwall is ~150 m above river level (Fig. 3-6). Correlation of lateritic terraces across the fault provides a minimum offset since the footwall has been uplifting due to displacement on the Changhua fault (Mouthereau et al., 1999). This difference in terrace elevation is interpreted to be caused by uplift along the Chelungpu fault, and indicates at least 200 m of uplift in the last ~40,000 years, or approximately 5 mm/yr vertical uplift rate. This is similar to the vertical uplift rate of 5-7 mm/yr calculated for the Chelungpu fault near in the southern region (J. C. Lee et al., 2001).

Lateritic terraces are rarely preserved in the hanging wall in the southern region of the Chelungpu fault (Fig. 3-2) (Chen et al., 2000). This is likely due to continual uplift in the southern region along the Chelungpu fault that caused the terraces to be continually eroded from the hanging wall, burying the terraces in the footwall. Lateritic terrace surfaces are well preserved, however, in the footwall above the Pakuashan and Tatushan anticlines a few kilometers west of the fault (Fig. 3-2). This is due to uplift of these anticlines in the hanging wall of the Changhua thrust since approximately 0.5 Ma (Mouthereau, et al., 1999). The anticline provides accommodation space in the Taichung Basin for sediment eroding from the Chelungpu fault hanging wall. The lateritic terraces are simultaneously buried in the Taichung Basin and preserved above the anticline west of the Chelungpu fault, resulting in preservation of these terraces only on the crest of the Pakuashan and Tatushan anticlines.

Lateritic terraces are preserved in the northern region because the uplift has been fast and recent. The process of fault migration into the hanging wall of the Sanyi fault may have occurred over a period of time, most likely propagating northward from the southern region. Therefore, the Chelungpu fault would become progressively younger to the north, implying the uplift has been most recent in the far northern end of the Chelungpu fault. Deformation of fault rocks is least at the northern tip of the fault in the Tachia River, and the fault gouge becomes narrower towards the north (Chapter 2). This is also supported by the largest, most intact, uplifted, lateritic terraces found in the extreme northern tip of the Chelungpu fault. Rapid uplift on a new, very young fault is therefore the reason for the terrace preservation at high elevations above stream level in the hanging wall. Without recent, rapid uplift the terraces would not be preserved and would have eroded away in the tropical Taiwan climate, as probably occurred in the southern region.

North of the Chelungpu fault along the Sanyi fault region, lateritic terraces are preserved in both the hanging wall and footwall (Fig 3-2) (Chang, 1994). Terrace offset across the fault is minimal (<50 m) (Hsieh et al., 2001), indicating less activity (25%) on the Sanyi fault than the northern region of the Chelungpu fault since 46 ka. This is strong evidence for minimal activity on this fault segment. With significant uplift on the Sanyi fault, the lateritic terraces in the footwall would be buried with Holocene alluvium in a similar manner to the Taichung basin, where correlative terrace surfaces were surely formed, but subsequently buried by sediment from the continually uplifting Western Foothills. The lateritic terraces should also be found with similar elevations to the terraces in the northern Chelungpu region. The lack of buried footwall terraces and low hanging wall terrace elevations is evidence for low activity on the Sanyi fault since 46 ka, relative to the northern Chelungpu fault.

### Timing of faulting

Timing of faulting in the Western Foothills fold-and-thrust belt is difficult to constrain precisely (Hung and Wiltschko, 1993). The Shuantung fault cuts the Pleistocene Toukashan Formation in its footwall, while the Chelungpu/Sanyi fault system cuts Holocene alluvium in its footwall. This indicates that both faults are active during the Quaternary. Paleomagnetic evidence suggests that deposition in the foreland basin increased at approximately 1.1 ma (Chen et al, 2001) due to uplift in the proximal foothills, that is, on the Chelungpu/Sanyi and Shuantung faults. The Chelungpu fault may be younger than the Shuantung fault, consistent with foreland progression of the fold-and-thrust belt (Davis et al., 1983). If so, then the Shauntung thrust initiated during the early Quaternary around 1.1 Ma., followed by the Chelungpu fault between approximately 0.7-1 Ma. (Y. G. Chen et al., 2001; Lee et al., 2001). The Chelungpu/Sanyi fault is currently more active than the Shuantung fault, based on the fact that it cuts Holocene deposits and the Shuangtung fault does not. Estimates for the initiation of the Changhua thrust are  $\sim 0.5$  Ma (Mouthereau et al., 1999). This is in agreement with in-sequence progression of faulting towards the foreland in the fold-and-thrust belt (Davis et al., 1983).

### Fault Structure

Migration of the Chelungpu fault into the hanging wall of the Sanyi Fault has produced significantly different structures in the different regions. The bed-parallel, young fault in the northern region produced a narrow (0.20 m) gouge zone where slip was localized during the earthquake (Chapter 2) (Fig. 3-8). The Chelungpu fault in the southern region consists of a 20-70 m zone of intensely sheared mudstone and siltstone (see Chapter 2). The primary reason for the structural differences is the much greater total displacement in the southern region than in the northern region of the Chelungpu fault. Additionally, the dip of bedding and lithology through which the fault cuts appears to play an important role in

defining the width of the fault zone. The structure of the Sanyi fault is interpreted as similar to the southern region of the Chelungpu fault, based on similar ramp-geometry and lithology across the fault.

### Discussion

The evolution of the Chelungpu/Sanyi fault system can be observed through the varying structures on the fault. The southern Chelungpu fault and the Sanyi fault initiated together between 0.7-1.1 Ma (Y. G. Chen et al., 2001; Lee et al., 2001). The faults were active together until ~50 ka, and developed similar geometry with a footwall ramp. Both faults have thick (>1500 m), relatively flat-lying, Quaternary Toukoshan Formation in their footwall and total displacement on the fault of 8-15 km (Hung and Wiltchko, 1993; Suppe, 1980). This displacement caused the hanging wall rocks to be tilted to the angle of the footwall ramp, as they were carried up the fault. For this reason the hangingwall rocks roughly parallel the dip of the fault.

The Sanyi fault between Taichung and the Tachia River appears to have a listric structure, steepening towards the surface (Fig. 3-9). This is inferred from cross-sections (Chang, 1994; Y. H. Lee et al., 2001), and by the dips of hanging wall rocks. The steep dip of the Sanyi fault in the near surface (Fig. 3-3) caused increased friction on the footwall ramp with continued east-west convergence in the region. Therefore, the fault tended to migrate into its hanging wall due to less frictional resistance in the steeply dipping bedding planes in the hanging wall. Migration into the hanging wall has caused the older Sanyi fault to be "abandoned", since contraction is now accommodated along the newer, northern Chelungpu fault. This is seen by the minimal displacement since 45 ka through the lateritic terraces north of the Tachia River. Y. G. Chen et al. (2001) discussed the Holi fault, which is between the Sanyi fault and northern Chelungpu fault that represents an intermediate stage of migration into the hanging wall (Fig. 3-2, 3-9c). The southern Chelungpu fault did not



migrate into its hanging wall in the southern region because the fault is planar there, and dips approximately  $30^\circ$  east.  $30^\circ$  is the optimum angle for thrust fault rupture in a contractional setting, based on Mohr-Coulomb failure analysis. Therefore, even though both the Sanyi and southern Chelungpu faults have similar footwall (Toukoshan conglomerate) and hanging wall (Pliocene and Miocene siltstone and shale) lithologies, the angle of the fault ultimately determined the frictional resistance on the fault and the tendency for the fault to migrate into its hanging wall.

Such out-of-sequence structures are observed in a variety of settings (Ford and Stahel, 1995; Norris and Cooper, 1997). Willemin (1984) examined the mechanics of emergent thrusts and the problem of how long a thrust toe can be. He showed that for an isotropic, homogeneous thrust toe there exists a maximum stable length, for which over a certain displacement under steady erosion rates the thrust toe will internally deform (break-back). This "breaking-back" essentially will cause the thrust toe to become shorter, shortening the total displacement and making the toe again stable.

Stress on the Sanyi fault may well have been increased as the thrust emerged over the flat-lying Quaternary Toukoshan Formation, especially when compared to the optimally oriented geometry of the hanging wall bedding. The Chelungpu fault developed in the hanging wall bedding because the stress was less than on the toe, and this also provided a way to regain stability in the thrust toe (Willemin, 1984). Additionally, the Tachia river may have caused significant unloading so as to create a change in the frontal load of the thrust sheet, inducing break-back into the hanging wall. Thus, the Chelungpu fault's out-of-sequence development may have been caused by the combined mechanical effects of changes in frictional properties of the basal thrust, and erosion effects in the hanging wall.

The evolution of the Chelungpu fault in the northern region (Fig. 3-9) can be described from the data collected in this manuscript. The Sanyi fault initiated as a listric fault at  $\sim 1$  Ma. Fault activity occurred for  $\sim 0.95$  Ma along this listric fault, carrying the Pliocene

and Miocene sandstone and shale in the hanging wall up on the listric fault (Fig. 3-9a). At  $\sim 0.45$  Ma, fault activity temporarily ceased to allow formation of lateritic soil profiles on alluvial terrace surfaces (Fig. 3-9b). The fault reactivated after 46 ka, but migrated into its hanging wall along bedding planes parallel to the Sanyi fault trace (Fig. 3-9c). The new fault produced large displacements that allowed preservation of the lateritic terraces at elevation  $>200$  m above river level. Lateritic terraces are not preserved in the southern region probably because continual uplift of small displacements caused the terraces to be eroded and not preserved.

This investigation indicates that in some cases, individual emergent thrust faults may have a tendency to migrate towards the hinterland. When and if the frictional forces on the fault exceed those in the hanging wall (forces that have been produced through past displacement and deformation of bedrock), combined with changes of the vertical loading due to erosion, the fault will migrate "out-of-sequence" towards the hinterland. Analysis of the Chelungpu/Sanyi fault system indicates that the fault only migrates into its hanging wall where the original fault ramps steeply ( $>50^\circ$ ) to the surface. This creates an unfavorable angle for thrust fault rupture, and therefore the fault may have a tendency to seek a weaker plane to rupture (shale bedding) than the ramp above a thick package of Quaternary conglomerate and sandstone.

### Conclusions

The southern region of the Chelungpu fault was contiguous with the Sanyi fault from  $\sim 1.0$  Ma. (Y. G. Chen et al., 2001; W. S. Chen et al., 2001). The fault ruptured along flat and ramp surfaces within late Miocene and early Pliocene sedimentary units (Hung and Wiltchko, 1993). At  $\sim 46000$  y.b.p., the lateritic terraces were formed along the river valleys and in the coastal plain (Fig. 2). After formation of these terraces, faulting resumed along the Chelungpu/Sanyi fault segment. The fault, however, migrated back into its hanging wall

north of Wufeng. This was due to formation of optimally oriented bedding planes ( $\sim 50^\circ$ ), which provided a less-friction surface for the fault to rupture. The fault did not migrate into its hanging wall south of this point because the fault was already at its optimum angle ( $30^\circ$ ) for Thompsonian thrust fault rupture.

The bed parallel geometry and low total displacement on the Chelungpu fault in the northern region caused the fault to be confined along narrow, pre-existing zone of weakness between two similar lithologies. This produced a narrow (0.07-0.20 m) gouge zone where slip was localized, producing large surface displacements but little, high-frequency ground motion (Chapter 2). By contrast, the fault in the southern region has >10 km of displacement and juxtaposes the Chinsui shale with flat-lying Toukoshan Formation sandstone and conglomerate (Lee et al., 2001). This sharp lithologic contrast resulted in the inability for the fault to localize in one specific area, thus resulting in a diffuse (>20m) shear zone in the fault.

The evolution of the Chelungpu fault indicates that the fault has migrated into the hanging wall of the Sanyi fault in the northern region. This has produced 2 different geometries along the fault trace that ruptured in the 9/21/99 earthquake: the northern and southern regions of the Chelungpu fault. This implies that any given thrust fault may have different structures along strike resulting from a different histories of each section of the fault.

#### References

- Birkeland, P. W. (1999). *Soils and Geomorphology*, Oxford University Press, 430 p.
- Chang, H. C. (1994). *The geological map and explanatory text of Tachia, Taiwan*, Central Geol. Surv., Ministry of Economic Affairs, R.O.C., scale 1:50,000.

- Chang, S. L. (1971). Subsurface geologic study of the Taichung Basin, Taiwan, *Petrol. Geol. Taiwan* **8**, 21-45.
- Chen, C. H., H. C. Ho, K. S. Shea, W. Lo, W. H. Lin, H. C. Chang, C. S. Huang, C. W. Lin, G. H. Chen, C. N. Yang, and Y. H. Lee (2000). Geologic map of Taiwan, Ministry of Economic Affairs, R.O.C., scale 1:500,000.
- Chen, W. S., K. D. Ridgeway, C. S. Horng, Y. G. Chen, K. S. Shea, and M. G. Yeh (2001). Stratigraphic architecture, magnetotratigraphy, and incised-valley systems of the Pliocene-Pleistocene collisional margin foreland basin of Taiwan, *Geol. Soc. Amer. Bull.* **113**, 1249-1271.
- Chen, Y. G., W. S. Chen, Y. Wang, P. W. Lo, T. K. Liu, and J. C. Lee (2002). Geomorphic evidence for prior earthquakes: lessons from the 1999 Chichi earthquake in central Taiwan, *Geology* **30**, 171-174.
- Chen, Y. G., W. S. Chen, J. C. Lee, C. T. Lee, H. C. Chang, and C. H. Lo (2001). Surface rupture of the 1999 Chi-Chi earthquake yields insights on active tectonics of Central Taiwan, *Bull. Seismol. Soc. Am.* **91**, 977-985.
- Chi, W.R., J. Namson, and J. Suppe (1981). Stratigraphic Record of Plate Interactions in the Coastal Range of Eastern Taiwan: *Geol. Soc. China Mem.* **4**, 155-194.
- Davis, D., J. Suppe, and F. A. Dahlen (1983). Mechanics of fold-and-thrust belts and accretionary wedges, *J. Geophys. Res.* **88**, 1153-1172.
- Ford, M., and U. Stahel (1995). The geometry of a deformed carbonate slope-basin transition: The Ventoux-Lure fault zone, SE France, *Tectonics* **14**, 1393-1410.
- Ho, C. S. (1986). A synthesis of the geologic evolution of Taiwan, *Tectonophysics* **125**, 1-16.
- Ho, H. C., and Chen, M. M. (2000). The geological map and explanatory text of Taichung, Taiwan, Central Geol. Surv., Ministry of Economic Affairs, R.O.C., scale 1:50,000.

- Hsieh, M. L., Y. H. Lee, T. S. Shih, S. T. Lu, and W. Y. Wu (2001). Could we have pre-located the northeastern portion of the 1999 Chi-Chi earthquake rupture using geological and geomorphic data? *Terr., Atm. and Oceanic Sci.* **12**, 461-484.
- Hsieh, S. L. (1990). Fission-track dating of zircons from several east-west sections of Taiwan Island (M. S. thesis), Taipei, National Taiwan University, 134 p. (in chinese).
- Hung, J. H. and D. V. Wiltschko (1993). Structure and kinematics of arcuate thrust faults in the Miaoli-Cholan area of western Taiwan, *Petrol. Geol. Taiwan* **28**, 59-96.
- Knuepfer, P. L., and Long, H. M. (1996). Geomorphic evidence for westward propagation of the Taiwan fold-and-thrust belt in the Holocene, *Abstracts with Programs, Geol. Soc. Amer. annual meeting* **28**, 394.
- Lee, J. C., Y. G. Chen, K. Sieh, K. Mueller, W. S. Chen, H. T. Chu, Y. C. Chan, C. Rubin, and R. Yates (2001). A vertical exposure of the 1999 surface rupture of the Chelungpu fault at Wufeng, western Taiwan: structural and paleoseismic implications for an active thrust fault, *Bull. Seismol. Soc. Am.* **91**, 914-929.
- Lee, J. F. (2000). The geological map and explanatory text of Tungshih, Taiwan, Central Geol. Surv., Ministry of Economic Affairs, R.O.C., scale 1:50,000.
- Lee, Y. H., W. Y. Wu, T. S. Shih, S. T. Lu, M. L. Shieh, and H. C. Cheng (2001). Deformation characteristics of surface ruptures of the Chi-Chi earthquake, east of the Pifeng bridge, *Cent. Geol. Surv. Special Issue* **12**, 27-40 (in chinese).
- Lin, A., T. Ouchi, A. Chen, and T. Maruyama (2001). Co-seismic displacements, folding and shortening structures along the Chelungpu surface rupture zone occurred during the 1999 Chi-Chi (Taiwan) earthquake, *Tectonophysics* **330**, 225-244.
- Liu, T. K. (1990). Neotectonic crustal movement in northeastern Taiwan inferred by radiocarbon dating of terrace deposits, *Proc. Geol. Soc. China* **33**, 65-84.

- Lo, W., L. C. Wu, and H. W. Chen (1999). The geological map and explanatory text of Kuohsing, Taiwan, Central Geol. Surv., Ministry of Economic Affairs, R.O.C., scale 1:50,000.
- Meng, C. Y. (1963). The San-i overthrust, *Petrol. Geol. Taiwan* **2**, 1-20.
- Mouthereau, F., O. Lacombe, B. Deffontaines, J. Angelier, H. T. Chu, and C. T. Lee (1999). Quaternary transfer faulting and belt front deformation at Pakuashan (western Taiwan), *Tectonics* **18**, 215-230.
- Norris, R. J., and A. F. Cooper (1997). Erosional control on the structural evolution of a transpressional thrust complex on the Alpine Fault, New Zealand, *J. Struc. Geol.* **19**, 1323-1342.
- Suppe, J. (1980). A Retrodeformable Cross Section of Northern Taiwan, *Proc. Geol. Soc. China* **23**, p. 46-55.
- Suppe, J. (1987). The Active Taiwan Mountain Belt in *The Anatomy of Mountain Ranges*, J. P. Schaer and J. Rodgers, (Editors), Princeton University Press, 277-293.
- Wang, C., T. H. Huang, I. C. Yen, S. L. Wang, and W. B. Cheng (2000). Tectonic environment of the 1999 Chi-Chi earthquake in central Taiwan and its aftershock sequence, *Terr., Atm. and Oceanic Sci.* **11**, 661-678.
- Willemin, J. H. (1984). Erosion and the mechanics of shallow foreland thrusts, *J. Struc. Geol.* **6**, 425-432.

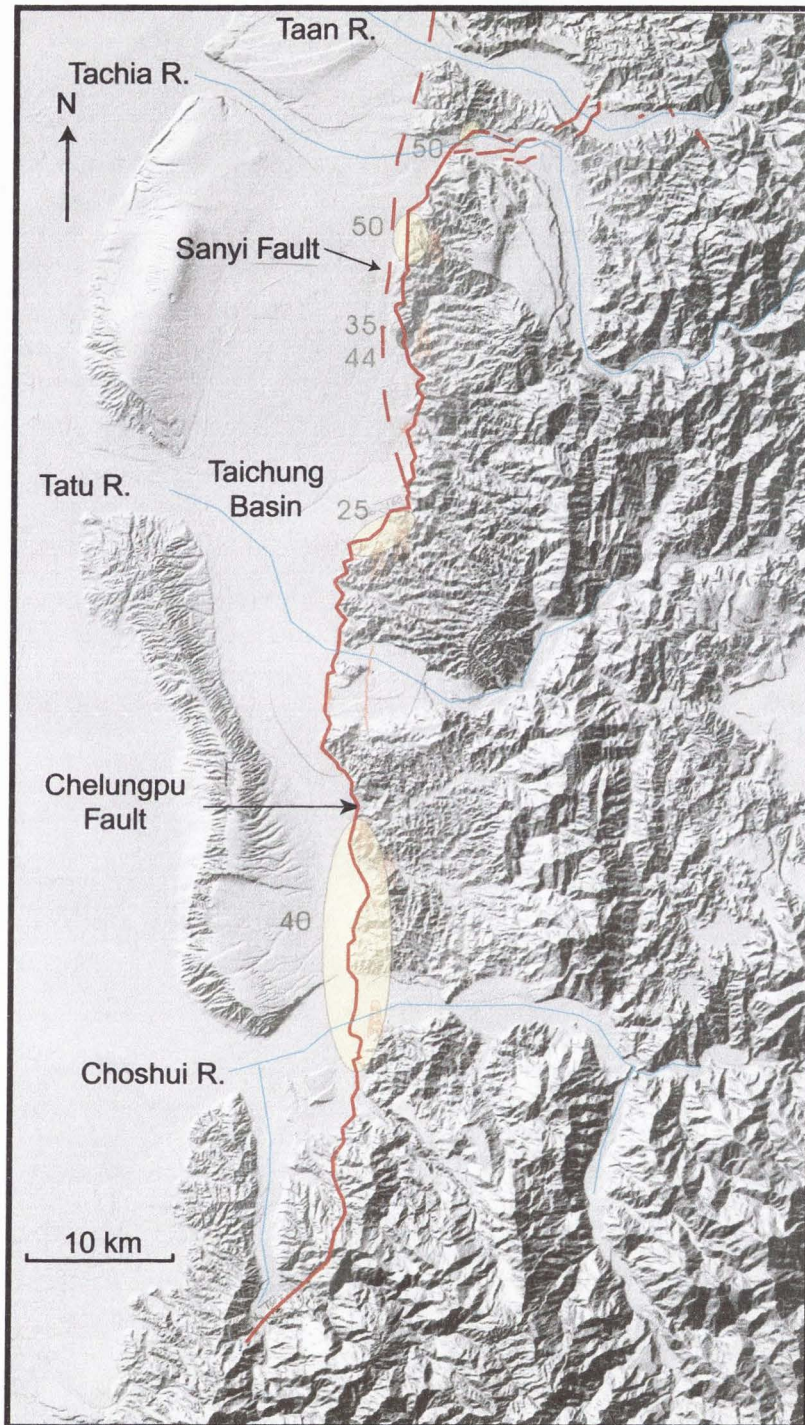


Figure 3-1. Digital elevation model of the Chelungpu fault rupture. Solid red line is the 1999 rupture trace. Dashed red line indicates the hidden trace of the Sanyi fault. Numbers indicate the fault dip based on Central Geologic Survey of Taiwan borehole data (Y. H. Lee, pers. comm.).

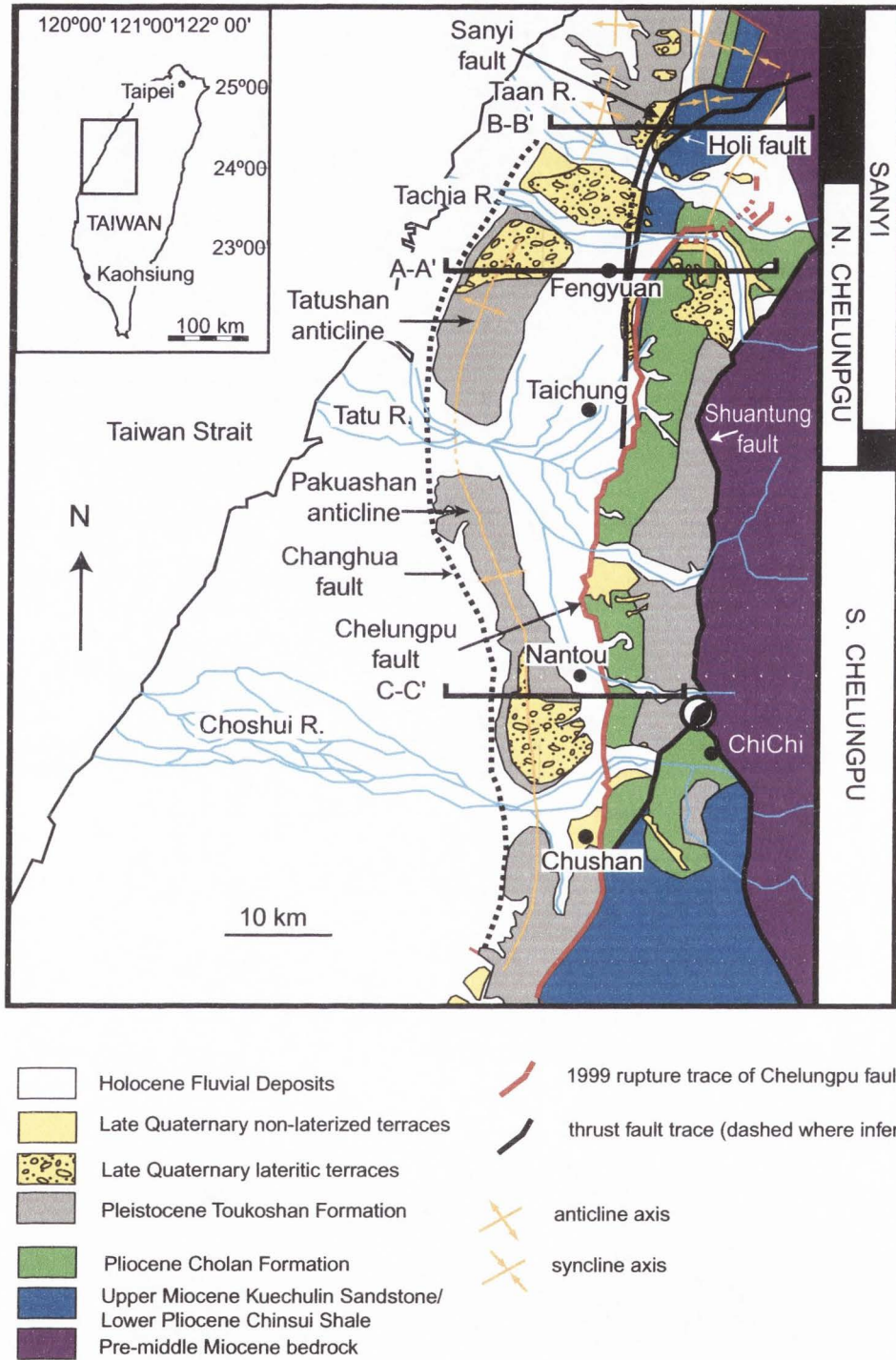


Figure 3-2. Geologic map of the Chelungpu/Sanyi fault region. Faults are shown as the bold red (9-21-99 earthquake trace) and black lines (dashed where inferred). All faults are west vergent thrust faults. Cross sections A-A', B-B', and C-C' are shown. Map modified from on Chang (1994), Chen et al. (2000), Ho and Chen (2000), and Lo et al. (1999).



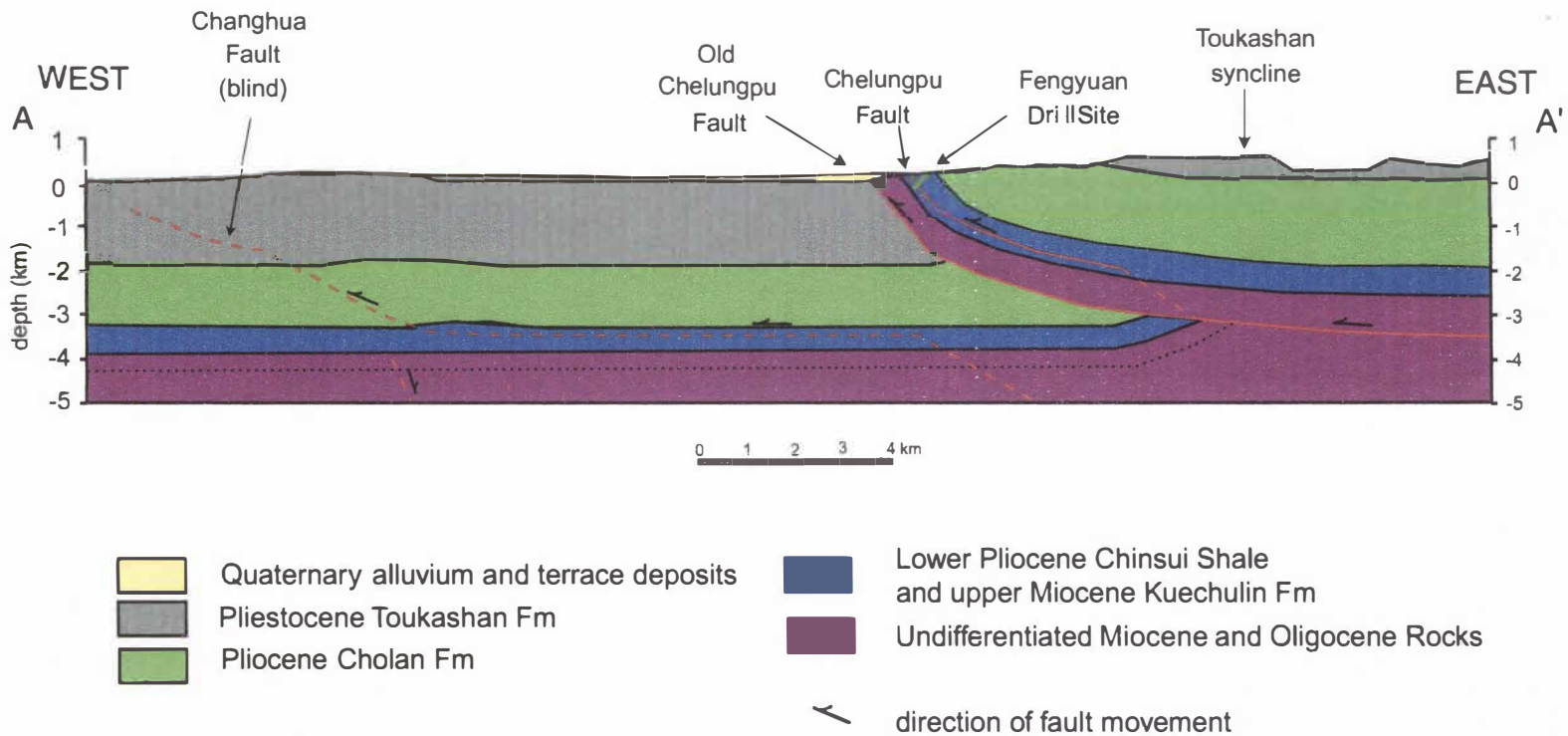


Figure 3-3. Cross section A-A' through the northern region of the Chelungpu fault. Drill hole is shown in green. Cross section based on field mapping and Central Geologic Survey geologic maps (Ho and Chen, 2000; Lo et al., 1999).

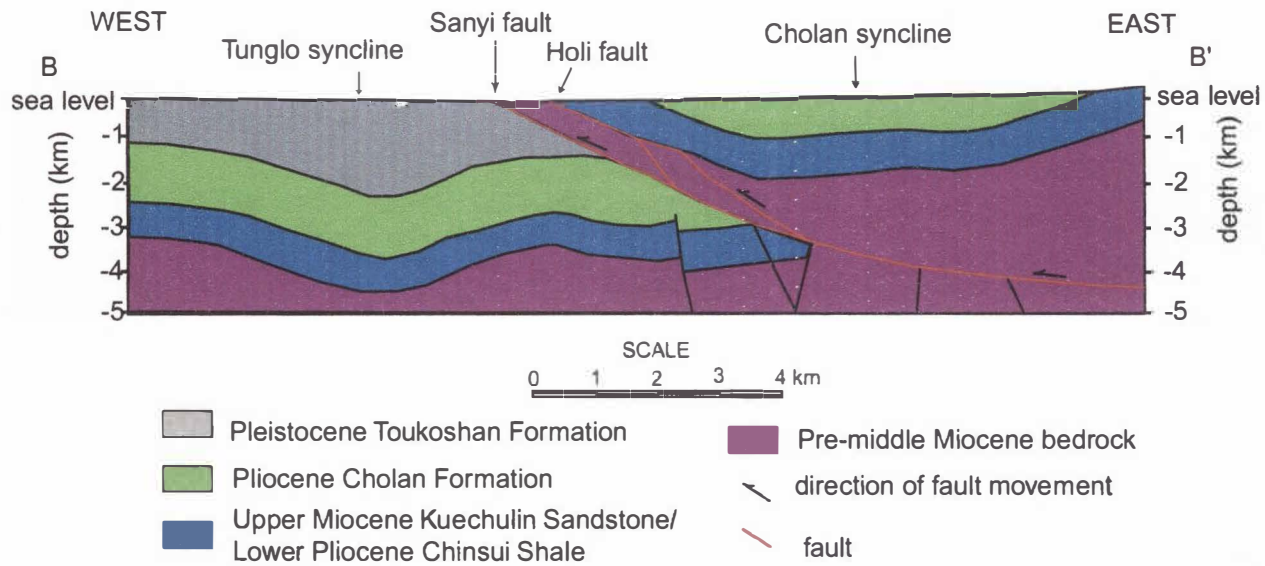


Fig. 3-4. Cross-section B-B' through the Sanyi region, modified after Hung and Wiltchko (1993).

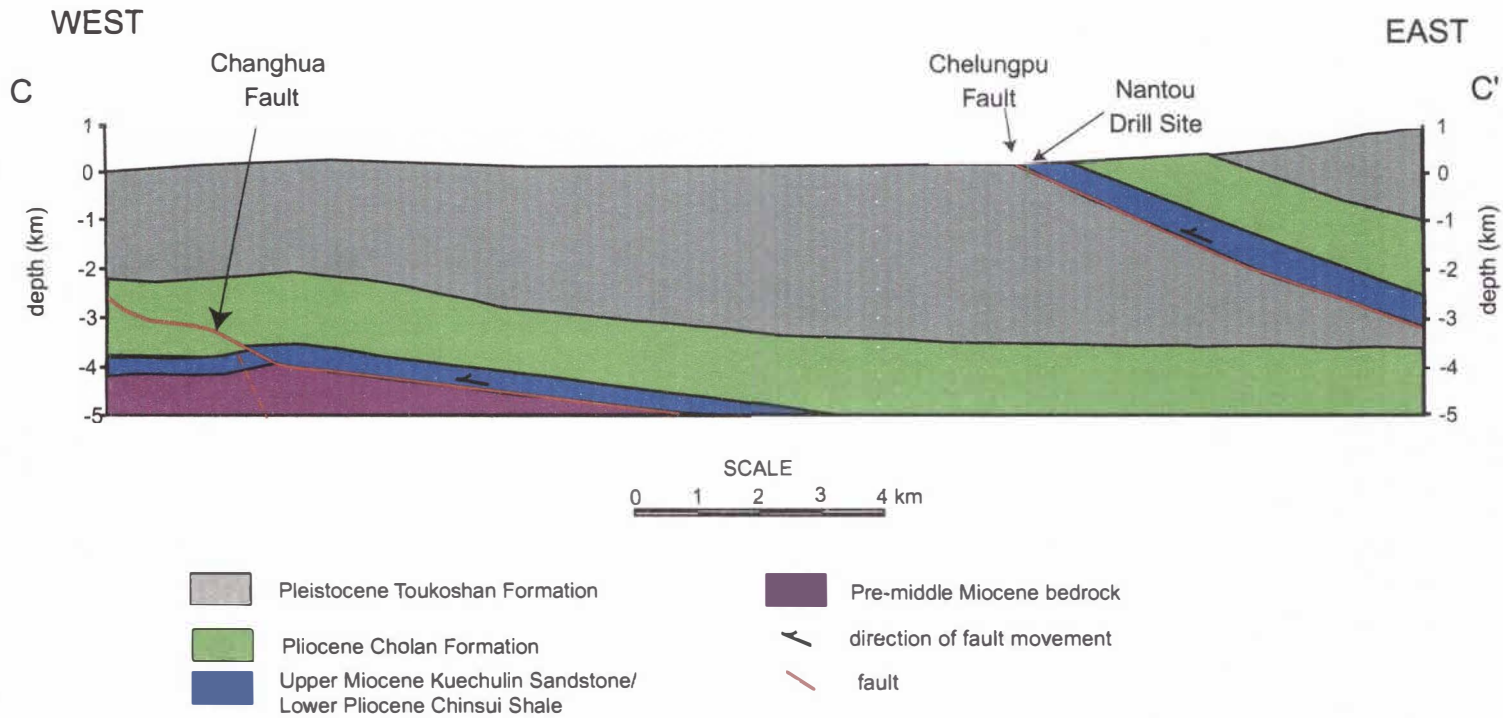


Fig. 3-5. Cross-section C-C'. Section based on seismic from Chang (1971).

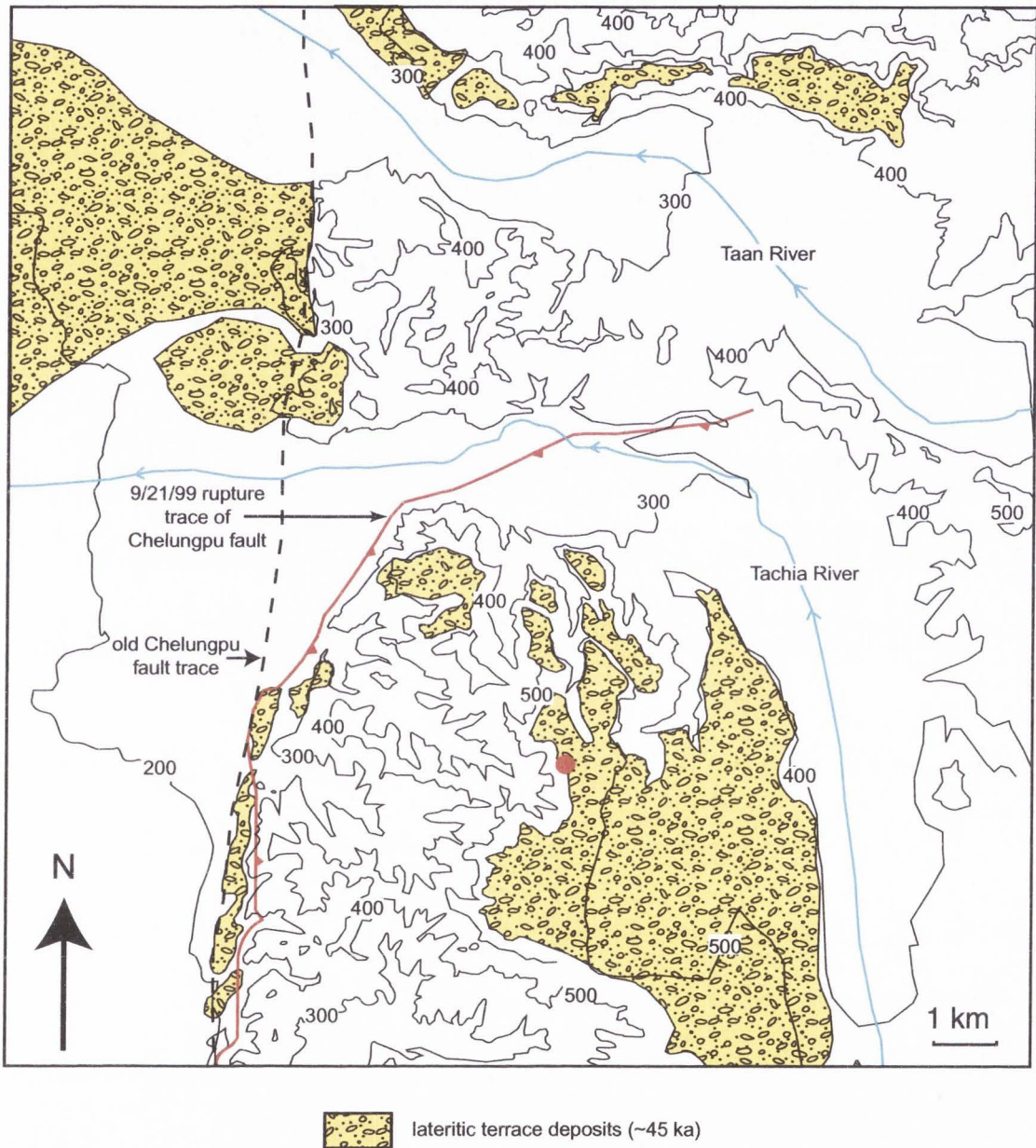


Figure 3-6. Map of lateritic terraces in the northern region of the Chelungpu fault. Elevations are shown by the 100 m contour lines (Chang, 1994; Lo et al., 1999; Lee, 2000; Ho and Chen, 2000). Fault traces are shown with teeth on upthrown side. Blue lines depict major river valleys with arrows indicating flow direction. Red dot in photo is location of photo in figure 3-6.



Figure 3-7. Uplifted lateritic terrace in hanging wall of the northern region of the Chelungpu fault. Person at base is 1.75 m tall. The terrace is a fill terrace ~10 m thick and 350 m above the adjacent river level. The angular unconformity with the underlying Cholan Fm. can be seen in the middle of the figure (shown with arrow). Bedding is depicted with the dashed lines. View is to north.



Figure 3-8. Fault zone outcrop from the Tongtuo Bridge site at the southern terminus of the Chelungpu fault. The red circles enclose the shear zones in photo. This photo is from 70 m from the fault and is viewed to the north. This photo typifies the fault zone in the southern region of the Chelungpu fault.

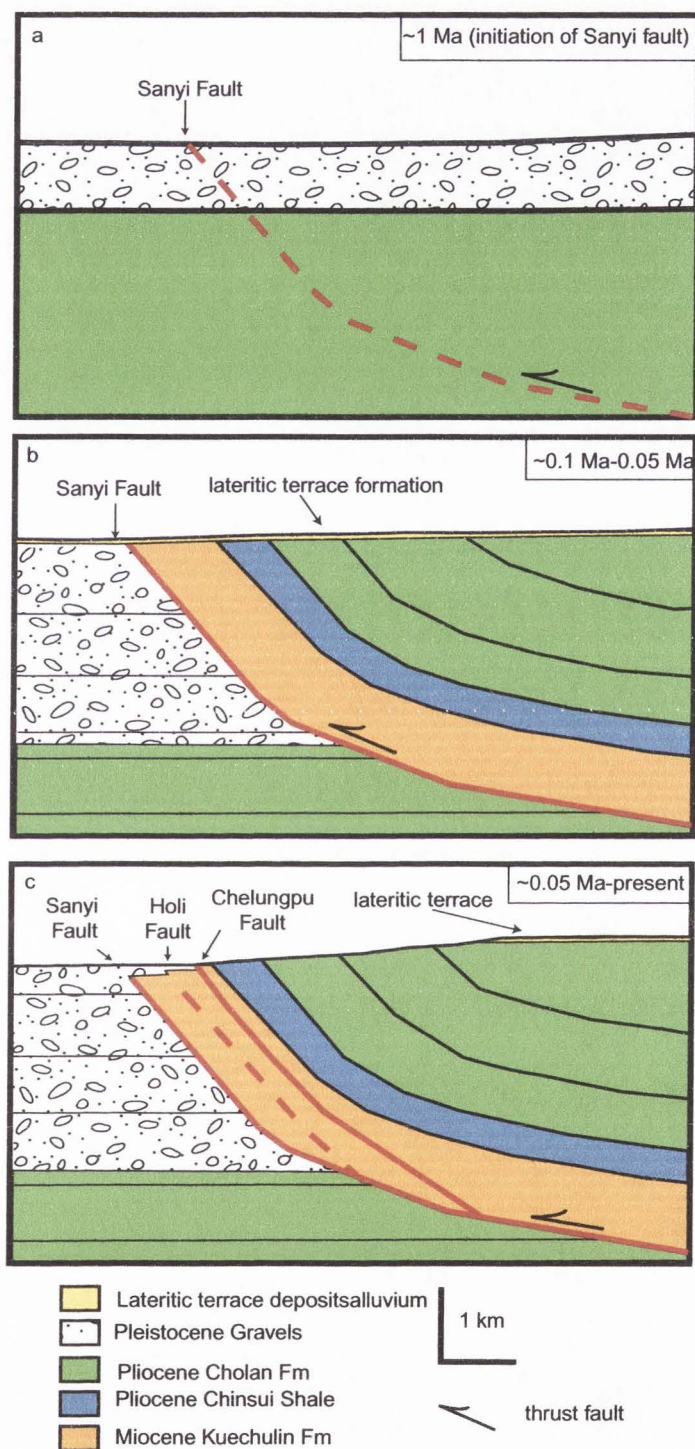


Figure 3-9. Schematic cross sections through time of the Chelungpu fault in the northern region. These show the evolution of fault as it migrates into its hanging wall. a) Sanyi fault initiated  $\sim 1$  Ma as a listric fault. b) Lateritic terraces formed during across fault. c) Reactivation of faulting caused bed-parallel rupture in the hanging wall of the Sanyi fault, where friction was less than on the older Sanyi fault. This uplifted the lateritic terraces in the hanging wall.

## CHAPTER 4

### CONCLUSIONS

The September 21, 1999,  $M_w$  7.6 earthquake on the Chelungpu fault in central Taiwan provided a large data set on the seismic and rupture characteristics of a large-magnitude earthquake. The present study examined in-situ fault properties and compares them with the rupture and seismic properties observed in the earthquake. The physical properties of the fault zone, such as width and structural setting of the rupture, were obtained through detailed examination of outcrops and drilled cores through the fault. Analysis of 3 localities in the northern region shows how slip is localized within the fault as a result of fault geometry. These results are compared with strong motion data and surface rupture characteristics to understand the slip distribution during the earthquake. Large displacements, combined with the less high frequency ground motion than in the southern region, were associated with a bed-parallel, flat-on-flat geometry, and thin ( $<0.02$  m) gouge zone in the northern region. Analysis from 2 localities in the southern region indicate the fault contains a wide ( $>20$  m), sheared zone with no obvious single zone of slip. The wide fault zone in the southern region produced lower displacements but higher frequency ground motion in the southern region. The wide fault zone developed from large amounts of displacement above a footwall ramp.

Data collected from the Fengyuan drill site constrains the fault dip at  $52^\circ$  east to at least 250 m depth. This correlates well with the Takeng site 6 km south of the Fengyuan drill site, and with surface rupture observations from Lin et al. (2001) that indicate that the fault dips  $50-80^\circ$  at the surface in the northern region. The fault dip measured through the Fengyuan borehole ( $52^\circ$ ) matches bedding dips in the hanging wall ( $56^\circ$ ) and footwall ( $53^\circ$ ) in the area, indicating the fault is bed parallel and confined to the Kueichulin Formation at this location in the near surface. Analysis of the drilled core indicates the fault consists of a zone 7 mm-thick of sheared, dark-gray, clay gouge. The narrow zone was associated with a planar break in the core and the largest increase in fracture density observed in the core.



A similar gouge zone was observed at the surface outcrop in Takeng, where the gouge was 20 cm thick. Microstructural analysis of the Takeng rupture revealed a foliated, sheared fabric and a very-narrow, 50-300  $\mu\text{m}$ -thick, zone of ultracataclasite interpreted to be the slip surface of the 1999 rupture. The clay gouge sampled from the Takeng site is assumed to be correlative with the gouge observed in the Fengyuan core. It has similar color, foliation, and is located at the rupture surface of the 9/21/99 earthquake. Therefore, the fault is interpreted as a very narrow zone confined to a narrow gouge that is unique to the fault within the host lithologies. The gouge also correlates with a 15 cm gouge observed at 60 m (Liao et al., 2002) due west of the Fengyuan drill site along the cross-section (Fig. 2-5). These gouge zones constrain the fault to a narrow gouge to at least 250 m total vertical depth.

Qualitative analysis of the drilled core through the fault in the southern region indicates a large sheared zone ( $\sim 20$  m) at the fault. No single, unique gouge was observed in the core, and the fault is considered to be a large, diffuse zone dipping approximately  $35^\circ$  in this region. The fault juxtaposes east-dipping Pliocene Shale on a footwall ramp with 2000-3000 feet of flat-lying, Quaternary, alluvial deposits of the Toukoshan Formation in the footwall (Lee et al., 2001).

Fracture density in the drill hole increases 30-50 m above the fault gouge, and this zone is interpreted as a damage zone related to the fault. This zone is predominately localized in the hanging wall of the fault, and is characterized by wide fractures ( $< 1.5$  m) filled with brecciated siltstone and sandstone clasts suspended in a massive, clay-rich matrix. These brecciated zones are compositionally indistinguishable from the host Pliocene sedimentary rocks, based on XRD analysis of these rocks, and there is very little evidence for shearing and foliation in these zones, indicating that slip and shear were localized in the narrow gouge zones.

The thickness and material properties of the Chelungpu fault has important implications for understanding the seismic characteristics of the 9/21/99 earthquake. These factors may influence the amount of high-frequency ground motion during an earthquake (Ma et al., submitted; Brodsky and Kanamori, 2001; Kanamori and Heaton, 2000). Our conclusion of a thin (50-300  $\mu\text{m}$ ), clay-rich

slip surface within a narrow gouge supports the model by Ma et al. (submitted) for the 1999 earthquake that states that lubrication pressure will be increased in such a narrow zone to decrease friction in the fault zone. This model also suggests that very fast (4.5 m/sec) and large (12 m) slip can deform the fault walls, reducing asperities along the fault. This reduction in asperities would result in less friction, producing less, high frequency shaking. Lubrication pressure would not be increased sufficiently to widen the fault with the wide fault zone in the southern region, due to the large width of the fault slip surface in the southern region. Therefore, slip is dispersed into the wide zone, resulting in greater amounts of high frequency ground motion and lower displacement during and earthquake in the southern region.

The different fault geometry between the northern and southern regions contributed to the observed fault structural heterogeneity along strike. The bed parallel geometry in the northern region allowed the fault to be confined along a narrow, pre-existing zone of weakness between two similar lithologies. This produced a smooth, narrow fault surface. The fault in the southern region juxtaposes east-dipping, Pliocene Chinsui Shale with poorly consolidated, flat-lying, conglomerate and sandstone in the Quaternary Toukoshan Formation. This sharp contrast, between the hanging wall flat and footwall ramp produced a "rough," wide zone with no pre-determined zones of weakness. This undoubtedly contributed to the inability of the fault to localize in one specific area. Slip may easily be lost in the flat-lying Quaternary sediments, and there are no existing planes of weakness for slip to localize. Therefore, slip on the "rough" footwall ramp resulted in a diffuse fault zone.

The different displacement histories led to the different structures along the Chelungpu/Sanyi fault system. The southern region of the Chelungpu fault and the Sanyi fault were originally continuous. This continuous fault, however, changed shape from an  $\sim 30^\circ$  dipping fault in the south to a listric fault in the north, steeply dipping near the surface ( $\sim 50^\circ$ ) (Fig. 2-2). Sometime after 50 ka, the fault migrated into its hanging wall in the northern region, whereas in the southern

region the fault has remained on its original footwall ramp. Migration occurred due to the presence of optimally oriented bedding planes in the hanging wall that provided a fault pathway to the surface with less friction than the  $\sim 50^\circ$  dipping footwall ramp above  $<2000$  feet of Quaternary alluvial deposits. Timing of uplift in the northern region is partially constrained by correlative dating of lateritic terraces in the hanging wall of the Chelungpu northern region (Liu, 1990). Therefore, we concluded that the fault in the northern region is a young fault ( $<50$  ka) based on lack of deformation in the fault zone, the bed-parallel, stratigraphic sequence across the fault, and terrace dates in the hanging wall. By contrast, the fault in the southern region is much older ( $\sim 1$  Ma) (Lee et al., 2001). The different displacement histories on the fault produced the differing structures observed along strike.

The data collected here show how fault zone structure and composition are the result of regional structural setting and lithology. The fault orientation and lithology across the fault greatly impact the nature of how slip during an earthquake gets to the surface, and ultimately the rupture characteristics of the earthquake. Therefore, by understanding the fault properties, we may interpret how the fault will behave during an earthquake event. Large displacements but relatively low amounts of high-frequency ground motions are associated with a young, bed-parallel fault at the surface. This fault consists of a narrow gouge zone (cm-scale) and contains an associated, asymmetric damage zone in the hanging wall. Small displacements but large amounts of high-frequency ground motion are associated with a wide (m-scale) shear zone (gouge?). This can be associated with a footwall ramp geometry between two contrasting lithologies, such as observed in the southern Chelungpu and Sanyi fault regions. These factors should be considered when developing geotechnical regulations and seismic zones of intensified shaking along active thrust fault traces. The 9/21/99 earthquake in Taiwan has provided important insight into active earthquake processes that can be used to prevent future earthquake casualties.

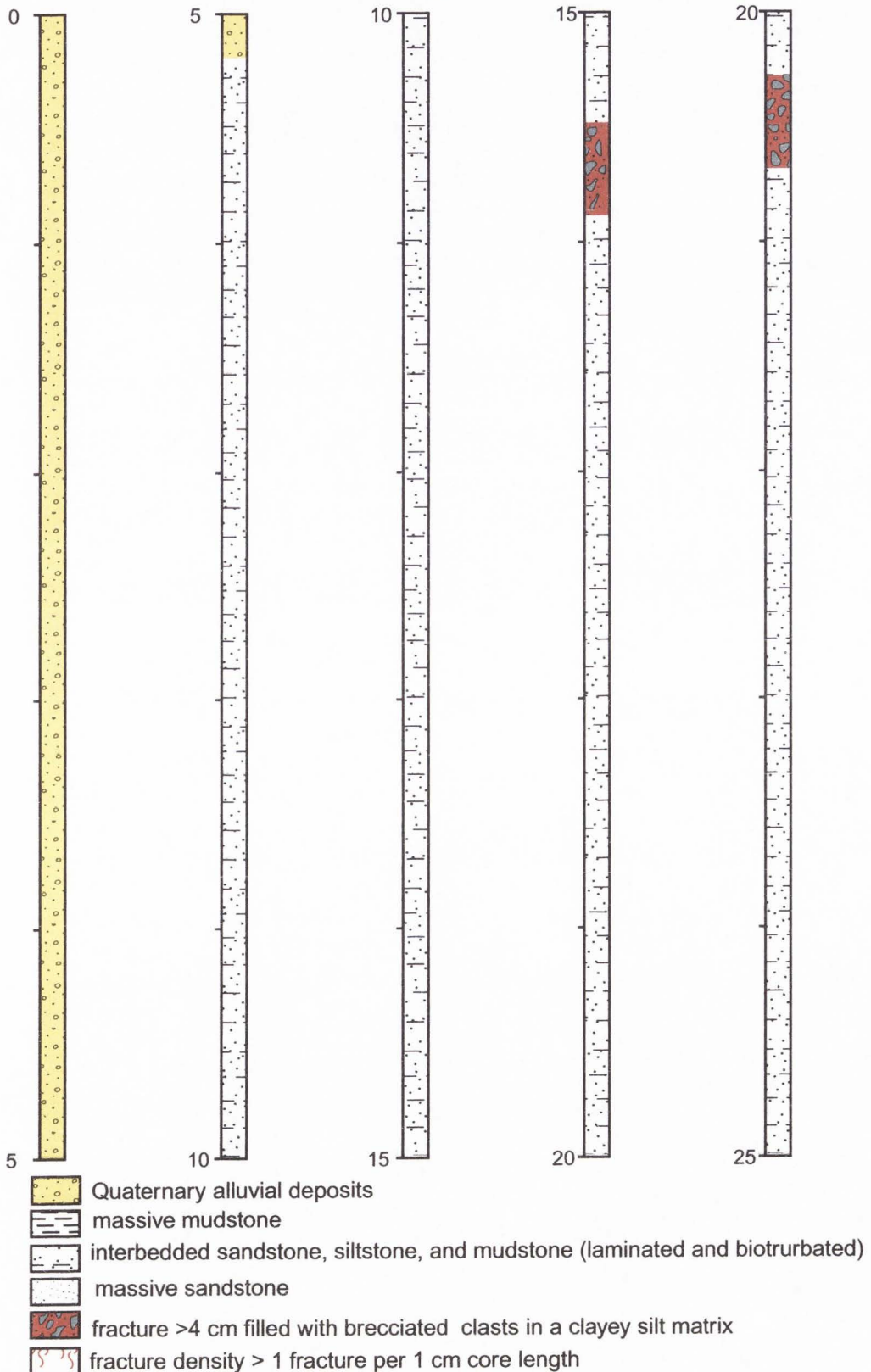
## References

- Brodsky, E. E. and H. Kanamori (2001). Elastohydrodynamic lubrication of faults, *J. Geophys Res.* **106**, 16357-16374.
- Kanamori, H., and T. H. Heaton (2000). Microscopic and macroscopic physics of earthquakes, *Am. Geoph. Un. Mono.* **120**, 147-161.
- Lee, J. C., Y. G. Chen, K. Sieh, K. Mueller, W. S. Chen, H. T. Chu, Y. C. Chan, C. Rubin, and R. Yates (2001). A vertical exposure of the 1999 surface rupture of the Chelungpu fault at Wufeng, western Taiwan: structural and paleoseismic implications for an active thrust fault, *Bull. Seismol. Soc. Am.* **91**, 914-929.
- Liao, C-F., Hung J. H., and Lee, C-T (2002). Analysis of clay minerals and fractures from cores of Chelungpu fault zone (abstract), in *Geol. Soc. China, Annual Meeting*.
- Lin, A., T. Ouchi, A. Chen, and T. Maruyama (2001). Co-seismic displacements, folding and shortening structures along the Chelungpu surface rupture zone occurred during the 1999 Chi-Chi (Taiwan) earthquake, *Tectonophysics* **330**, 225-244.
- Liu, T. K. (1990). Neotectonic crustal movement in northeastern Taiwan inferred by radiocarbon dating of terrace deposits, *Proc. Geol. Soc. China* **33**, 65-84.
- Ma, K. F., E. E. Brodsky, J. Mori, J. Chen, T. R. A. Song, and H. Kanamori (submitted, 2002). Evidence for fault lubrication during the 1999 Chi-Chi, Taiwan, earthquake (Mw7.6).

APPENDIX

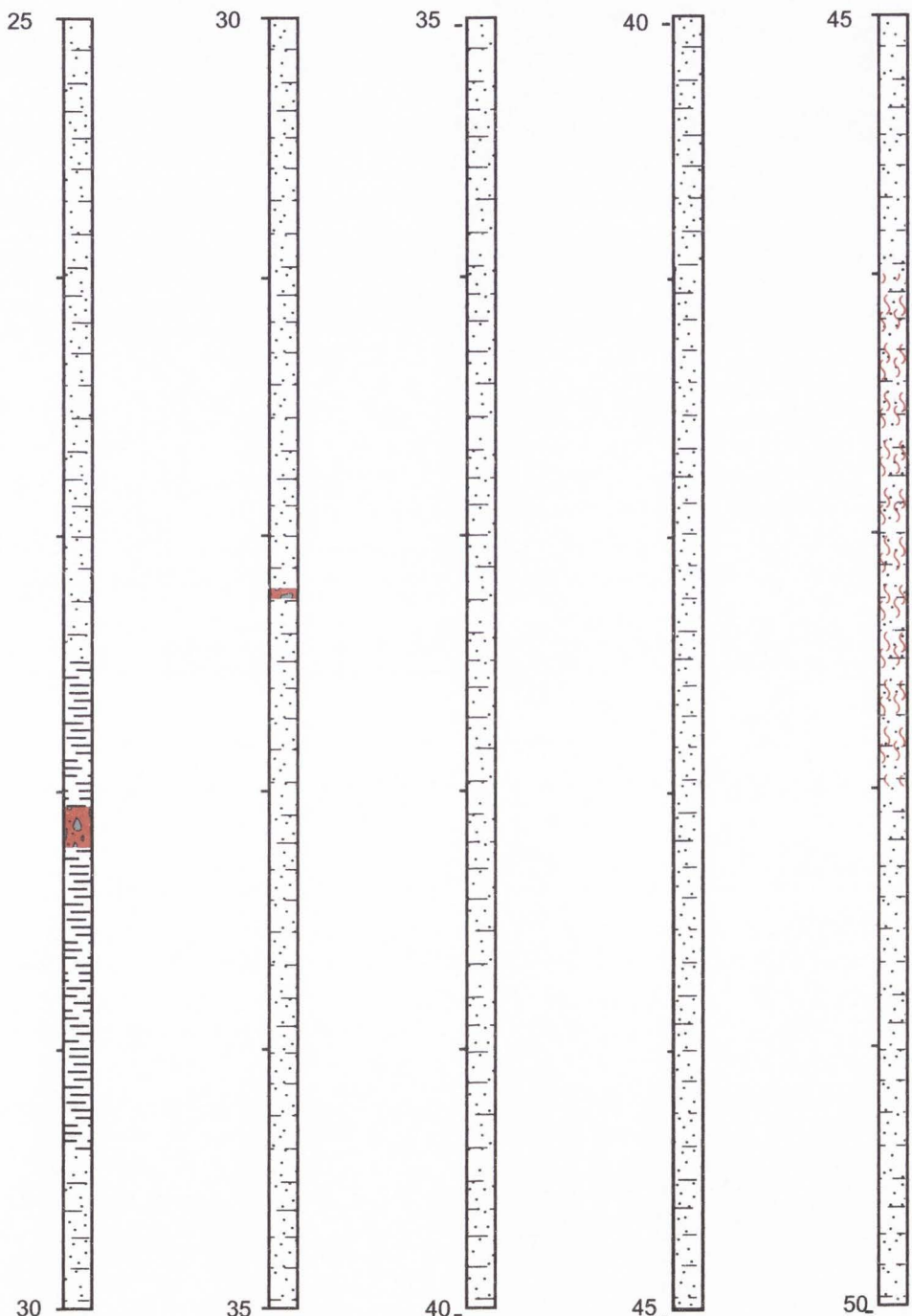
# Graphic log of core from Fengyuan drill site

Scale 1:25 (2x horizontal exaggeration), all depths in meters



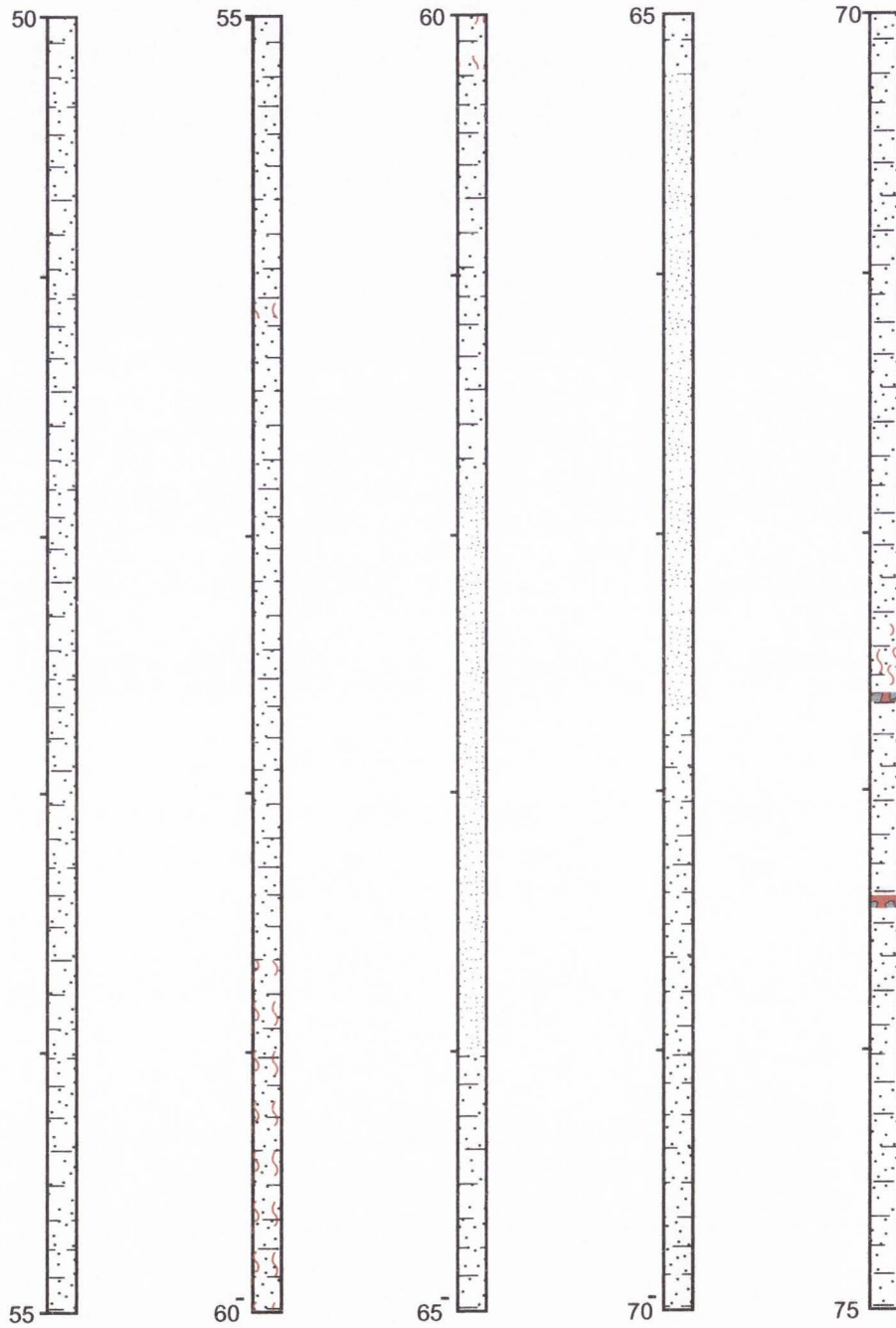
### Graphic log of core from Fengyuan drill site






Scale 1:25 (2x horizontal exaggeration), all depths in meters



- massive mudstone
- interbedded sandstone, siltstone, and mudstone (laminated and bioturbated)
- massive sandstone
- fracture >4 cm filled with brecciated clasts in a clayey silt matrix
- fracture density > 1 fracture per 1 cm core length

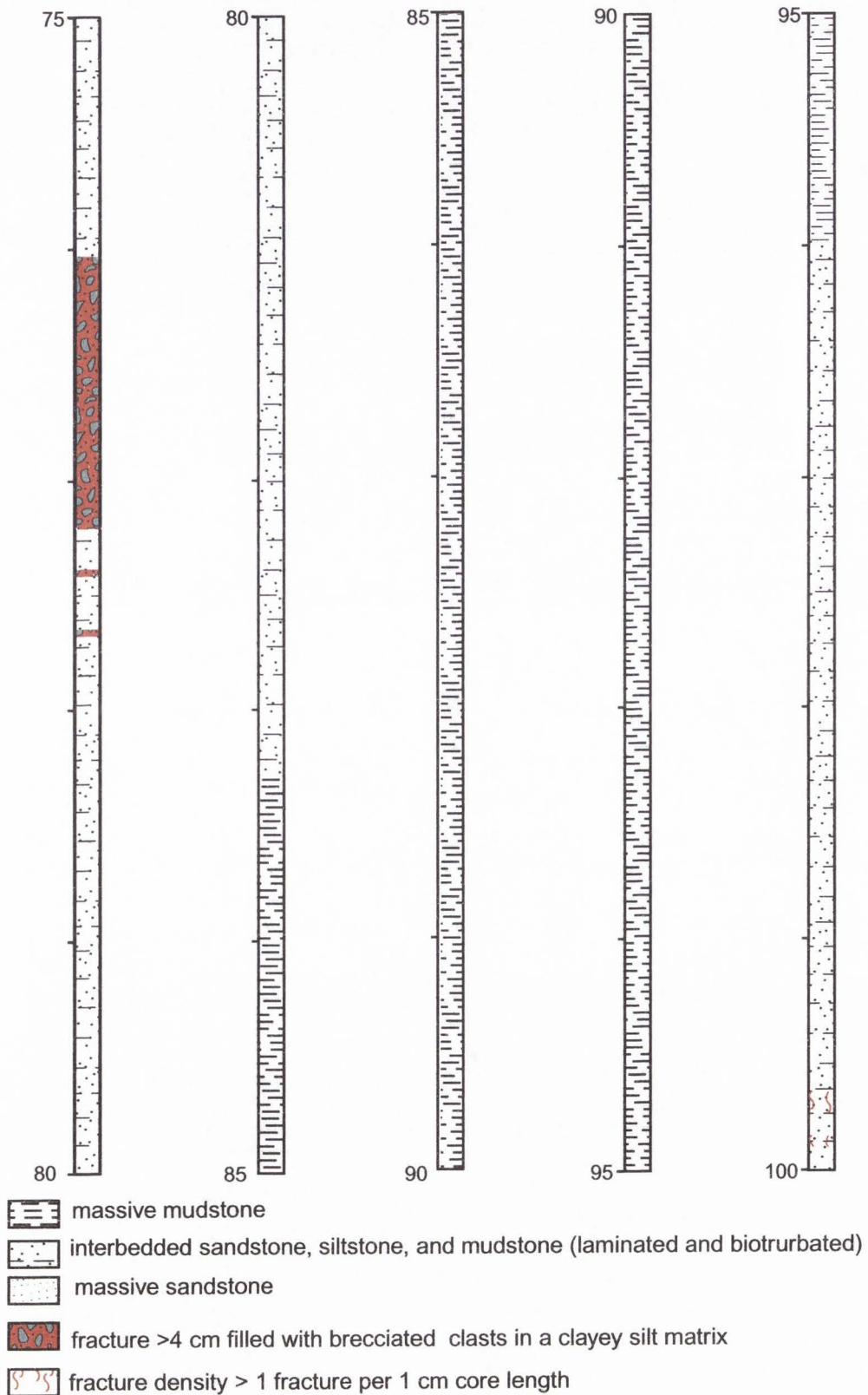
Graphic log of core from Fengyuan drill site  
 Scale 1:25 (2x horizontal exaggeration), all depths in meters



-  massive mudstone
-  interbedded sandstone, siltstone, and mudstone (laminated and bioturbated)
-  massive sandstone
-  fracture >4 cm filled with brecciated clasts in a clayey silt matrix
-  fracture density > 1 fracture per 1 cm core length

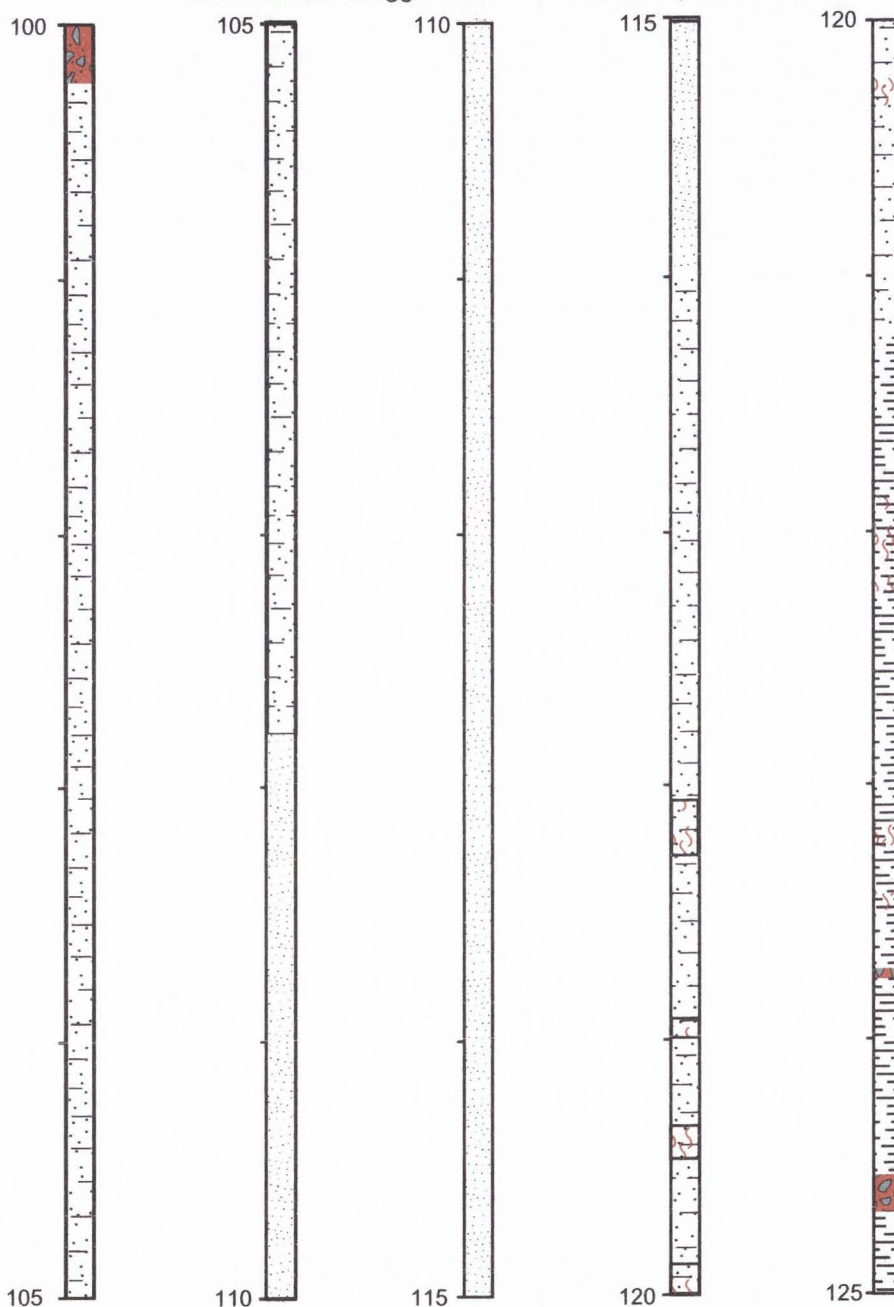




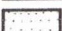


### Graphic log of core from Fengyuan drill site 2x horizontal exaggeration of cores, all depths in meters



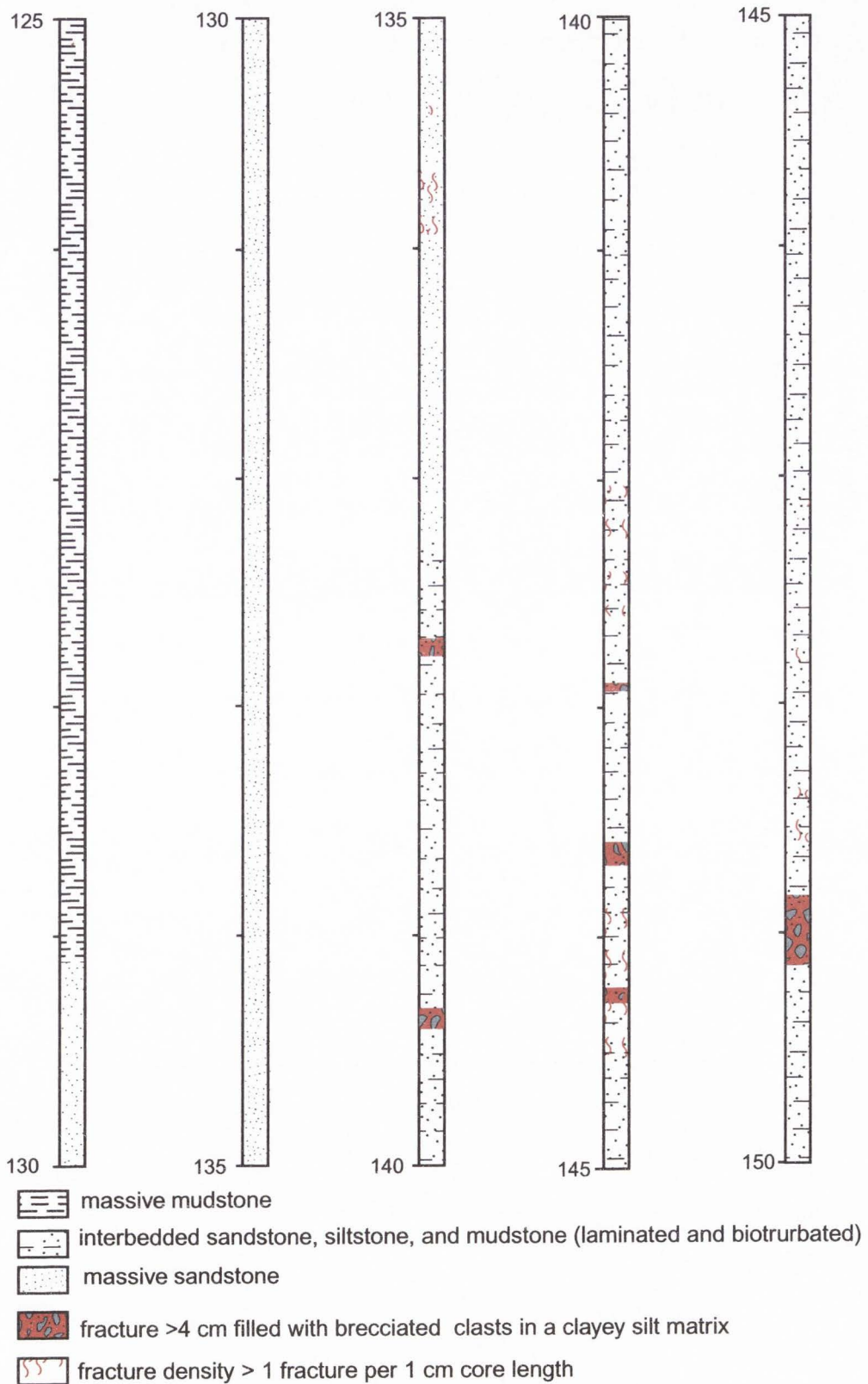
### Graphic log of core from Fengyuan drill site

2x horizontal exaggeration of cores, all depths in meters



-  massive mudstone
-  interbedded sandstone, siltstone, and mudstone (laminated and bioturbated)
-  massive sandstone
-  fracture >4 cm filled with brecciated clasts in a clayey silt matrix
-  fracture density > 1 fracture per 1 cm core length

Graphic log of core from Fengyuan drill site  
 Scale 1:25 (2x horizontal exaggeration), all depths in meters

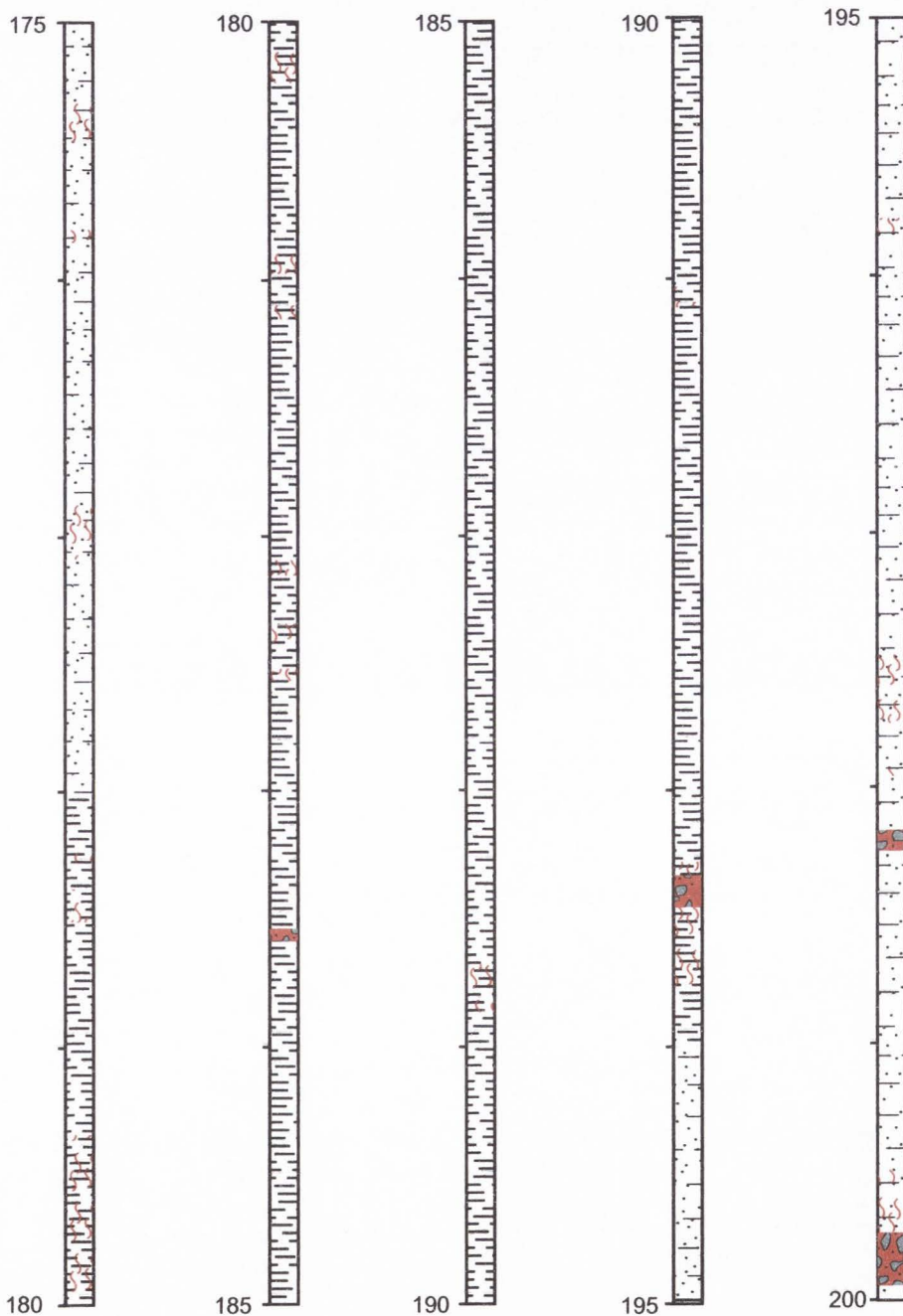



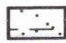


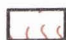
Graphic log of core from Fengyuan drill site  
 2x horizontal exaggeration of cores, all depths in meters



### Graphic log of core from Fengyuan drill site

2x horizontal exaggeration of cores, all depths in meters



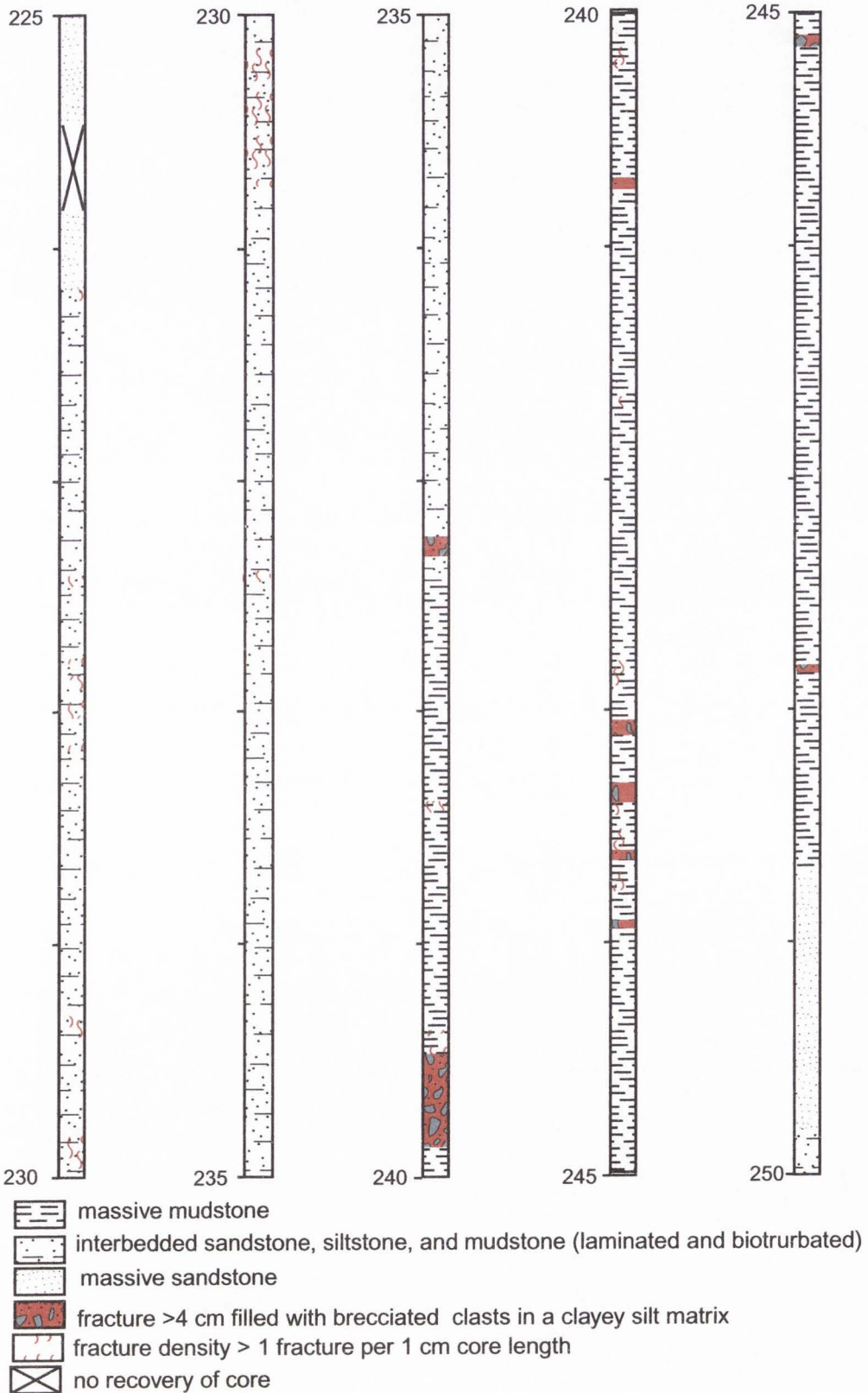
-  massive mudstone
-  interbedded sandstone, siltstone, and mudstone (laminated and bioturbated)
-  massive sandstone
-  fracture >4 cm filled with brecciated clasts in a clayey silt matrix
-  fracture density > 1 fracture per 1 cm core length

### Graphic log of core from Fengyuan drill site

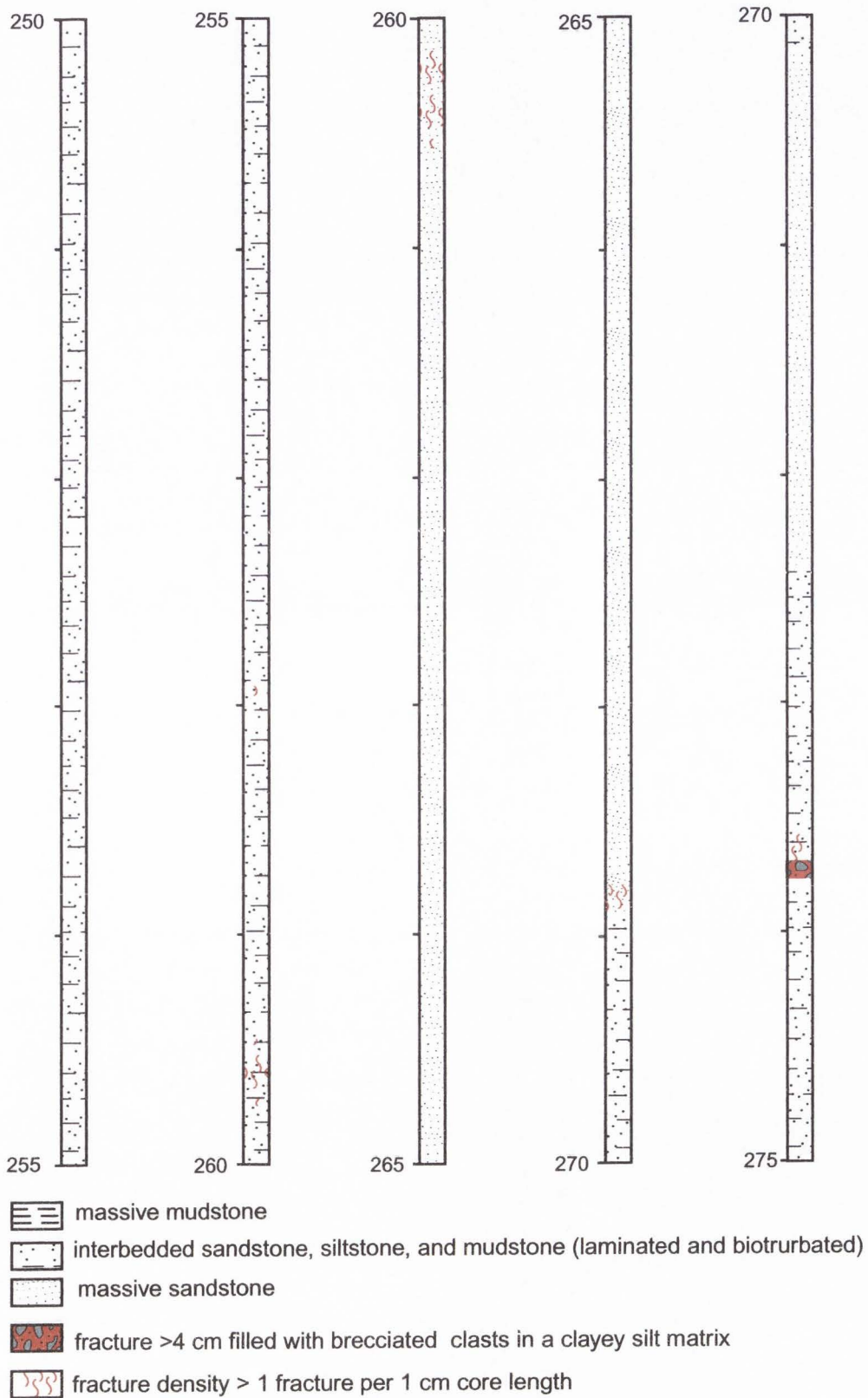
2x horizontal exaggeration of cores, all depths in meters



Graphic log of core from Fengyuan drill site  
 2x horizontal exaggeration of cores, all depths in meters

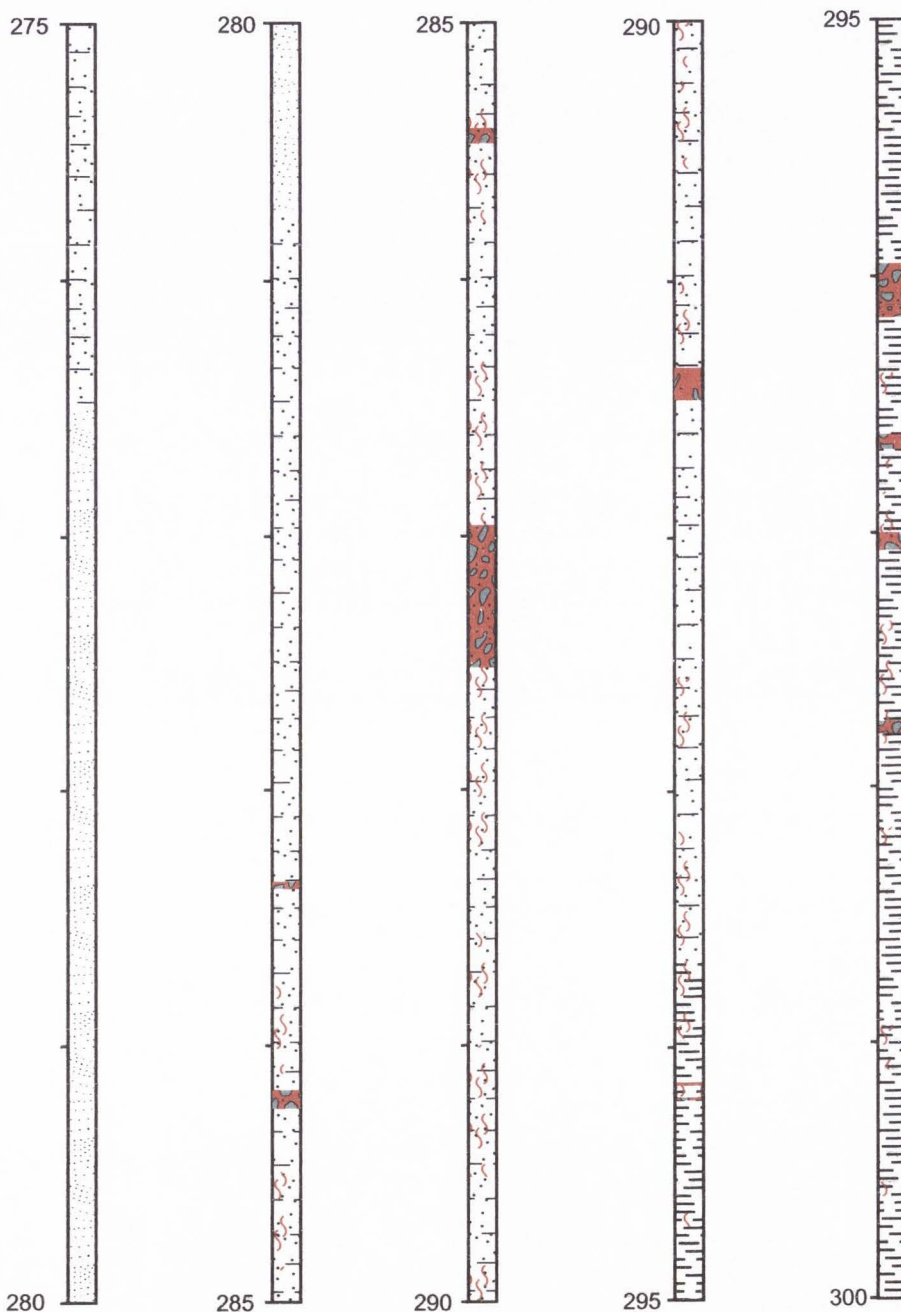







Graphic log of core from Fengyuan drill site  
 2x horizontal exaggeration of cores, all depths in meters



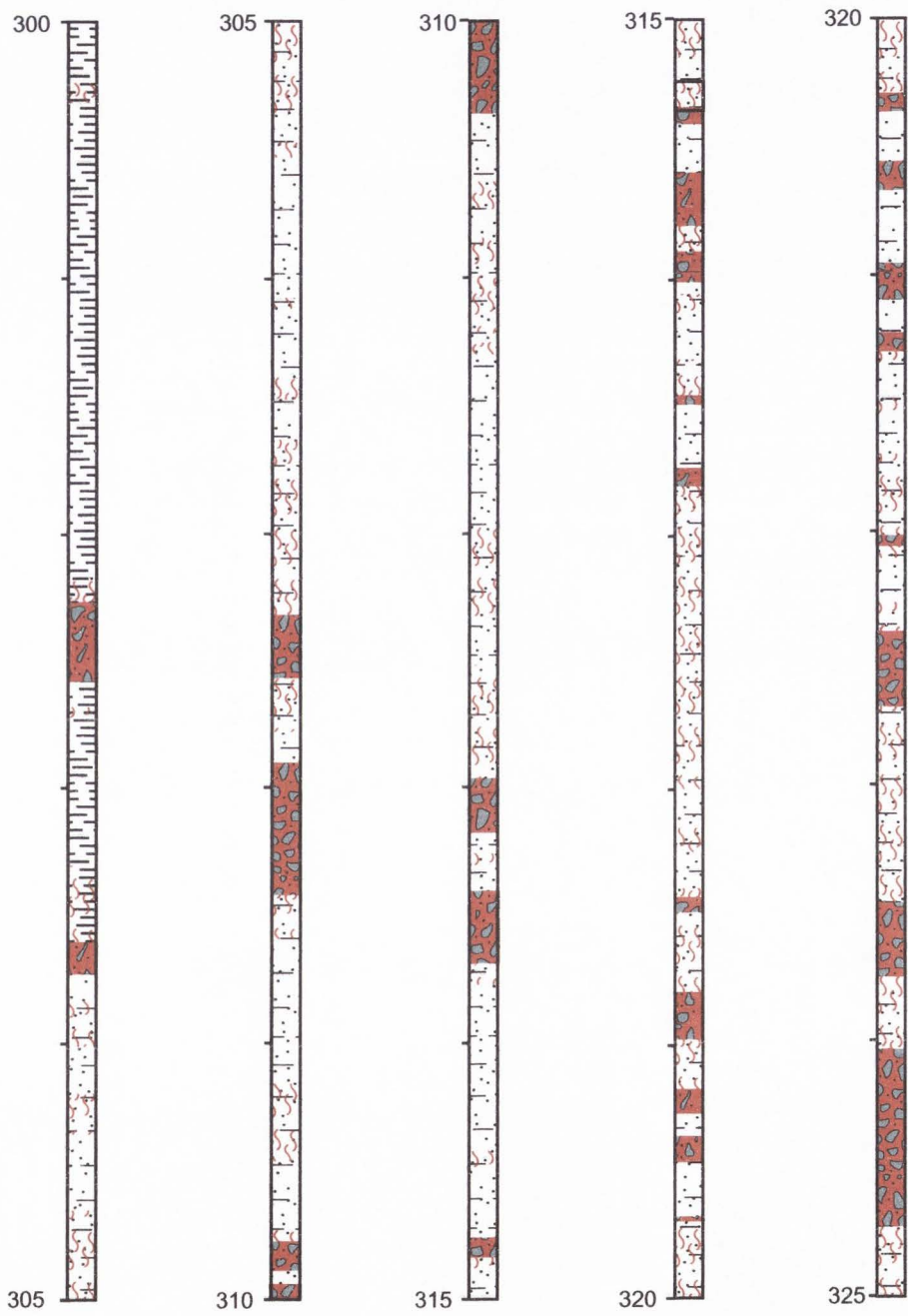




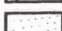


Graphic log of core from Fengyuan drill site  
 2x horizontal exaggeration of cores, all depths in meters



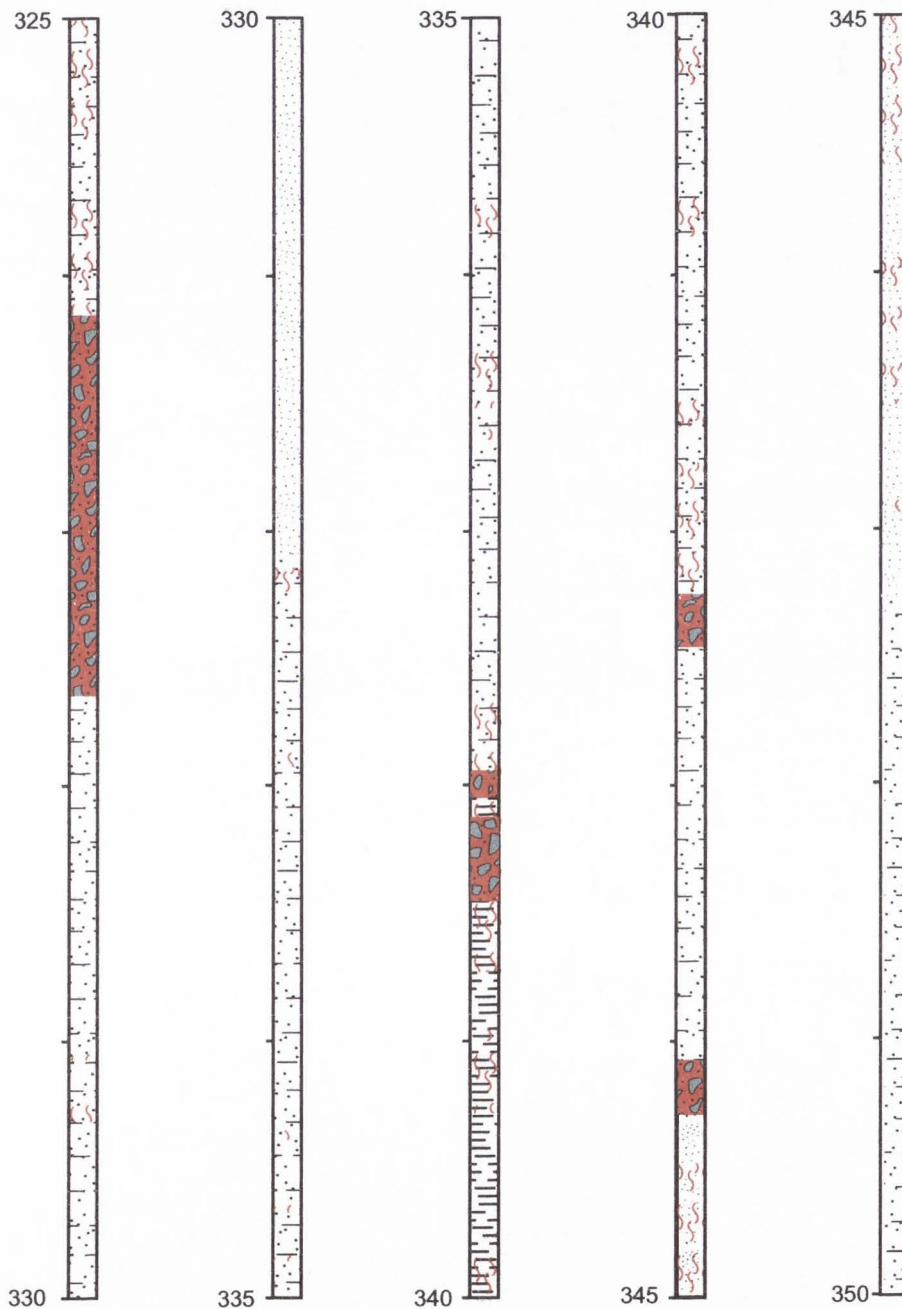
-  massive mudstone
-  interbedded sandstone, siltstone, and mudstone (laminated and bioturbated)
-  massive sandstone
-  fracture >4 cm filled with brecciated clasts in a clayey silt matrix
-  fracture density > 1 fracture per 1 cm core length






Graphic log of core from Fengyuan drill site  
 2x horizontal exaggeration of cores, all depths in meters



-  massive mudstone
-  interbedded sandstone, siltstone, and mudstone (laminated and bioturbated)
-  massive sandstone
-  fracture >4 cm filled with brecciated clasts in a clayey silt matrix
-  fracture density > 1 fracture per 1 cm core length

Graphic log of core from Fengyuan drill site  
 2x horizontal exaggeration of cores, all depths in meters


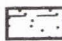





-  massive mudstone
-  interbedded sandstone, siltstone, and mudstone (laminated and bioturbated)
-  massive sandstone
-  fracture >4 cm filled with brecciated clasts in a clayey silt matrix
-  fracture density > 1 fracture per 1 cm core length

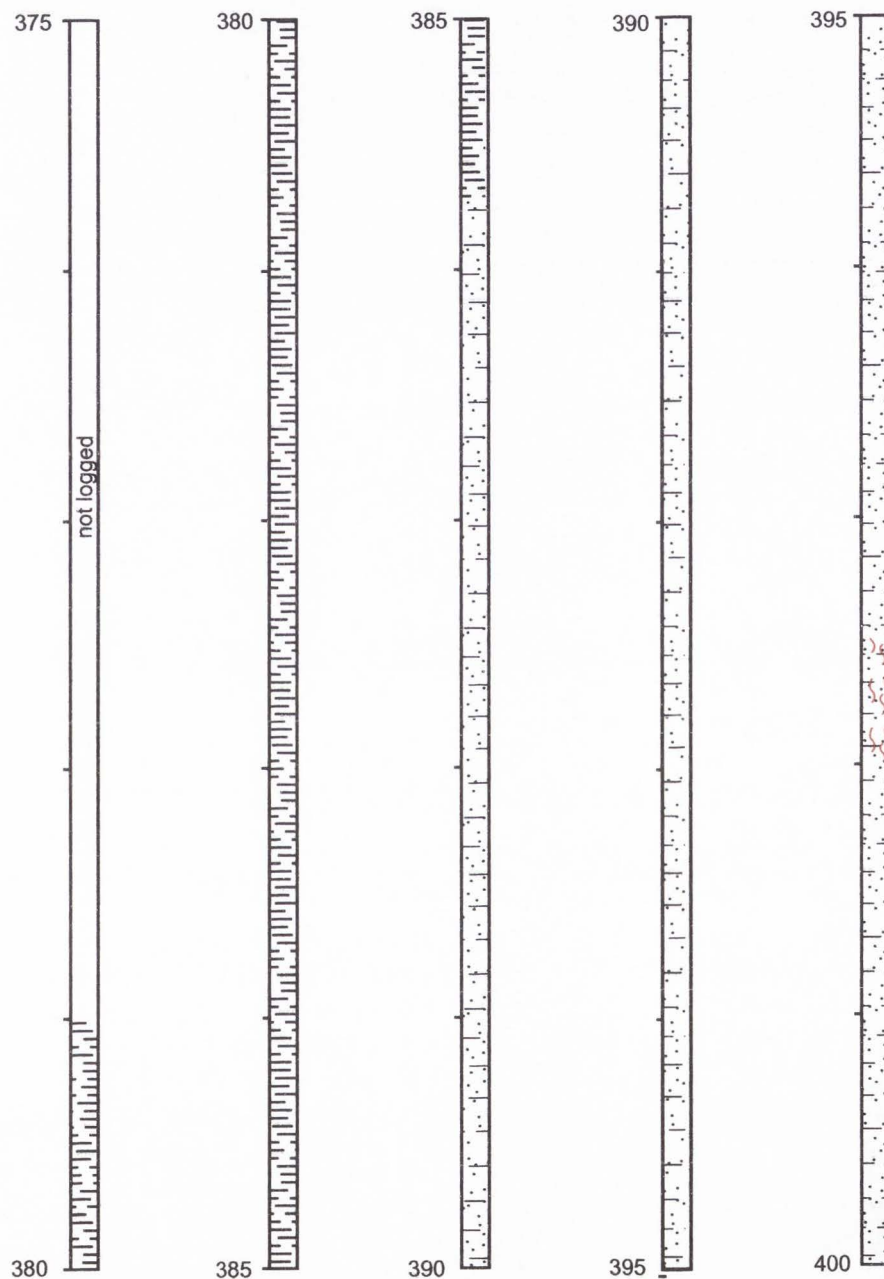
### Graphic log of core from Fengyuan drill site

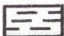
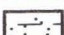



2x horizontal exaggeration of cores, all depths in meters



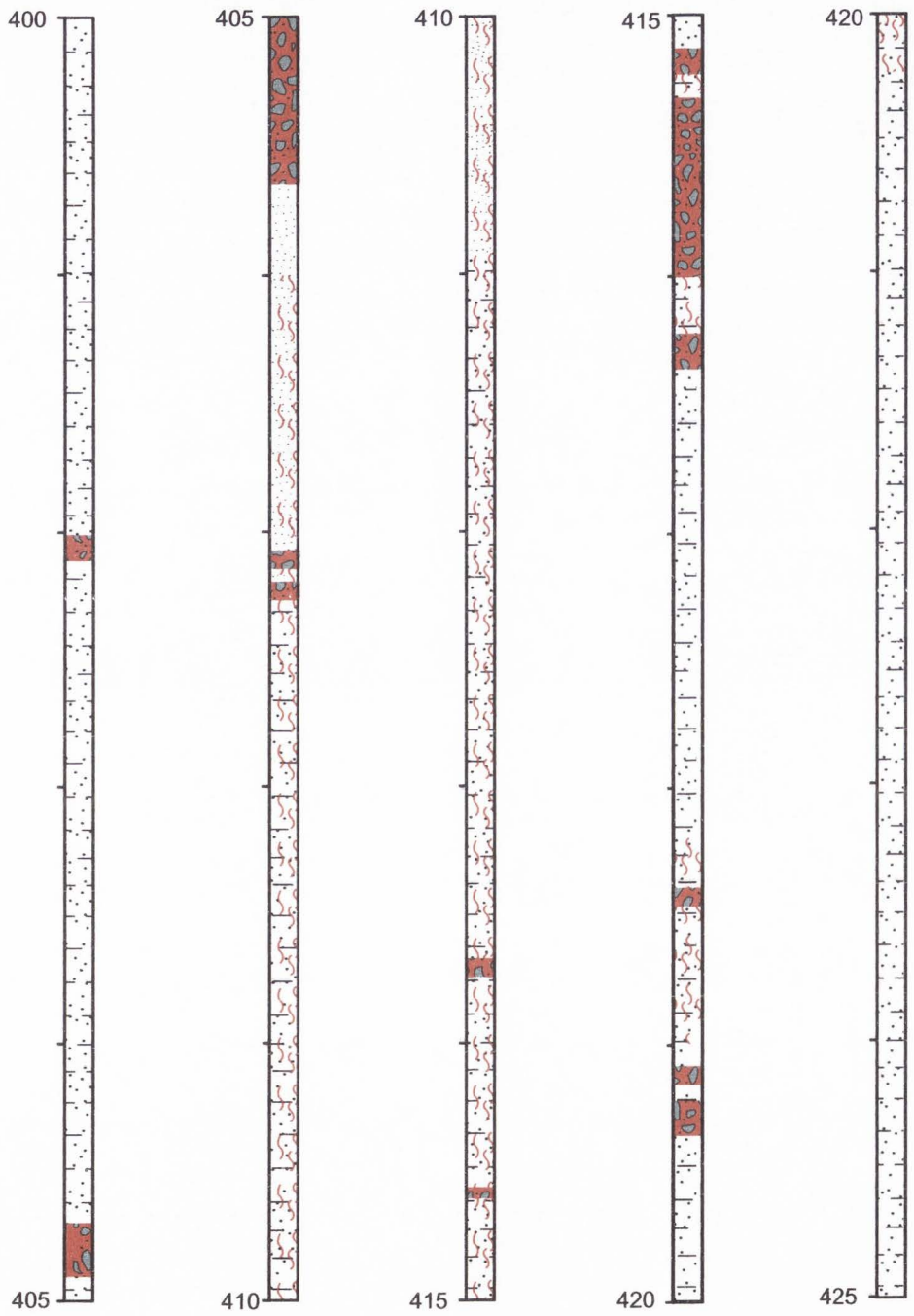
-  massive mudstone
-  interbedded sandstone, siltstone, and mudstone (laminated and bioturbated)
-  massive sandstone
-  fracture >4 cm filled with brecciated clasts in a clayey silt matrix
-  fracture density >1 fracture/1 cm





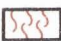
Graphic log of core from Fengyuan drill site  
2x horizontal exaggeration of cores, all depths in meters



-  massive mudstone
-  interbedded sandstone, siltstone, and mudstone (laminated and bioturbated)
-  massive sandstone
-  fracture >4 cm filled with brecciated clasts in a clayey silt matrix
-  fracture density >1 fracture/1 cm

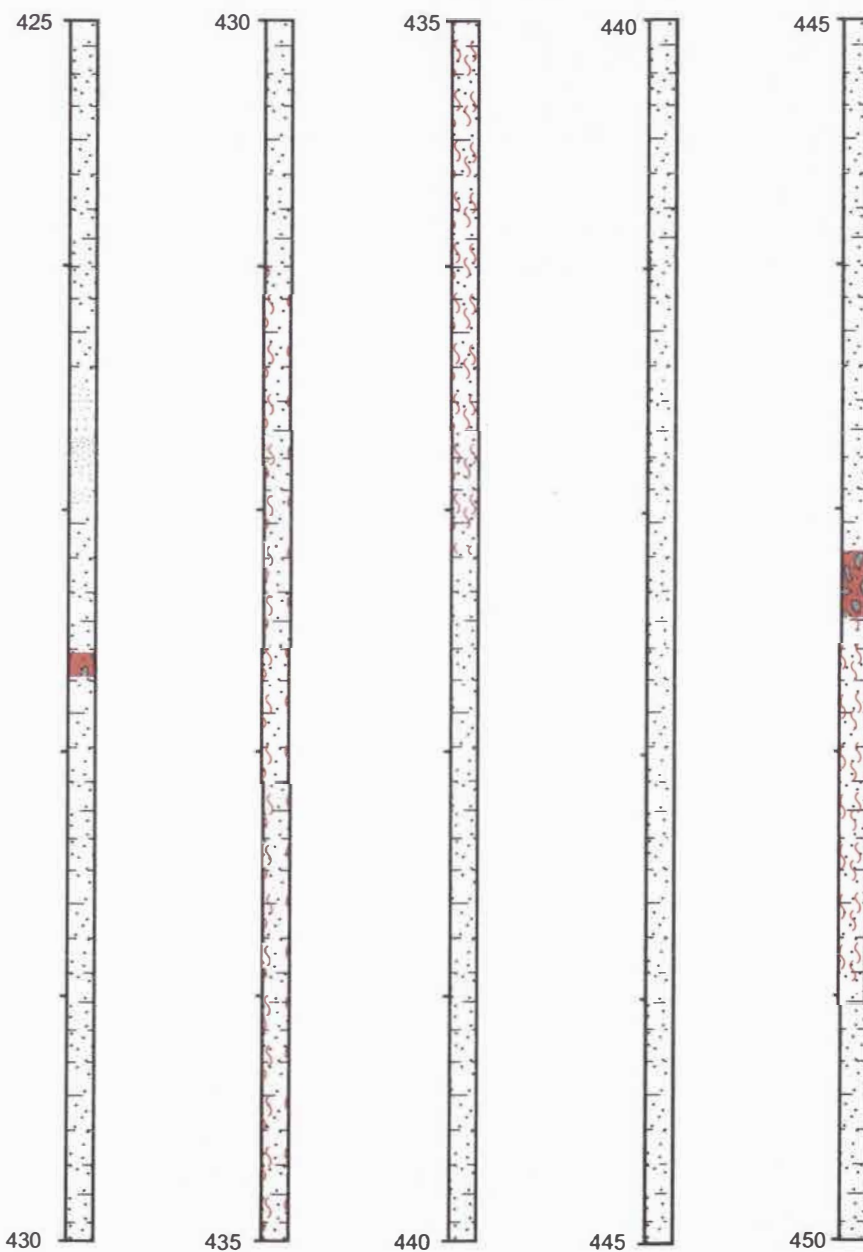
### Graphic log of core from Fengyuan drill site 2x horizontal exaggeration of cores, all depths in meters








-  massive mudstone
-  interbedded sandstone, siltstone, and mudstone (laminated and bioturbated)
-  massive sandstone
-  fracture >4 cm filled with brecciated clasts in a clayey silt matrix
-  fracture density > 1 fracture per 1 cm core length

### Graphic log of core from Fengyuan drill site

2x horizontal exaggeration of cores, all depths in meters



-  massive mudstone
-  interbedded sandstone, siltstone, and mudstone (laminated and bioturbated)
-  massive sandstone
-  fracture >4 cm filled with brecciated clasts in a clayey silt matrix
-  fracture density > 1 fracture per 1 cm core length